Studying spatial trends of heavy metals in soil from a tropical region

Susanne Jøntvedt Jørgensen

Thesis for the Master's

Degree in Chemistry

60 Study points

Department of Chemistry

Faculty of Mathematics and Natural Sciences

UNIVERSITY OF OSLO

2020

Studying spatial trends of heavy metals in soil from a tropical region

2020

Title: Studying spatial trends of heavy metals in soil from a tropical region

Author: Jørgensen, Susanne Jøntvedt

http://www.duo.uio.no

Printed at Reprosentralen, University of Oslo

Abstract

Fast-economic growth in some emerging economies brings forth potential environmental challenges due to increased population, industrialization and urbanization. A lack of regulatory framework and enforcement of these in emerging economies may therefore lead to increase in the pollution of heavy metals and persistent organic pollutants (POPs). The majority of these nations are located in tropical regions where there is a lack of synoptic studies assessing the biogeochemical processes governing the spatial distribution of heavy metals. The aim of this study was to obtain knowledge about the levels of heavy metals in soil and the role of drivers and pressures governing the spatial trends of these metals such as the physicochemical properties of the soil and distance to known sources. As the POPs have distinctive application areas, POPs data were included in order to observe the different sources of heavy metals.

A key pathway for which heavy metals and POPs may enter the terrestrial environment is via atmospheric deposition, both due to the volatile nature of some POPs and Hg, as well as the transport through eolian dust in air in these tropical environments. The physicochemical properties of soil in this region is different compared to those in temperate regions which will affect the ability of the soil to hold the heavy metals.

Surface soil samples were collected in a transect from the 40km upwind southeast of Dar es Salaam, Tanzania, through the city and up to 60km downwind northwest of the city. This transect followed the general wind direction. Additional samples were collected from a transect that incorporated the major city waste dumpsite and an e-waste recycler plant to assess the heavy metal pollution at these sites.

The samples were analyzed for Arsenic (As), Cadmium (Cd), Cobalt (Co), Chromium (Cr), Copper (Cu), Lead (Pb), Selenium (Se) and Zinc (Zn) using Inductively Coupled Plasma – Mass spectrometry after microwave assisted acid digestion. Total Mercury (Hg) content was determined by DMA-80. Physiochemical properties of the soil like pH, organic matter (OM) and cation exchange capacity (CEC) were determined. clay content was estimated based on soil texture feel.

The main governing factor for the spatial distribution was the distance to the city. This was supported by the significantly higher levels of Cd, Cu, Pb and Zn in urban areas than in rural areas. The levels of As, Co, Cr, Ni and Se were additionally governed by the soil's physicochemical properties.

The results indicated pollution at hotspot locations and higher levels of Cu, Pb, Cd and Zn in the city of Dar es Salaam than rural. Cd, Co, Cr, Ni and Se were found in background levels in all samples. Hg was found in low concentrations mainly due to the physicochemical properties of the soil and high temperature in the region which hinder the retention of the metal in soil.

Inclusion of POPs data allowed for a discrimination of general waste and e-waste.

Preface

First and foremost, I would like to thank Rolf Vogt for taking me on as his master student and for his constant belief in me as a researcher and chemist. Your great advice and optimism have been motivating when the work was challenging.

I am grateful for my co-supervisor, Maja Nipen, who included me on her field trip and for having her office door open for me to ask questions about field work, POPs, statistics and lab work.
I am also thankful for Knut Breivik, who allowed me to contribute to the Anthrotox project.

The field work in Dar es Salaam would not have been successful without Eliezer Mwakalapa and Samwel Ntapanta who not only managed to transport us to every location, also were great help when trying to find adequate sample locations.

I am grateful for Hilde Uggerud at NILU who joined me during the first sample digestions and for her valuable insight and help regarding sample preparation for trace element analysis.

The ICP-MS analysis and sample digestion would not have been possible without the help from our department engineer, Eline Færgestad. Thank you for valuable input during lab work and for trusting me with the ICP-MS.

The Mercury analysis was conducted at the department of Biology, and I am therefore thankful for Berit Kaasa and the Ecotoxicology group for their great help and hospitality.

Thank you to the whole Environmental Chemistry group for our interesting discussions during coffee breaks and long lunches. I am especially grateful for Camille Crapart for helping me with R and for Alexander Håland who helped whenever assistance was needed in the lab.

Last but not least, I would like to express my deepest gratitude to my family and friends who kept me somewhat sane during these last months. Thank you for being a safe haven to come home to whenever things are stressful.

Table of Contents

List of figures

List of Tables

Abbreviations

As	Arsenic
Be	Beryllium
Cd	Cadmium
Co	Cobalt
CP	Chlorinated paraffins
Cr	Chromium
Cu	Copper
Dec syn	Dechlorane Syn
Dec anti	Dechlorane Anti
DMA	Direct Mercury Analyzer
EEE	Electrical and electronic equipment
E-waste	Electronic Waste
Fe	Iron
GPS	Geographical Position System
Hg	Mercury
ICP-MS	Inductively Coupled Plasma – Mass Spectrometry
LOD	Limit of Detection
MDL	Method Detection Limit
MeHg	Methyl Mercury
Ni	Nickel
NW	Northwest
OM	Organic Matter
PCA	Principal Component Analysis
POP	Persistent Organic Pollutant
PZC	Point of Zero Charge
R^2	Correlation Coefficient
QA	Quality Assurance
QC	Quality Control
Se	Selenium
SCCP	Short Chain Chlorinated Paraffins
MCCP	Medium Chain Chlorinated Paraffins
SE	Southeast

STD	Standard Deviation
UiO	University of Oslo
Zn	Zink

1 Introduction

Heavy metal pollution has been a significant environmental concern for decades given the elements toxicity, potential for bioaccumulation and biomagnification in the food web and their potential for long-range transport.

Emerging economies that experiences rapid economic growth, increased population, consumption, urbanization, and industrialization faces environmental challenges related to pollution of heavy metals and other pollutants. This is mainly due to lack of legislation or capacity of enforcement and inadequate infrastructure required to handle toxic waste.

1.1 Heavy metals

There is no official definition of "heavy metals" in the scientific community, which can lead to confusion regarding what is being referred to when discussing this topic.

In chemistry, the term "heavy metal" commonly refer to metals that have a specific density greater than 3.5-7gmL^{-1} (Duffus, 2002). However, the term is commonly understood as referring to toxic metal contamination. This terminology can be misleading as some metals of lower density are toxic such as Beryllium (Be), while some heavier metals are essential at low concentrations, e.g. Iron (Fe), Copper (Cu) and Zinc (Zn). The term was originally applied to toxic metals such as Lead (Pb), Mercury (Hg) and Cadmium (Cd), but the high density of these elements does not infer any specific biological property nor behavior in the environment.

Ahrland et al. (1958) introduced a way of classifying metals which was based on their sorption properties, where metals were differentiated by their affinities to donor ligands, indicated by the covalent index (i.e. Electronegativity^2 · radius). The covalent index classifies metal ions as either Type A (hard metals), Type B (Soft metals) or borderline. This thesis focuses on several type B and borderline metals, which herein are referred to as heavy metals as this is the term commonly used. Selenium (Se) is not a metal, but a metalloid. It was nonetheless included in the study and included in the term "heavy metal".

Including the ionic index (i.e. charge^2/radius) in the classification, as illustrated in Figure 1-1, also separates the metals in terms of their ability to form ionic bonds and complex stability when binding to Organic matter (OM).

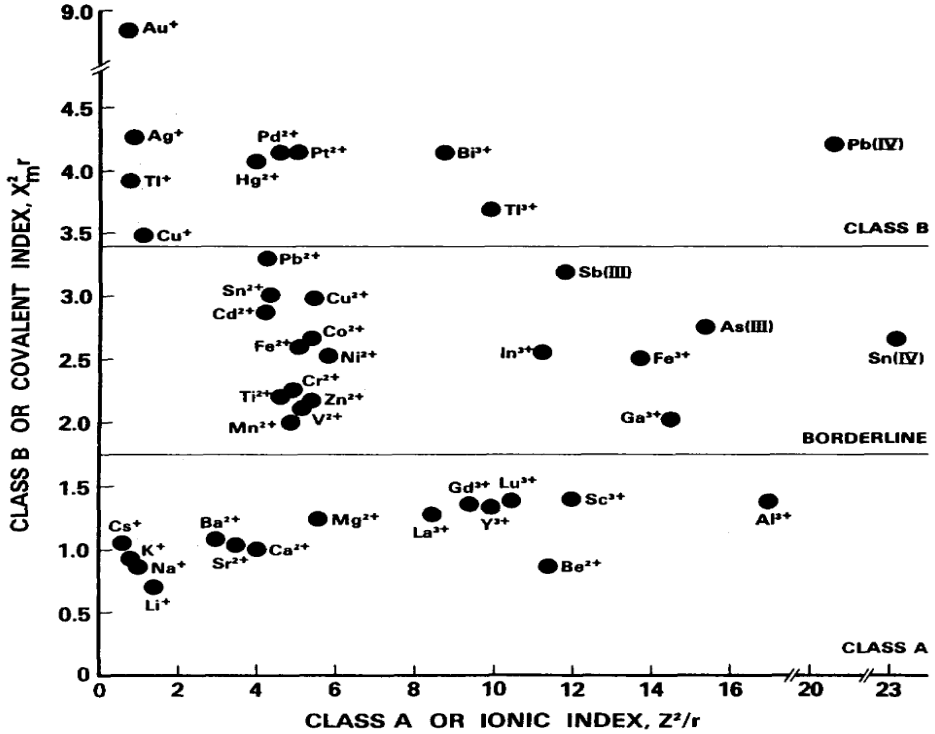

Figure 1-1: Classification system of metals into Type A, B or borderline based on sorption properties, reproduced from Nieboer and Richardson (1980).

1.2 Heavy metals as toxic substances

Pb, Cd and Hg are some of the metals of most concern due to their highly toxic traits. Although humans have utilized these metals for centuries, their detrimental aspects gained attention during the industrial revolution after being in used in a wide range of industries, such as metal plating and in electronics and electronic equipment (EEE). During this period several studies documented the toxic effects of heavy metals such as Pb and Cd, and reports of Hg poisoning in the Minamata area in Japan were published, later known as Minamata disease (Tong et al., 2000, Aoshima, 2016, Harada, 1995). Type B metals are generally the most toxic followed by the borderline metals (Appelo and Postma, 2005).

Public knowledge of the toxic traits associated with heavy metals resulted in collection and handling of waste containing heavy metals as well as phase out processes for many heavy metals in industry and domestic products. For Pb this included a phase out of the compound from gasoline and paint. Similarly, Cd was phased out of production of alloys, pigments and

stabilizers (UNECE, 1998). An international agreement on phasing out products containing Hg and prohibition of establishing new Hg mines are more recently made in the Minamata convention (UNEP, 2013).

1.3 Challenges in emerging economies

Heavy metal pollution from sources such as industries, transportation, power plants and agriculture are still occurring in countries with developed economies as these metals are utilized in a numerous amount of applications. However, emissions of heavy metals from these sources have decreased due to abatement efforts towards reducing the use of heavy metals. Given the element's persistence in the environment, there remains a legacy to this day of historic use of these hazardous metals (AMAP, 2011). On the other hand, in emerging economies there is generally a poor regulatory framework and inadequate enforcement of these regulations. In addition, there is a lack of management standards and monitoring of the waste containing heavy metals which may lead to elevated levels of heavy metals in the environment in these regions.

Such emerging economies are facing pollution from the same sources as the developed economies of the 21st century in addition to sources such as uncontrolled waste dumps and e-waste handling (Fayiga et al., 2018). An increasing population in urban areas leads to more traffic, which further increases the pollution from roadside emission.

The concern regarding environmental contamination is not limited to heavy metals but include other contaminants such as persistent organic pollutants (POPs). POPs are toxic, persistent and bioaccumulative substances which are, similarly to heavy metals, restricted in developed economies, but remains in use in emerging economies due to lack of regulation or infrastructure to enforce regulation (Wania and Mackay, 1996, UNEP, 2011) POPs are used in various industrial applications such as pesticides in agriculture and as plasticizers or flame retardants in plastics and in EEE. Dechlorane Plus, which contains two isomers of dechlorane, syn and anti (dec syn and dec anti respectively) are used as flame retardants in televisions and computer monitors, wire coating and furniture (Sverko et al., 2011).

Chlorinated paraffins (CPs) such as short and medium chain chlorinated paraffins (SCCP and MCCP respectively) are used as softeners in plastic and as flame retardant in rubber, textiles and PVCs and as additives in metal working fluids and paint (Denier van der Gon et al., 2007,

Fiedler, 2010). Both the dechloranes and chlorinated paraffins are in use to this day and are thus of environmental concern and included in this study. Dechlorane 602 and 603 were included though their applications are not widely discussed in literature.

The input of heavy metals and POPs to the environment from e-waste in emerging economies is enhanced by the illegal export of used, broken and obsolete EEE from developed economies to emerging economies (Robinson, 2009). The environmental challenges in developing economies arise when the EEEs are considered defective and are at the end of their lifetime. Due to the high content of valuable metals in the components of EEEs, the scavenging, extraction and selling of precious metals from e-waste generate an income and is thus a large industry in developing economies. Conducting formal and legal recycling is not as profitable due to the large fees and taxes for processing e-waste formally (Mahenge et al., 2018). However, the informal e-waste handling processes, as opposed to formal processes, generally fail to include pollution emission control. In a performance audit report from 2018 regarding electronic waste management in Tanzania it was concluded that "Despite the continuous efforts to improve the state of the environment in the country, the government has failed to effectively manage the e-waste" (Mahenge et al., 2018).

There is limited information on sources contributing to pollution as well as levels of heavy metals in the African environment. Even in South-Africa, which is considered one of the most industrialized African countries, there is a lack of data regarding emission and levels of heavy metals in the environment (Leaner et al., 2009). While some African countries have implemented abatement efforts (such as standards for discharge of effluents to surface waters), high levels of regulated compounds are still found in the environment, reflecting that there is an absence of enforcement of the standards and regulations, as well as a lack of monitoring of discharges to surface waters (Fayiga et al., 2018).

1.4 Pollution tropical regions

Some pollutants released into the environment have the potential to evaporate or absorb to aerosols and thereby be advected with airmasses, resulting in contamination at long distances from the source. A long lifetime in the atmosphere, as some metals and POPs hold, promotes the transportation of these contaminants over long distances.

Hg is mainly present in the atmosphere as elemental gaseous Hg ($Hg^0(g)$). In the atmosphere the element is oxidized to divalent Hg (Hg^{2+}). The transformations between these species greatly affects the transport and deposition of the element as the deposition is mainly dominated by wet and dry deposition of Hg^{2+} (Lindberg and Stratton, 1998). Some of the deposited Hg^{2+} is reduced to Hg^0 in soils and re-emitted to the atmosphere. Re-emission of Hg^0 from soil is a part of the global cycling of the element (UN Environment, 2019). Deposited Hg^{2+} is additionally prone to accumulation in boreal areas where soil OM content is high due to the element's complexing nature with OM (Lindqvist et al., 1991). In a tropical region where soil OM are low, one can expect that the retention in soil of heavy metals with a high affinity for OM is low.

Volatile and semi-volatile compounds, such as Hg and POPs respectively, are even more prone to atmospheric transportation in tropical areas due to high temperatures and low content of soil OM which can bind the compounds. Previously deposited contaminants can thereby readily be re-emitted to the atmosphere from soil surfaces and waterbodies in gaseous form. This process of repetitious evaporation and deposition is referred to as "the grasshopper effect" which is illustrated in Figure 1-2. In warm regions (i.e. tropical and subtropical) the temperature will favour the evaporation of volatile and semi-volatile compounds, in temperate regions the evaporation and deposition are run by seasonal changes in which pollutants frequently evaporate and deposits due to temperature changes (Wania and Mackay, 1996). At higher latitudes, such as the Arctic, deposition exceeds the evaporation and pollutants can therefore ultimately accumulate in these regions, making the Arctic a sink for Hg (AMAP, 2011, Ariya et al., 2004) .

Less volatile contaminants such as Pb, Cd, Zn, and some of the lower volatile POPs, such as the Dechloranes, are not transported in the atmosphere in gas form but can be transported adsorbed to particulate matter.

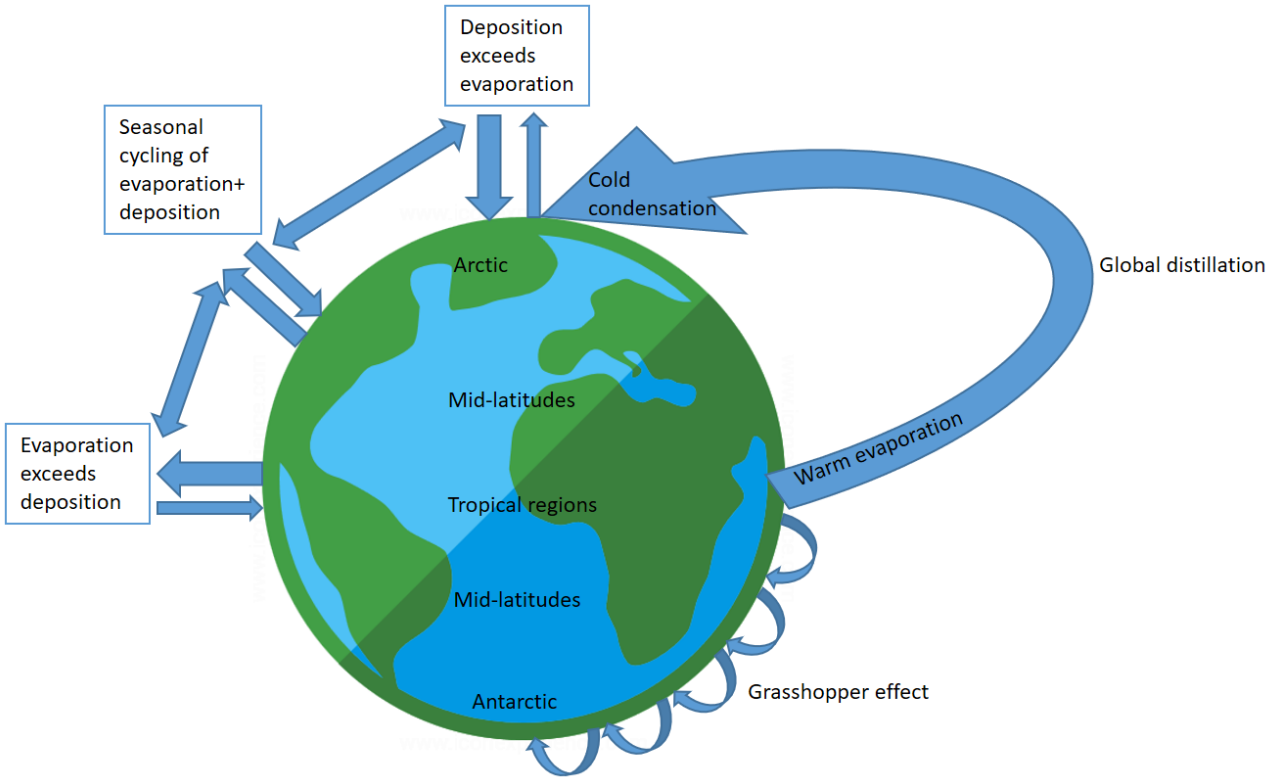

Figure 1-2: The Global Distillation Process, adapted from (Wania and Mackay, 1996)

In short, the tropical environment results in a soil that does not favour retention of heavy metals or POPs as the soils contain low amount of OM and high temperature favors evaporation of volatile compounds.

1.5 The AnthroTox project

This master thesis is a part of the AnthroTox project that is assessing the environmental, social, political, and economic processes that affect the emission, mobilization and transport of toxicants in societies and ecosystems in countries with emerging economies (Anthrotox, 2017).

Over the last few decades, Tanzania has experienced rapid development, making the Tanzanian economy one of the fastest growing among the non-oil nations in Sub-Saharan Africa (The World Data Bank, 2009). Tanzania was therefore used as a representative country experiencing fast-economic development, and which thus faces a set of challenges regarding environmental pollution

The Environmental Sciences section at the Department of Chemistry, UiO, is an integral part of the project, and aims to understand the governing factors for spatial distribution and temporal trends of hazardous compounds, such as heavy metals and POPs in and around the largest city in Tanzania, Dar es Salaam.

Various metals from the type B and borderline category was included in this study. The metals were included due to the significant urban pollution of some heavy metals, as well as their content in e-waste, though some were chosen due to natural background association. This was done to observe potential trends in urban and rural environments.

Heavy metals often associated with urban pollution are Cu, Pb and Zn although this varies a great deal, however, Pb is a common pollutant for most urban areas (Karim et al., 2014, Guo et al., 2012, Manta et al., 2002). Metals usually associated with pollution from e-waste are Cd, Cu, Hg, Nickel (Ni), Pb, Zn and hexavalent Chromium (Cr) (Frazzoli et al., 2010). Arsenic (As), Cobalt (Co), Cr and Ni have been shown to be associated with natural background (He et al., 2017, Manta et al., 2002, Guo et al., 2012). Se is a metalloid that interacts with some of the heavy metals as Cd, Hg and Pb, and detoxifies the elements (Christophersen et al., 2013).

Heavy metals included in this study is therefore As, Cd, Co, Cr, Cu, Hg, Ni, Pb, Zn and Se.

1.6 Aim of study

Research conducted on spatial trends of heavy metals in tropical regions is limited, thus little is known regarding the levels and spatial distribution of these contaminants in a tropical environment like the Dar es Salaam region. The objectives of this thesis was therefore i) to assess the levels and spatial trends of the various heavy metals in the region, ii) describe the physicochemical properties of the soil that governs the soils ability to hold heavy metals such as pH, OM content, cation exchange capacity (CEC) and clay content and iii) use multivariate analysis to assess the influence of physicochemical properties and potential pollution sources of spatial trends.

There are multiple potential sources of heavy metals in the city of Dar es Salaam.

It was therefore hypothesized that the levels of heavy metals are at background levels in the southeast (SE) rural locations. The levels will increase upon entering the urban areas of Dar es Salaam and will gradually decrease towards the northwest (NW) rural locations and reach background levels at the end of the transect.

The levels of heavy metals and POPs will be high at hotspot locations, such as e-waste recycling plants and the waste dump. It was expected that the levels of heavy metals were to be governed by physicochemical properties.

2 Theory

This chapter provides theoretical background regarding the physochemical soil properties that govern the soil's ability to hold heavy metals. The chapter also provides information about the different heavy metals included in the study, with focus on Hg, Cd, and Pb due to their type B behavior in the environment.

2.1 Soil properties

Important properties of the soil that govern to what extent they accumulate heavy metals are the content of OM, pH, CEC and clay content.

The manner in which these properties control the mobility and thus the accumulation of the different types of heavy metals are addressed in the following subchapters.

2.1.1 Organic matter

Inorganic material constitutes the major fraction of the mineral soil profile, but the minor fraction of OM plays a disproportionate role in governing the soils ability to sorb metals.

The OM mainly consists of dead and decomposing biological material, as well as biomass of living plant tissue, bacteria, fungi, actinomycetes, and protozoa (VanLoon and Duffy, 2011). The amount of OM in soil depends on the climate, type of vegetation that grows in the area, land use, landscape and the inorganic composition of the soil.

Litterfall and its decomposition products mainly constitute the main source of OM. The product of the partial decomposition process is humic matter which is a chemical and microbial stable compound. The properties of humic matter are important for the CEC of soil (See following section on CEC) due to its weak organic acid groups that generates a pH dependent net negative surface charge on soil particles (Schlesinger and Bernhardt, 2013).

Humic matter is mainly composed of carbon, oxygen and hydrogen and is structurally built up of aliphatic and aromatic moieties as well as carbohydrates (Perdue, 2009).

An important component of the humic matter is the large number of weak organic acid functional groups. Along with the hydroxyl groups, these acids contribute to a pH dependent net negative charge on the OM. The cations on the cation exchanger are type A metals.

Additionally, the oxygen in the protolyzed weak organic acid functional groups in the humic matter forms stable chemical complexes with both Type B metals and borderline metals (described in more detail in section 2.2.1 and 2.2.2). The OM has thus a large capacity to bind heavy metals. The amount of OM in the soil is therefore an important explanatory factor for the spatial variation in accumulation of heavy metals in soil (VanLoon and Duffy, 2011).

The content of OM varies greatly in different types of soils. General ranges of content of OM in different climates and land-use soils are found in Table 2-1.

Table 2-1: Organic matter content in different types of soil. Reproduced from vanLoon and Duffy (2011) (VanLoon and Duffy, 2011).

Soil type	Organic matter content (%)
Temperate agricultural soils	1-5
Tropical agricultural soils	0.1-2
Forest soils (surface horizons)	>10
Peat soils	>20

As observed from Table 2-1, tropical soils have low content of OM, mainly because the warm and dry climate favor the complete mineralization of litterfall rather than the partial humification (Kalpage, 1976).

In addition, the intense rainfall episodes over a short period in tropical and subtropical areas causes considerable surface runoff that flushes out the litterfall and causes erosion of the mineral soil. Moreover, during the dry season, rainfall is too irregular and insufficient to facilitate plant growth which further reduces the potential for OM to be incorporated in the soil (Kalpage, 1976).

2.1.2 Cation Exchange Capacity

CEC of a soil is defined as the soil's ability to hold and exchange type A cations (Fergusson, 1990). This capacity originates from the net negative charge of the soil surface, in which there are two kinds of charges, the pH-independent and the pH-dependent charge.

The pH-independent charge of soil is a result of a process in which an atom in the crystal lattice in the clay mineral is replaced by another atom. Clay minerals are built up of tetrahedra Silica (Si) and Aluminum (Al) octahedra structures with oxygens in the corners and Si or Al, respectively, are residing in the middle. A negative charge occurs when the cation in the middle of the structure is replaced by a cation with a lower charge. For example, Si^{4+} can be replaced by Al^{3+} and Al $^{3+}$ replaced by Mg^{2+} (Appelo and Postma, 2005) .

The second source for negative charge is the pH-dependent charge of the soil. These charges are a result of weak organic acids in the humic material, OH groups at the edges of the clay particles and iron and aluminum oxyhydroxides exposed to soil solution. At high pH, the OH-groups dissociates and becomes negative ($-O^-$).

The strength of the sorption of a type A cation to an exchangeable site is determined by its ionic index (Z^2/r), which is determined by charge (z) and hydration radius (r).

2.1.3 Soil pH

The soil pH has a great influence on the solubility and adsorption of heavy metals to the soil, and is the key property of the soil that has the strongest influence on the level of heavy metals (Young, 2013). Soil pH depends on the type of the unconsolidated material, the local climate and the land-use history and age of the soil

pH of water infiltrating the soil will change depending on the pH of soil the water is infiltrating. Easily eroded minerals, like carbonates, take up much of the H^+ (Equation 2-1), while minerals less prone to erosion, such as quartz, are inert to H^+ ions in the water. Soils with a significant content of carbonates have thus a higher pH than soils with lower content of carbonates.

$$CaCO_3(s) + 3H^+(\text{aq}) \rightarrow Ca^{2+}(aq) + CO_2(g) + H_2O(l) \qquad \text{Equation 2-1}$$

pH in carbonate free soils depends on the amount of humic material, as well as Fe/Manganese oxyhydroxide minerals which will also react with H^+ ions of the infiltrating water. The reaction with H^+ is dependent on the charge of humic matter and the oxyhydroxides, which is determined by point of zero charge (PZC). PZC is the pH were the pH dependent positive charged on the hydroxyl- and acid functional groups compensate for the negative charge caused by isomorphic substitution inside the clay lattice, so that the net surface charge equals 0 (Appelo and Postma, 2005). The protonation of functional groups on oxyhydroxide minerals and humic matter at pH below the PZC causes a positive charge on the functional groups and thus low complexation of cationic heavy metals (VanLoon and Duffy, 2011). At pH over PZC the deprotonated functional groups will provide a net negative charge, rendering the sites available for cationic heavy metal binding.

The pH at PZC differ among minerals Goethite (FeOOH), Boehmite (AlOOH) and Bernalite ($Fe(OH)_3$) have PZC within the soil range between 6 and 8.5, which is within the pH range encountered in this study. These are common minerals expected to be present in the equatorial soils where there is a total dissolution of the primary mineral and neo-formation of clay and oxides (Vogt, 2020). This pH dependency can be observed for various metals sorbed to goethite at various pH (Figure 2-1).

Goethite has pH dependent groups on the surface ($-O^-$, -OH, $-OH_2$, $-OH^{\pm}$) which at pH below 8 will be protonated and cause the surface to have a net positive charge and thus little sorption of heavy metals, while at pH higher than PZC (pH 8 for Goethite) the surface will have a net negative charge and the surface is thus more prone to binding cationic heavy metals (Vogt, 2020).

The different positions of the curves reflect the affinity of the heavy metals to the surface. In addition to the pH dependent net positive or negative surface charge of the common Fe and Al oxyhydroxides in the pH range of these soil, the covalent index of the heavy metal determine their affinity to the oxygen functional group (Fischer et al., 2007). The steep curve for Al and Cr is the result from formation of stronger complexation to $-O^-$.

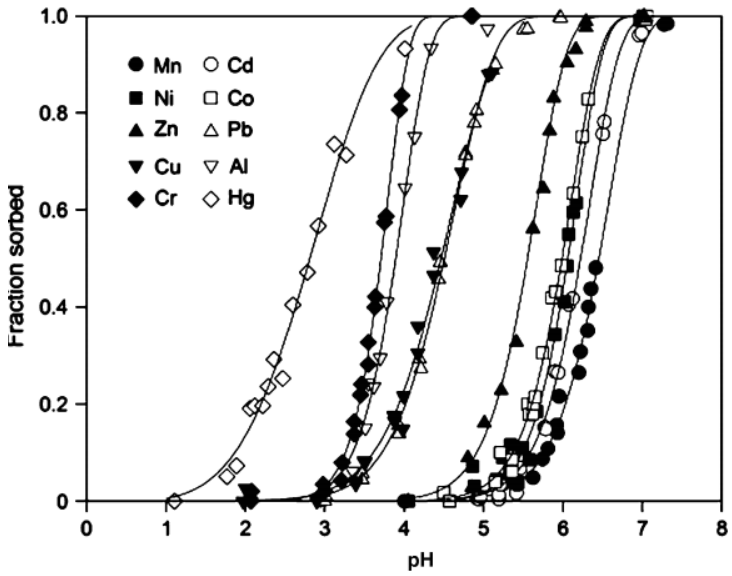

Figure 2-1 - pH dependency of sorption of various heavy metals. Experiment done on Goethite and data recorded after 2h (Reproduced from Fischer et al. (2007)).

In regard to Goethite, which may be considered representative for the soil in this region, only sorption of Cd, Ni and slightly Zn are influenced by the pH in the range from 6.0-8.5. This may indicate that the complexation of these heavy metals may be to some extent governed by the soil pH, while pH is high enough to not be an important factor for Hg, Cr, Cu and Pb.

2.1.4 **Clay content**

The inorganic fraction of the soil consists of particles of different sizes fractions, classified as sand, silt and clay. The relative amounts of these fractions determine the soil texture. It is the clay size fraction that has the most important role in dictating the soils ability to bind heavy metals due to the much larger surface area of clay compared to other size fractions (Fergusson, 1990). The larger surface area provides larger opportunity for heavy metal sorption.

2.2 Heavy metals in the environment

Heavy metals are naturally present in the lithosphere and are part of the parent rock material, but due to widespread anthropogenic use they are found at elevated levels in atmosphere, water, soil and sediments.

Important anthropogenic sources of heavy metals to the environment are acid seepage to surface waters from mining, emission with flue gases to the atmosphere from metal smelters,

coal fired power plants, fertilizers in agriculture, and emission from industries and transportation (Alloway, 2013b).

2.2.1 Type B metals

Metals classified as type B tend to form more stable complexes than type A metals, because type B metals displays a preference to form covalent bonds with other highly polarizable, big (large radius) and low charged donor ligands. The type B metals also prefers ligands of low electronegativity as the type B metals themselves displays relatively high electronegativity (VanLoon and Duffy, 2011).

These metals form stable complexes with sulfides, organosulphides, ligands containing nitrogen and functional groups on humus that acts as ligands

The heavy metals addressed in this study that belong in this category are Hg and Pb. The cations Hg^{2+} and Pb^{2+} form strong complexes with organic carbon, where MeHg is of great concern.

2.2.2 Borderline metals

The metals in this class exhibits traits that are intermediated to type A and B. They can form complexes with all types of ligands.

Of the borderline metals, type B behavior is displayed for the elements more to the right in the periodic table than those to the left due to higher electronegativity. Second row transition metals also show more type B behavior than the first row (VanLoon and Duffy, 2011).

Cations included in this study that belong in this group are Cd^{2+}, Cu^{2+}, Co^{2+}, Ni^{2+}, Zn^{2+}, As^{2+} and Cr^{2+}.

2.2.3 Mercury – Applications, speciation and toxicity

Despite its low natural concentration in the lithosphere, Hg is a compound of great concern due to its toxicity, persistence in the environment and potential for long range transport. Due to its unique properties, Hg compounds have been utilized by humans since antiquity and is still being used in certain industries and in applications to this day (Steinnes, 2013b).

Due to the element's broad application range, the anthropogenic sources of Hg are many. Approximately 31 tons of Hg were released from anthropogenic sources to the environment in Tanzania in 2016 (Vice President's Office: Division of Environment, 2017), not accounting for reemission of previously deposited Hg – which is an process of interest due to high temperature in the tropics.

The largest source was primary metal production, followed by waste incineration as illustrated in Figure 2-2.

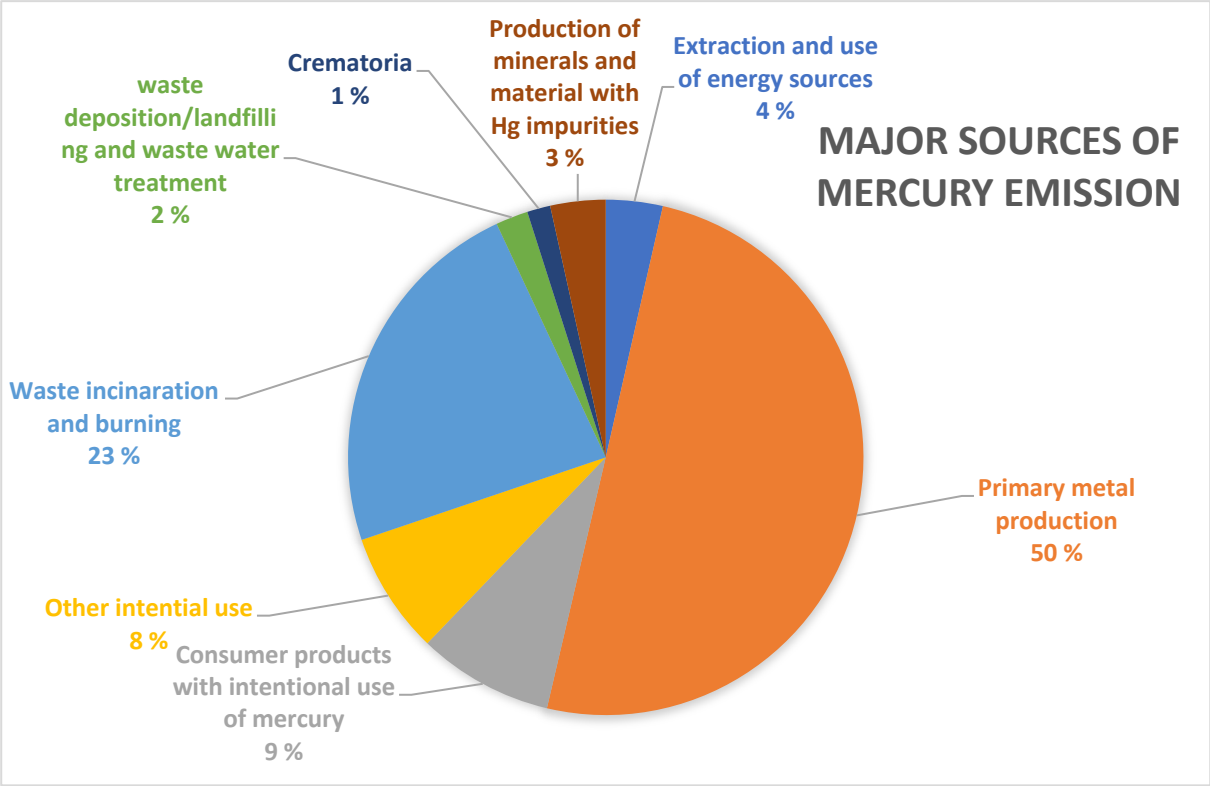

Figure 2-2: The major anthropogenic sources of Mercury in Tanzania(Numbers from Vice President's Office: Division of Environment (2017))

Hg released as a product of waste incineration or from waste deposition is a result of products containing Hg. These wastes includes e-waste in which Hg is used in fluorescent lamps, LCD monitors and electrical switches (EPA, 2019).

2.2.3.1 Hg in atmosphere

$Hg^0(g)$ has a lifetime of approximately 1 year in the troposphere, allowing for transport over long distances (Slemr et al., 1981). The oxidized (Hg^{2+}) is the dominant form that is deposited by dry and wet deposition, though gaseous elemental Hg^0 can also be deposited by dry

deposition. The Hg^{2+} specie is more reactive and more soluble than elemental Hg, which increases the total deposition of Hg^{2+}, both through dry and wet deposition. Hg^{2+} has thus a considerably shorter lifetime in the atmosphere (UNEP, 2002). Although Hg exists predominantly in the atmosphere as gaseous Hg^0, trace amounts of Hg^{2+} species control the total deposition of Hg (Lindberg and Stratton, 1998).

2.2.3.2 Hg in soil

Speciation of Hg in soil is controlled by redox conditions, pH and content of various ligands, mainly OH^-, Cl^-, S^{2-} and organic anions (Steinnes, 2013b).

Several species of Hg occur in soil media, but the most abundant redox states found in soil are Hg^0 and Hg^{2+}. Hg^{2+} is rarely found in its free aqueous form in soil due to its ability to form stable complexes with OM, such as humic material, and sulphur species. A study from Tiveden area in southern Sweden showed that 75-80% of annually deposited mercury was retained in soil due to the high content of OM in the area (Lindqvist et al., 1991), which indicate that the element, in addition to the Arctic, accumulates is OM rich soils.

The studied soil has pH above 6, which according to Figure 2-1 indicated that pH is not a governing physicochemical property for Hg in the studied soil. The dominant mechanism of sorption is complex formation with soil OM rather than ion exchange (Schuster, 1991).

2.2.3.3 Toxicity

Hg has no use in biological systems, and all forms of the element are toxic to humans, although some forms of mercury are of more concern than others. This includes methylmercury (CH_3Hg^+ or simply MeHg) and Hg vapour (Hg^0). Exposure to $Hg^0(g)$ is of concern as an occupational hazard for workers in environments where Hg is used, for e.g. silver mining, where it was mined and refined or where urban mining of precious metals is conducted (UNEP, 2002).

For the general public MeHg is of great concern due to exposure through diet, especially through seafood diet. For some populations rice may be a major pathway for MeHg exposure (Zhang et al., 2010). Hg is converted to MeHg in a process called mercury methylation illustrated in Figure 2-3. Inorganic Hg is most likely methylated as a by-product by sulphate-

reducing bacteria in slightly anoxic environment (Compeau and Bartha, 1985, Gilmour et al., 2011). MeHg is readily assimilated by plankton and thus enter the food chain. The Hg binds with thiol groups in proteins and is therefore found in the muscular tissue in organisms (Landis et al., 2018). Once the compound is in the food chain, it thus biomagnifies with each trophic level making the concentrations higher in top predators. The compound bioaccumulates in an organism over time, and concentration is at more elevated levels in older more long-lived organisms than in younger and short-lived organisms.

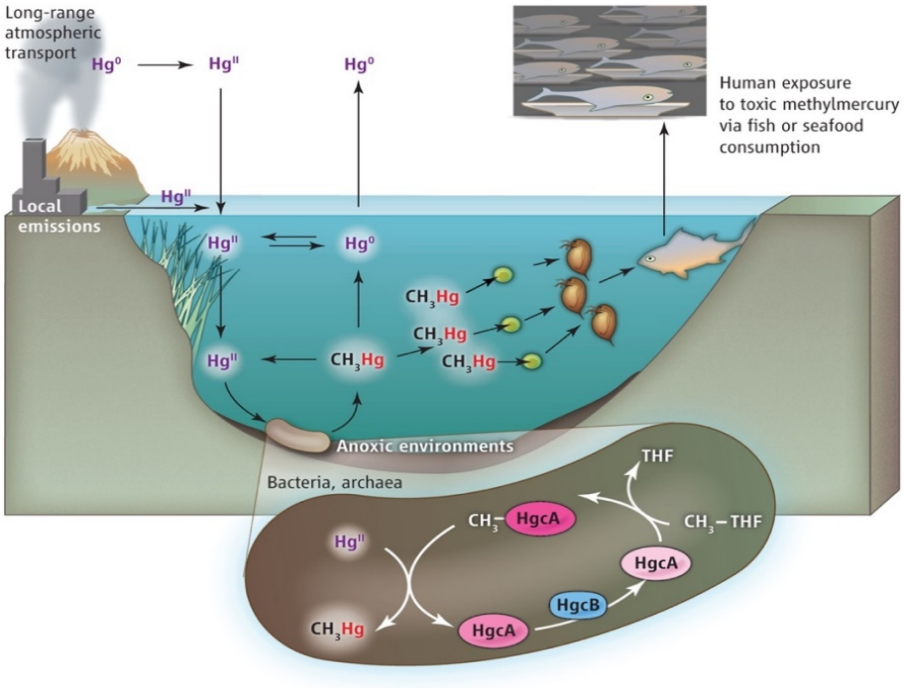

Figure 2-3: Methylation process, reproduced from Poulain and Barkay (2013).

Once a person is exposed to MeHg through their diet, 90-95% of the compound is absorbed in the gastrointestinal tract (Landis et al., 2018). The toxin passes the placental barrier and blood-brain barrier easily. MeHg function as an enzyme inhibitor and causes disintegration of cells. MeHg exposure is affecting the central nervous system (CNS) of the exposed with main consequences including paresthesia, loss of coordination, and damaged visual coordination (Fergusson, 1990). The compound's ability to cross the placental barrier have serious adverse effects of the embryo's developing brain. Infants who are born to mothers with high MeHg intake have shown symptoms of motor- and mental impairment (UNEP, 2002).

2.2.4 Cadmium - Applications, speciation and toxicity

The main sources of Cd in atmosphere include metallurgical processes, combustion of fossil fuel and incineration of Cd containing consumer products (e.g. EEE and plastics) (Landis et al., 2018).

Cd has undergone numerous phase out processes from pigment, PVC stabilizer and plating, but remains a popular component in EEEs, e.g. in Ni-Cd batteries. Even though these batteries somewhat have been replaced by lithium ion batteries, they are still commonly used in less expensive EEEs (Tolcin, 2020).

Cd is commonly associated with Zn ores where it is present in a 1:200 ratio resulting in Zn mining being a pollution source of Cd (Smolders and Mertens, 2013). Elevated concentrations of the element in the environment has additionally reported to originate from the use of phosphate fertilizers (UNEP, 2010a).

2.2.4.1 Cadmium in Soil

Cd a borderline metal that can form complexes with most ligands, though main adsorbent in soil are OM, oxyhydroxides and clay. The element binds to surface oxygens in carboxylic or phenolic groups on humic matter and to hydroxyl groups of hydroxides (Smolders and Mertens, 2013). Similar to many heavy metals, the sorption is low at low pH as illustrated in Figure 2-1 were hardly any Cd is sorbed at pH 5 and 100% sorbed at pH 7.

2.2.4.2 Cadmium in atmosphere

Due to low volatility, the element only exists in the atmosphere adsorbed to aerosols which is advected with the wind, the element has a lower lifetime in the atmosphere than Hg and some POPs, however due to the large air masses covered by the atmospheric transport Cd has been found at higher levels than natural background in pristine environments such as Greenland, Antarctica and Andes (UNEP, 2010a).

2.2.4.3 Toxicity

The general exposure routes of Cd to the public is through diet. Where the element is available for uptake in plants (i.e. at low pH), exposure through diet often occur due to ingestion of plants that has accumulated the element, as reported being the case for the *itai itai* disease where highly Cd contaminated rice was ingested by farmers (Landis et al., 2018).

The metal has a relatively long biological half-life of 10-25 years and can thus bioaccumulate over time in the human body (Landis et al., 2018). Once in the blood, Cd inhibits enzymes by binding to thiol groups or by competing with and displacing Zn for the enzyme where Zn is a cofactor. It is indicated that osteoporosis is the main consequence of Cd exposure through food (Jaerup et al., 1998).

2.2.5 Lead – Applications, speciation and toxicity

Pb has numerous utilities for humans and has been in use since ancient times (Nriagu, 1983). In early 1900s, alkyl Pb was added to gasoline as an anti-knock additive but has been phased out by many countries due to the toxic nature of Pb. Use of leaded gas for the general public was banned in the majority of African countries in 2006, but high concentrations of Pb found in the environment of many sub-Saharan African countries are still attributed to the late phase out of leaded gasoline in the region as well as the rapid industrialization these nations experiences (Echegoyen et al., 2014, World Health Organization. Regional Office for Africa, 2015) .

Additional anthropogenic releases of the element include combustion of coal, metal smelters and products that contain Pb such as batteries, paint, solders, glass, rubber, plastic and insecticides. Pb has also been used in EEEs in Cathode ray tubes, tin-lead solder and in printed circuit boards (Herat, 2008). Tin-lead solders have been phased out and replaced with lead-free solder (The European Parliament and the Council of the European Union, 2011), though some of the e-waste generated today might contain Pb if the EEEs were produced before any phase out took effect.

2.2.5.1 Lead in soil

As Pb^{2+} is a type B metal it has high affinity to OM which, similar to Hg, causes the element to accumulate in organic rich soils.

As observed on Figure 2-1 the increase in Pb sorption occurs from pH 3 (~0% sorbed) to 5.5 (100% sorbed). For the soil studied in this thesis the pH was higher than 5.5 in all samples indicating that the levels of Pb is not governed by any variation in pH.

Transportation in soil of the element in edaphic and aquatic environment is therefore usually as Pb- organic complexes to dissolved humic substances (Steinnes, 2013a).

2.2.5.2 Lead in atmosphere

Pb is released to the atmosphere in particle form through high-temperature processes such as combustion of coal, smelting of Pb ore and from the legacy of exhaustion from automobiles that used leaded gasoline (Steinnes, 2013a). Pb absorbed to fine particles are prone to long-range atmospheric transport. The element has a relatively short residence time (days-weeks) in the atmosphere, and transport is therefore often over regional distances, but Pb has also been found to be prone to intercontinental transport due to reports of elevated levels in pristine environments (UNEP, 2010b).

2.2.5.3 Toxicity

Once in the blood system, the element interacts with thiol groups, and inhibit enzymes that depend on the thiol-group (Landis et al., 2018). The systemic toxin causes adverse effects in many aspects of the body in the neurological, cardiovascular, gastrointestinal, renal and hematological systems (UNEP, 2010b).

The element can also pass the placental barrier, affecting infants born to mothers who have been exposed to high levels of Pb. Moreover, the element affects the CNS, in which children are at most risk of suffering the consequences of exposure due to their developing brain. The effects in children manifests as development impairment such as poor speech and language, motor skills and coordination skills (Landis et al., 2018).

3 Materials and methods

The following chapter contains procedures for collection of samples and the procedure conducted to determine physiochemical properties and heavy metal concentrations. The chapter also describes quality assurance and quality control procedures (QA/QC) for the different analysis.

The computer programs used for data processing are described in the last sub-chapter.

3.1 Sample collection

Sampling was done in the Dar es Salaam Region of Tanzania in February 2019. The following subchapters describes the sampling area and procedures for collecting samples. A map over Tanzania and the sampling areas around and in Dar es Salaam is illustrated in Figure 3-1.

3.1.1 Sampling area and strategy

The tropical savanna climate in the study area is hot and humid. There are few seasonal fluctuations, except for heavy rainfall from March - May due to the intertropical convergence zone near the equator where the northern and southern trade winds meet resulting in intense rainfall over short periods of time. The average rainfall in Dar es Salaam is 619mm/y, in which 275mm of this precipitate between March – May (Metoblue, 2020).
The soil samples were collected at the end of the summer during dry season.

The levels of heavy metals in the Dar es Salaam region were expected to show urban to rural trends, i.e. heavy metals with anthropogenic origin would have higher levels in the city than in rural locations. It was expected that the heavy metals would to some extent be transported by advection with the wind masses. Hg will in its elemental form (Hg^0) have a large potential to be vaporized from soil due to low carbon content in the soil and the high temperatures (average temperature in the area is 21-30C° (Metoblue, 2020)). Less volatile elements are advected via eolian dust particles by the wind. To assess the potential for transportation out of the city with the wind, samples were collected both upwind and downwind, through urban, suburban and rural areas, relative to the prevailing wind direction.

Figure 3-2 illustrates the general wind direction and speed in the form of a wind rose (modelled, data from Julius Nyerere airport weather station) (Metoblue, 2020). The wind rose indicates that wind blows for the most part from southeast and south-southeast towards northwest and north-northwest. Due to these wind patterns, samples were collected along a transect from a SE rural area, following the general wind direction to suburban and urban areas of Dar es Salaam, and through suburban to rural areas 60 km (NW) of the city.

The rural, suburban and urban locations are indicated by green, red and blue markers respectively, at the bottom right map of Figure 3-1. A selection of visual description of the urban (Figure 3-3 and 3-4), suburban (NW suburban location in Figure 3-5 and SE suburban location in 3-6) and rural locations (NW rural location in Figure 3-7 and SE rural location in Figure 3-8) are given. A visual representation of the remaining location is given in Appendix A.2.

Additional sampling was carried out along a small transect west of the city through the major city waste dump-site (Figure 3-9), the Kimyamwezi landfill, and an officially registered e-waste recycling site (Figure 3-10). This was conducted in order to observe potential differences in heavy metal contamination and transportation patterns around the landfill and/or e-waste handling as these sites are potential hotspots for heavy metals. This transect is indicated by black markers in at the bottom right of Figure 3-1. Visual presentation of the remaining sample sites are found in Appendix A.2.

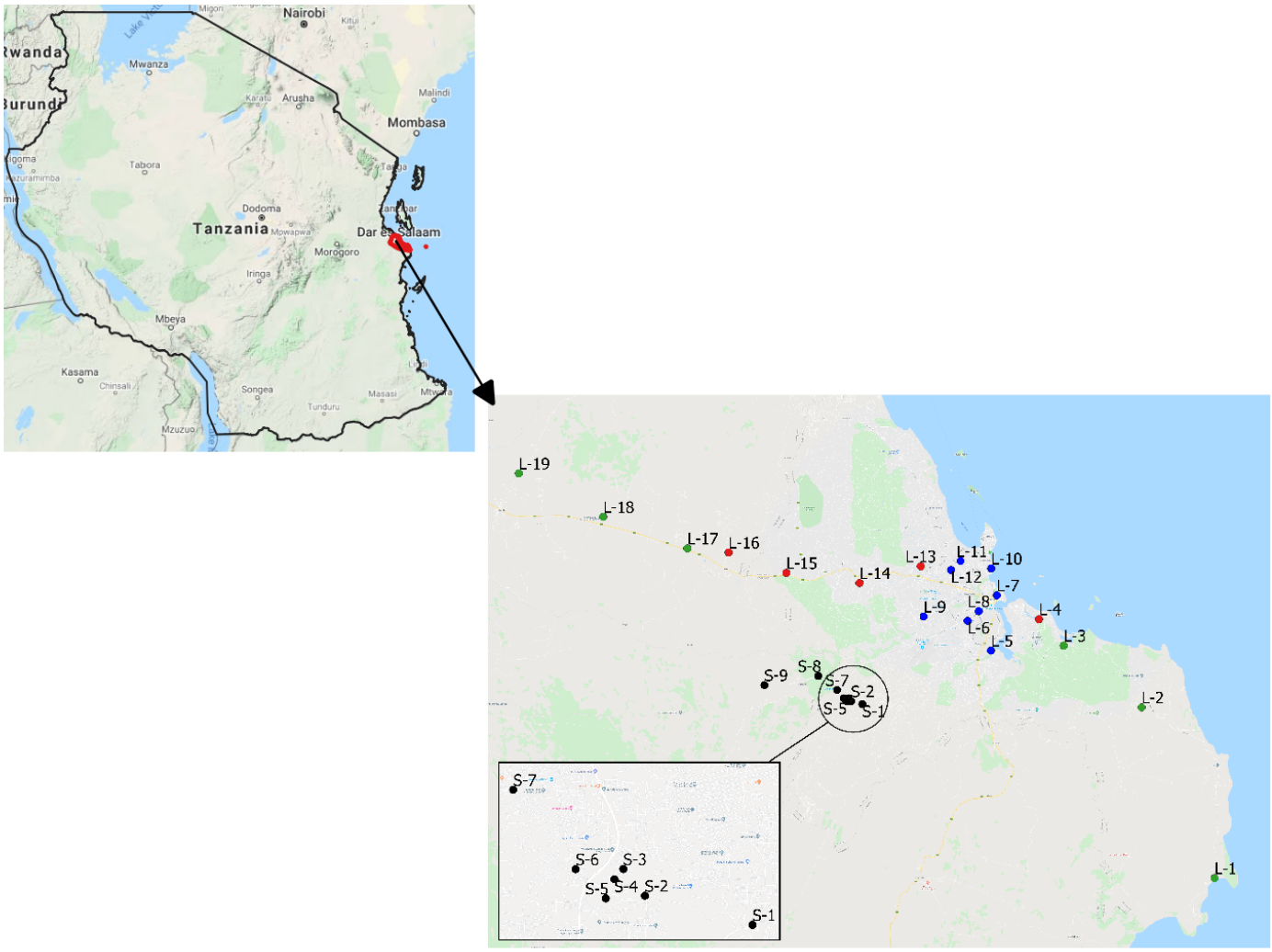

Figure 3-1: Map over Tanzania (top left) where the Dar es Salaam region is indicated by red outline. Sample locations in and around Dar es Salaam (bottom right). Maps made with QGIS 3.4.10 GPS coordinates are found in Appendix A.1

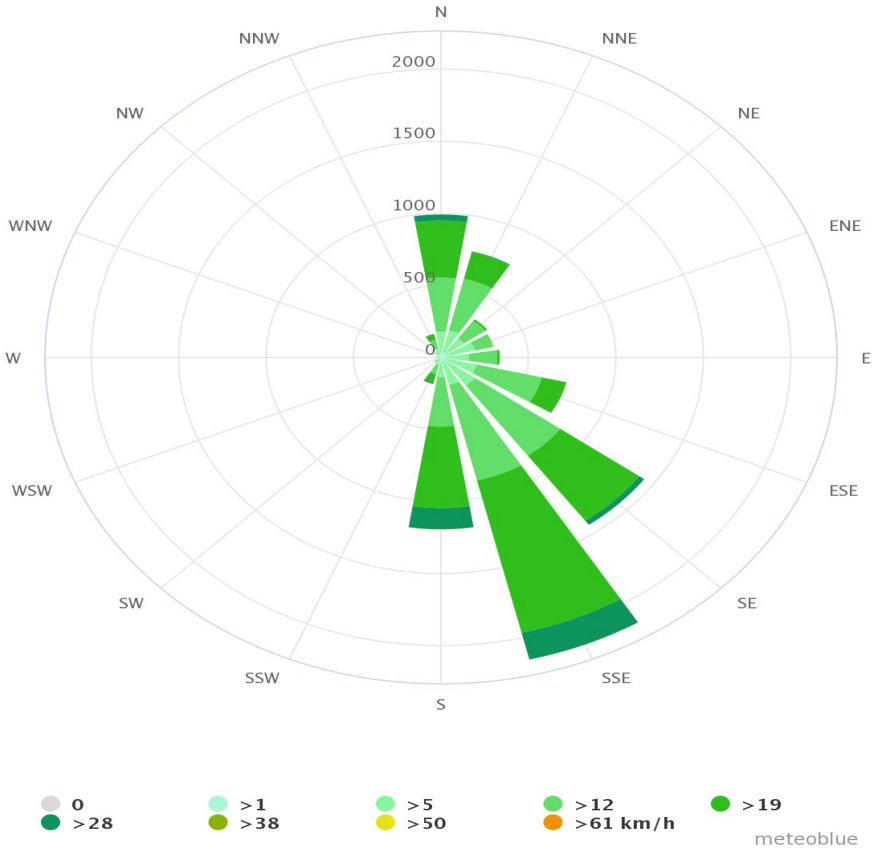

Figure 3-2: Modelled Wind rose of wind patterns in Dar es Salaam. The circles indicates hours/year. Downloaded from Metoblue (2020)

Figure 3-3: L-6, urban location close to an e-waste recycler plant.

Figure 3-4: L-8, Urban sampling location in Kariakoo which was defined as the city center of Dar es Salaam.

Figure 3-5: L-13, Suburban location, NW of the city.

Figure 3-6: L-4, Suburban location, SE of the city.

Figure 3-7: L-19, NW rural location.

Figure 3-8: L-1, SE rural location.

Figure 3-9: S-2, sampling location near the waste dump, e-waste transect. Photo: Rolf Vogt.

Figure 3-10: S-4, sampling location inside the e-waste recycler plant, e-waste transect. No trees were located at the property, soil was therefore collected in a minitransect diagonally through the property.

Soil sampling in strongly anthropogenically disturbed regions is challenging, as the land-use history of the soils at each site may be very different. The goal was to collect all samples from a similar local environment as possible, in order to promote comparability between locations, and be able to relate the differences in heavy metals concentration to regional trends. Especially, collecting soil that had been anthropogenically moved or dumped or dumped at the particular location was avoided. The soils were thus collected at locations were the soil most likely had been in place for the last 40 years, which is the period in which there has been significant anthropogenic input of heavy metals and POPs.

Additionally, the canopy of these trees function as air cleaner, absorbing compounds (dust with heavy metals and elemental Hg) from the air, which are washed out into the soil when it rains. The heavy metals associated with the dust, as well as Hg, will thereby accumulate in the soil underneath these trees rendering them as local hot-spots of metal contamination. Fallen leaves of the trees are also incorporated in the soil, contributing to the metal content as well as increasing the OM content.

3.1.2 Sampling and storage procedure

Soil samples were collected using a handheld corer (Figure 3-11) that collected the top 5-10 cm of soil profile. At each site, soil was collected from three spots that were mixed to a pooled sample, making up a total mass of approximately 500 g.

A total of 28 samples were collected.

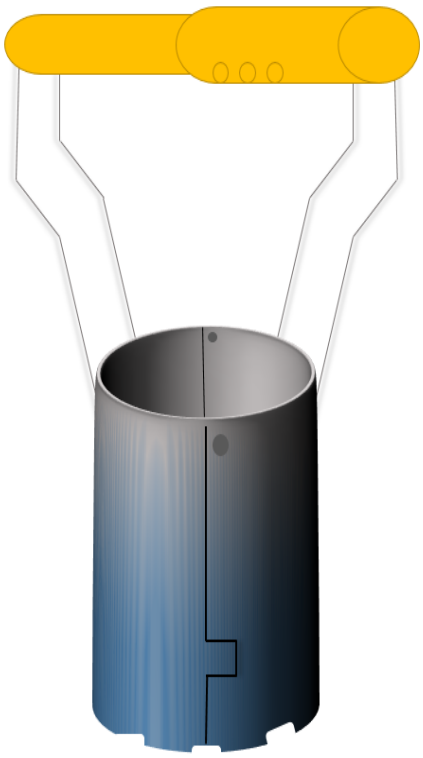

Figure 3-11: Sketch of handheld corer used to collect the top 5-10 cm of soil-profile.

3.1.2.1 Transport and storage of samples

Soil samples were wrapped in minimum two layers of alumina foil, placed in a zip lock bag and kept in a cooling bag. The samples were placed in a freezer at -18℃ after a maximum of 12hr. Transportation of samples from Dar es Salaam to Oslo was carried out in cooling bags for approximately 20hr until arrival at University of Oslo, where they were placed in a freezer at -18℃ until sample pretreatment.

3.2 Pretreatment

Soil samples were pretreated by drying and sieving following the method of ISO11464 – Air Drying (International Organizastion for Standardization, 2006). Drying was conducted by placing soil on pre-weighed paper plates, the soil and paper plate was weighed, and placed for drying on the lab bench at ambient temperature (21 ℃) under a paper plate for cover.

Depending on the moisture content of the soil, the samples were dried from 2 days up to 1 week until a stable weight was achieved (no more than 5% loss per 24 hour). The air-dried

samples were then sifted through a 2mm sieve allowing larger aggregates to be crushed carefully between gloved fingers. Both the mass of the soil passing the 2mm and the particles retained on this sieve size registered and stored.

Further analysis was conducted using the air-dried soil that had passed through the 2 mm sieve, as the particles smaller than 2mm constitute per definition the soil (Fergusson, 1990). The sifting also promoted homogenizing of the sample.

The soil samples were stored in cardboard boxes at room temperature and stirred thoroughly before taking out sub-samples for analysis.

3.3 Physicochemical properties of the soil

The following chapter describes the methods used for determining the physicochemical properties pH, hygroscopic humidity, OM content and CEC of the soil.

3.3.1 Determination of pH

The pH of the soil is a key parameter when discussing sorption of heavy metals to soil particles.

Determination of pH was conducted with type 1 water as the suspension agent according to ISO10390-Determination of pH in a soil/water ratio of 1:5 (International Organizastion for Standardization, 1994a). Two sample replicates were measured from each soil sample.

3.3.2 Determination of hygroscopic humidity

Soil is hygroscopic and absorbs water from the air making its weight higher and thus giving poor accuracy in analytical procedures if not accounted for. The heavy metal concentrations and OM are therefore corrected for hygroscopic humidity (w_{H_2O}) of the sample.

Determination of the hygroscopic humidity was done according to ISO11465 – Determination of Dry Matter and Water Content on a Mass Basis (International Organizastion for Standardization, 1993).

The relative amount of water in the air-dried samples were calculated gravimetrically based on loss of weight according to Equation 3-1 after drying at 110℃.
Three sample replicates were measured.

$$w_{H_2O} = \frac{m_1 - m_2}{m_2 - m_0} \cdot 100 \qquad \textit{Equation 3-1}$$

Where,

$$w_{H_2O} = water\ content(\%)$$
$$m_0 = the\ mass\ of\ empty\ container\ with\ lid(g)$$
$$m_1 = mass\ of\ air\ dried\ soil\ sample\ including\ container\ with\ lid(g)$$
$$m_2 = mass\ of\ oven\ dried\ sample\ including\ container\ with\ lid(g)$$

3.3.3 **Determination of organic matter content**

OM content is a physicochemical property of the soil that affect levels of heavy metals as Type B and borderline metals mainly form complexes with OM in the soil (VanLoon and Duffy, 2011).

The determination of OM content was based on Krogstad´s gravimetric method that determines the loss on ignition (LOI) after incineration at 550℃ for 4 hours (Krogstad, 1992).

The determination of OM can be calculated following Equation 3-2.

Three sample replicates were measured.

$$\%LOI = 100 - \frac{m_5 - m_3}{m_4} \cdot 100 - w_{H_2O} \qquad \textit{Equation 3-2}$$

Where,

$$\%LOI = loss\ on\ ignition(\%)$$
$$m_3 = weight\ of\ crucible(g)$$
$$m_4 = weight\ of\ air\ dried\ soil\ placed\ in\ crucible\ before\ combustion(g)$$
$$m_5 = weight\ of\ combusted\ soil\ and\ crucible(g)$$
$$w_{H_2O} = water\ content(\%), determined\ by\ Equation\ 3\text{-}1$$

Due to water bound in the clay fractions of the soil, the OM was corrected for content of clay.

3.3.4 **Determination of Cation Exchange Capacity**

The CEC of a soil affects its ability to hold Type A metals. The CEC is also a measure of the soils reactivity, where a high CEC reflects a high number of functional groups on the soil that can bind heavy metals.

Determination of effective CEC was conducted according to ISO11260 –using Barium Chloride Solution (International Organizastion for Standardization, 1994b), but Magnesium (Mg) measured with ICP-MS not flame emission spectrometry.

Due to the relative high pH values of all the samples (>6), one can assume that all the exchangeable sites on the soil particles are occupied by base cations (i.e. 100% base saturation) and it was thus decided to not measure the concentration of exchangeable cations.

The soil in type 1 water was added a surplus of $BaCl_2$ (0.1 M) which resulted in Barium (Ba^{2+}) exchanging for all the cations on the soil cation exchanger. Adding a known amount of excess $MgSO_4$ to the soil mixture after treatment with $BaCl_2$ caused the precipitation of Ba^{2+} as the highly insoluble $BaSO_4$ and Mg^{2+} replace Ba^{2+} on the exchanger. By determining the excess of Mg in solution with ICP-MS (see section 3.5.3 for ICP-MS operation), the CEC of the soil was determined by following Equation 4-4 and 4-5.

To assess the concentration of Mg^{2+} in solution, the concentration was corrected for liquid retained by the centrifuged soil after equilibration with 0.0025M $BaCl_2$ solution. This was done following Equation 3-3.

$$C_2 = \frac{C_1(30 + m_2 - m_1)}{30} \qquad \textit{Equation 3-3}$$

Where,

$$C_2 = \text{The } corrected\ Magnesium\ concentration\ in\ sample\left(\frac{mmoles}{L}\right)$$

$$C_1 = \text{The } Magnesium\ concentration\ in\ sample\left(\frac{mmoles}{L}\right)$$

$$m_1 = Mass\ of\ \text{the } centrifuge\ tube\ with\ air-dried\ soil(g)$$

$$m_2 = Mass\ of\ centrifuge\ with\ wet\ soil(g)$$

The CEC of the sample were then be determined by Equation 3-4.

$$CEC = \frac{(C_{b1} - C_2)}{m} * 3000 \qquad \textit{Equation 3-4}$$

Where,

$$CEC = Cation\ Exchange\ Capacity\ (cmol\ +/kg)$$

$$C_2 = The\ corrected\ Magnesium\ concentration\ in\ sample\left(\frac{mmol}{L}\right)$$

$$C_{b1} = Magnesium\ concentration\ in\ blank\ sample\left(\frac{mmol}{L}\right)$$

$$m = mass\ of\ air\ dried\ soil\ sample(g)$$

The concentration of Mg^{2+} in the blank sample was set as the concentration of Mg^{2+} added to the soil. Subtracting this concentration with the concentration found in soil solution gave the concentration that was exchanged, and thus the CEC.

Three sample replicates were measured.

3.3.5 Determination of soil texture by feel

A simplified assessment of soil texture was done by following the method of Thien (1979), which has been adapted by Ritchey et al. (2015). The flow chart of the method can be found in Appendix B.5.

The method is based on the brittleness, coherency and feel of the soil, which are governed by the soils texture given by its composition of sand, loam and clay. Based on the soil type, the proportion of clay was roughly estimated from a soil texture triangle as illustrated in Figure 3-12.

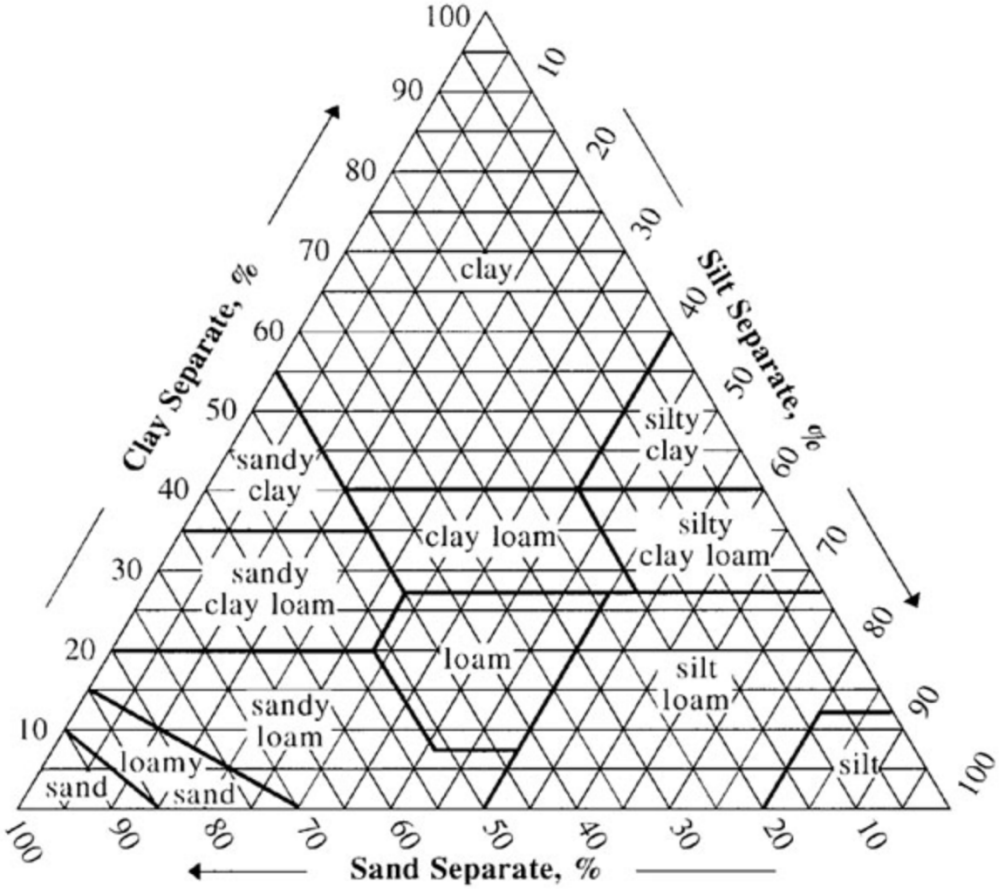

Figure 3-12: Soil texture triangle used for estimating the clay content of soils. reproduced from (USDA:Natural Resources Conservation Service Soils, 2020)

3.4 Determination of total Mercury content using DMA-80

The Hg content of the soil samples was determined using a Direct Mercury Analyzer (DMA-80) (Milestone, Sorisole, Italy) according to the application note HG/SC-10 for Calcareous soil (Application note in Appendix E.1).

3.4.1 **Analysis**

DMA-80 is an instrument that analyzes for total Hg content in solid samples with minimal sample preparation, except air drying of the sample.

The analysis is based on the principles of thermal decomposition, vaporization of Hg^0, amalgamation and atomic absorbance at 253.65nm for determining the levels of Hg (Milestone, 2018a). The instrumental scheme is shown in Figure 3-13.

50 mg of air-dried soil was weighed in a sample boat and placed on the autosampler. The sample was first dried at 200 °C and further combusted at 650 °C in an oxygen flow. Hg was oxidized to Hg^{2+} and Hg^{+} during the combustion process. The combustion products were carried to a catalyst furnace where the oxidation process was completed and Hg species reduced to Hg^{0} (Milestone, 2018b).
Hg vapors in the flue gas from the incinerator was selectively trapped in gold by amalgamation. It was subsequently separated from the gold by heating of the amalgamator, resulting in release of Hg vapor. The amount of Hg in the vapors was quantified based on atomic absorbance.

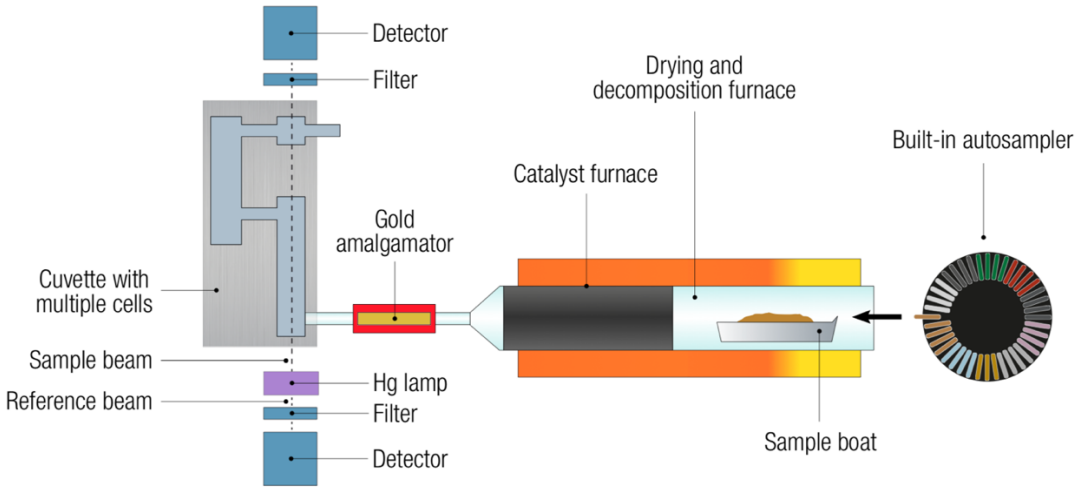

Figure 3-13: Instrumental sketch of DMA-80. reproduced from Thomas, Robert(2019)

The vapor in the DMA-80 cuvette is struck by light at 253.65nm. How much of the light is absorbed is proportional to the concentration of Hg in the sample (Vandecasteele, 1993) .

The output result of the DMA-80 is the total amount of Hg found in the sample boat. Calculation of the concentration in soil was done using Equation 3-5.

One sample replicate was measured.

$$C = {}^{m_{Hg}}/_{m_{sample}} \qquad \textit{Equation 3-5}$$

Where,

$$C = concentration\ in\ soil\left(\frac{mg}{kg}\right)$$

$$m_{Hg} = mass\ of\ \ Hg\ in\ dry\ soil\ sample\ (mg), corrected\ for\ \%H_2O$$

$$m_{sample} = mass\ of\ dry\ soil\ (kg)$$

3.5 Determination of heavy metal levels using ICP-MS

For the analysis of heavy metal content, soil samples needed to be in the aqueous phase. Microwave assisted digestion was used to the dissolve the soil samples for this purpose. Aqueous samples from the digestion were analyzed using inductively coupled plasma – mass spectrometry (ICP-MS).

3.5.1 Decomposing soil samples for ICP-MS analysis

Microwave assisted digestion technique utilizes microwaves that are absorbed by molecules with a dipole moment, such as water. This kinetic energy gives rise to rotational movement of the molecules, causing the temperature in the solution to increase following the rise in kinetic energy of the molecules (Bye, 2009).

As heavy metals bound inside silicate crystal lattice in soils are not available for human exposure and are most likely not a result of anthropogenic activities, it was determined that there was no need to dissolve the silicate minerals in the soil. Hydrofluoric acid for total decomposition was therefore not used, as a result of this the samples required filtration after digestion.

Microwave Ethos 1 (Milestone, Sorisole, Italy) was used for the decomposition of soil samples following the application note; “Sea sediment, Milestone application for Acid Digestion” (application note is found in Appendix E.1). 0.250 g of air-dried soil was digested in mixture of HNO_3 and H_2O_2 (9:1 ratio) in sample vessels made of Polytetrafluoreten. These vessels do not absorb the emitted microwaves allowing the microwaves to reach the sample directly, heating the sample solution quickly (Bye, 2009). The digestion process was performed in a closed system which prevented loss of volatile analytes and reagents.

The sample digest was filtered through a 0.45μm pore sized filter (Cellulose acetate filter, VWR collection) and stored in polypropylene tubes at 4°C. Prior to analysis, the aqueous sample was diluted 20 times based on recommendation to not run dissolved solid samples

with a higher percentage than 0.2% w/v on the ICP-MS in order to prevent clogging of the interface (U.S Environmental Protection Agency, 1994).

Blank samples were prepared by adding the same reagents to empty vessels as to the soil samples, and the resulting digest treated the same way as the soil samples.

The microwave program and details on reagents added are provided in Appendix E.2. Three sample replicates were prepared.

3.5.2 Calibration of the ICP-MS instrument

5 multi-element calibration solutions containing varying concentrations of 11 elements were made by diluting standard reference solutions. For As, Cu, Zn, Cu, Pb, Cr and Ni, the concentrations ranged from 0 to 200$\mu g/L$ and for Cd and Se the concentration ranged from 0 to 20 $\mu g/L$. The calibration solutions all contain 3.5% HNO_3 of suprapur grade, to match the acid concentration in the diluted digested samples. The calibration blank contains only 3.5% HNO_3. The instrument was calibrated prior to analysis and if the plasma had been shut off. The calibration approximation equation and correlation coefficient are found in Table F 3 in Appendix F.3.

3.5.3 Analysis

Quantification of heavy metals in the aqueous soil samples was conducted using the ICP-MS Nexion 300d (PerkinElmer Inc., Shelton, CT). A simple sketch of an ICP-MS instrument is shown in Figure 3-14.

A peristaltic pump introduced the sample solution to the nebulizer where it was converted to an aerosol. The instrument is equipped with a cyclonic spray chamber which separated the big droplets out of the sample aerosol. Through an injector, the aerosol was carried to the argon plasma which generated ions.
Via the interface (three metal cones) and the ion optics (quadrupole ion deflector) of the instrument, the ions were directed to the quadrupole which is the mass separation device. The quadrupole allows ions of certain mass/charge ratio to reach the detector which recorded the number of electronic signals per seconds (Thomas, 2013).

The ICP-MS measures a specific isotope of an element. The selection of which isotope to measure was based on minimal interference and abundance of the isotope. A common interference in ICP-MS is isobaric interferences originating from the argon plasma (U.S Environmental Protection Agency, 1994) . Isobaric polyatomic interferences are formed in the plasma and have the same mass/charge ratio as certain isotopes of the analyte. These interferences can be avoided by choosing other isotopes of the element However, choosing an isotope of lower abundance decreases the sensitivity of the analysis. The selected isotopes are given in Table F 2 in Appendix F.2.

It is generally recommended (but not required) to add internal standard (IS) to the samples, blanks and calibration solutions to correct for matrix differences in the samples and calibrations solutions. Many of the recommended elements used as IS are components in EEE and can thus be present in some of the soil samples, especially in samples from the e-waste sites. It was thus decided not to add IS.
A reference sample was instead analyzed to validate the accuracy of the method for digestion and quantification (See section 3.6.2).

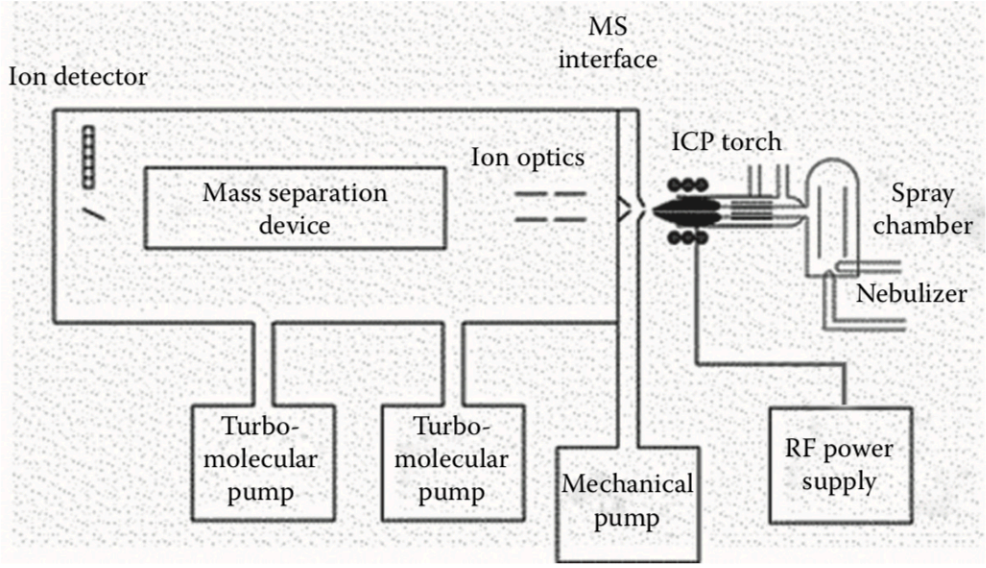

Figure 3-14: An instrumental sketch of an ICP-MS reproduced from Thomas (2013)

The concentrations of heavy metals in the soil samples were calculated using Equation 3-6. The concentration of the extracts was multiplied by the dilution factor.

$$C_{sample} = \frac{C_{extract} \cdot V_{extract}}{m_{sample}}$$ *Equation 3-6*

Where,

$$C_{sample} = \frac{mg}{kg\ dry\ soil}$$

$$C_{extract} = concentration\ in\ extract(\frac{mg}{L})$$

$$V_{extract} = Volume\ of\ extract(L)$$

$$m_{sample} = Mass\ of\ dry\ soil\ sample(kg), corrected\ for\ \%H_2O$$

3.6 QA/QC

3.6.1 Cleaning procedures

To minimize contamination of samples from the equipment, care was taken to thoroughly clean all glassware, sample boats, and digestion vessels.

3.6.1.1 Glassware and nickel boats

Glassware used for heavy metal determination was added 5% suprapur nitric acid and left over-night. The glassware was rinsed three times with Type 1 water before use.
Glassware used for CEC determination were washed in a Mielabor G7983 Multitronic laboraty dish washer.
Nickel boats used for Mercury determination were rinsed with Type II water and combusted at 550 ℃ prior to use.

3.6.1.2 Microwave digestion vessels

In between each microwave digestion run, the equipment was thoroughly cleaned to remove traces of soil. This was done by rinsing all parts in contact with sample with Type 1 water. Exterior equipment surrounding the sample vessels, such as lids and bombs, were rinsed with tap water. The vessels were further cleaned using a microwave program. Parameters of the program and reagents used for cleaning can be found in Table E 3 and Table E 4 in Appendix E.3. In between runs the sample vessels were stored in between runs in clean plastic boxes to prevent contamination from dust.

3.6.2 Reference material and method validation

When assessing analytical data, it is necessary to be aware of the precision and accuracy. In this study the focus has been on precision as it is the relative amounts of the metals that are studied when assessing the cause of spatial trends. The accuracy is relevant when addressing the absolute amounts and relating them to limit values as well as literature data. As the digestion method conducted in this study did not result in a total dissolution, the levels were compared to soil that had been treated either by aqua regia (Manta et al., 2002), HNO_3/H_2O_2 (Guo et al., 2012) or by a combination of HNO_3, H_2O_2 and HCl (Akortia et al., 2017).

A reference sample was used to validate the accuracy of the analytical methods used for determining the levels of heavy metals with ICP-MS, and for Hg levels with DMA-80. The chosen reference sample for this study was BCR-142 "Sandy soil". The sample was chosen due to its similar matrix with the sampled soil and because a reference concentration for a semi-total digestion of the material was available, as the samples in this study was not totally dissolved after decomposition.

The certificate of analysis can be found in Appendix D.5.

The recovery of the elements in the reference material was calculated following Equation 3-7. A recovery of 90-110% of the reference value was accepted.

$$Recovery = \frac{C}{C_{certified}} * 100 \qquad \textit{Equation 3-7}$$

Where,

$$Recovery = Recovery\ of\ analyte(\%)$$
$$C = measured\ concentration\ in\ reference\ sample(\frac{mg}{kg})$$
$$C_{certified} Certified\ concentration\ in\ reference\ sample\left(\frac{mg}{kg}\right)$$

Figure 3-15 illustrates the recovery (%) of various metals for the reference material (BCR142). The recoveries of Pb, Zn and Hg are within the accepted limits ($\pm$ 10%). It is worth noting that the recovery of Ni was not satisfactory with an average of only 65.4%. An explanation for this may be that Ni is passivated by concentrated nitric acid which leads to a poor recovery (Bye, 2009).

Although the accuracy of the element recovery is poor, the element was still included in the study due to its acceptable precision.

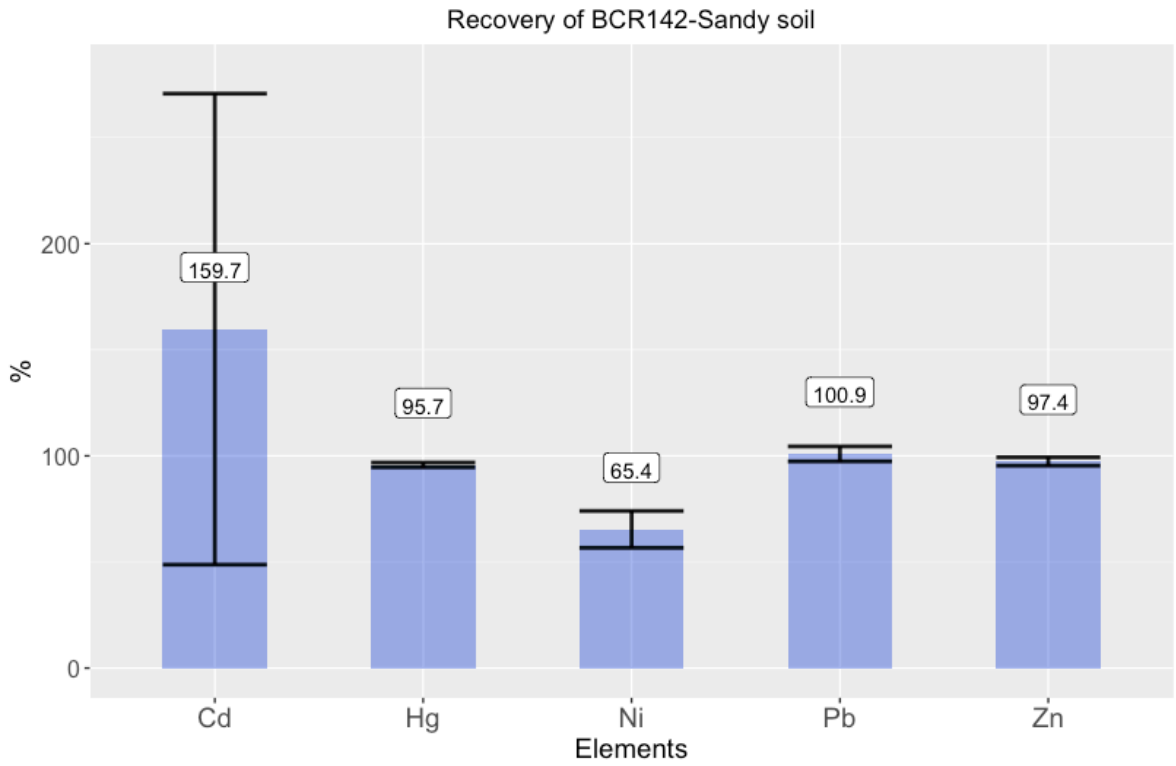

Figure 3-15: Recovery of reference material, BCR142

The recovery of Cd initially had poor accuracy (Figure 3-15). A contamination of Cd from the vessels in the microwave was the suspected cause for this as there was usually two sample replicates that had low concentrations and one replicate with high concentration among the three sample replicates. This was usually the case for one of the 10 vessels run in the microwave. A set of 10 blanks were therefore run in the microwave to check for Cd contamination of the vessels. One of the blanks had a significantly higher signal than the rest and was ruled an outlier by the Grubbs test (Table F 7 in Appendix F.7) supporting the suspicion of Cd contamination of one sample vessel. A Grubbs test was therefore conducted on all the Cd concentrations in which the outliers were omitted and a satisfactory recovery was obtained as illustrated in Figure 3-16. .

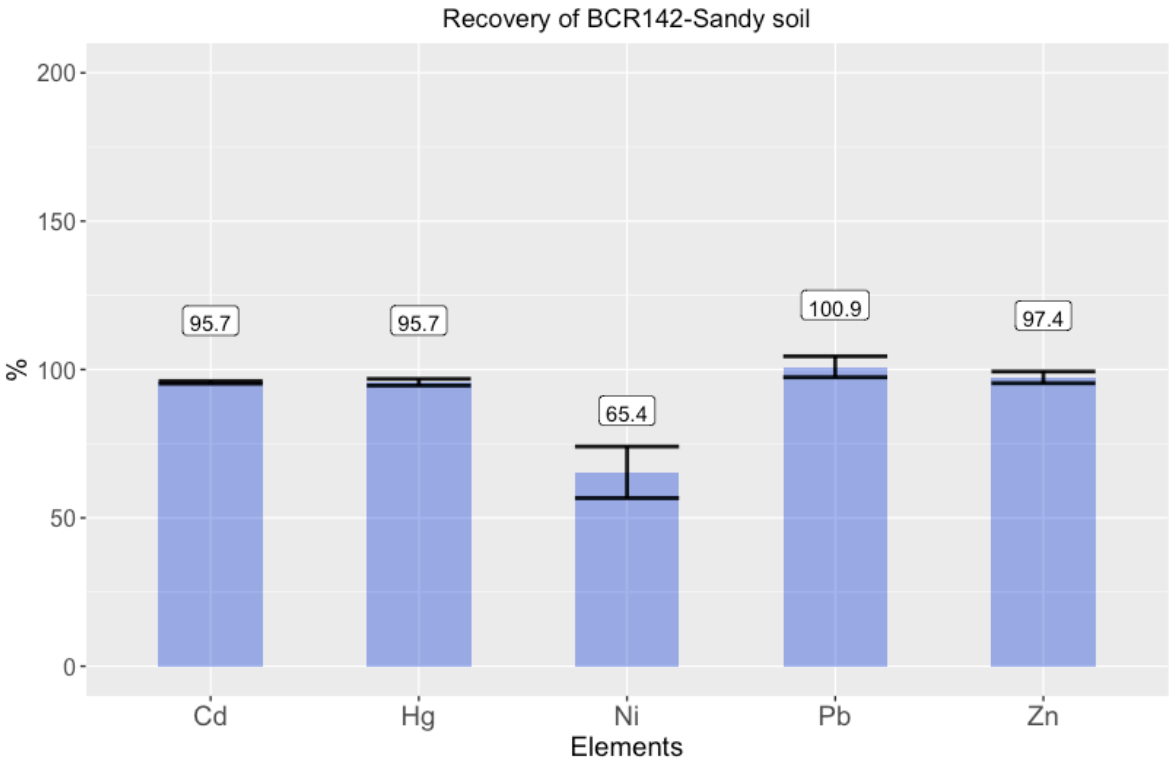

Figure 3-16: Recovery of reference material, BCR142, after conducting Grubbs test on Cd concentrations

3.6.3 **Method limit of detection**

Sample blanks were prepared to determine the method detection limit (MDL)

For heavy metal analysis using ICP-MS, the same reagents were added to the digestion vessel and the digest treated in the same manner as the sample digest.

For Hg analysis, empty sample boats were run as blank samples.

MDL is the lowest quantity of analyte that is statistically different from the calibration blank (U.S Environmental Protection Agency, 2016). It was defined as the average plus three times the standard deviation of the noise when analyzing blank samples.

The MDL was determined by analyzing 10 blank samples and calculated following Equation 3-8

$$MDL = \bar{X} + 3 * STD_b \qquad \textit{Equation 3-8}$$

Where,

$$MDL = Method\ detection\ limit\left(\frac{ug}{L}\right), (ng)$$

$$\bar{X} = Average\ concentration\ of\ blank\ samples\left(\frac{ug}{L}\right), (ng)$$

$$STD_b = Standard\ deviation\ of\ blank\ sample\ concentration\left(\frac{ug}{L}\right), (ng)$$

The MDL was converted to mg/kg soil following Equation 3-8 and Equation 3-9 for ICP-MS and DMA-80 respectively.

$$MDL_{mg/kg} = \frac{\frac{MDL * V_{extracts}}{m_{sample}}}{50} \qquad \textit{Equation 3-9}$$

Where,

$$MDL = method\ detection\ limit(\frac{\mu g}{L})$$

$$m_{sample} = mass\ of\ sample\ (25 * 10^{-5} kg)$$

$$V_{extracts} = Volume\ of\ sample\ digest(10^{-3} L)$$

$$MDL_{mg/kg} = \frac{MDL * 10^{-6}}{m_{sample}} \qquad \textit{Equation 3-10}$$

Where,

$$MDL = method\ detection\ limit(ng)$$

$$m_{sample} = mass\ of\ sample\ (5 * 10^{-5} kg)$$

Obtained $MDL_{mg/kg}$ can be found in Appendix F.6. for ICP-MS and in Appendix D.7 for DMA-80. Concentrations below MDL were included in the visualization of heavy metal concentrations as well as the statistical analysis.

3.6.4 Other

3.6.4.1 ICP-MS

To check for instrumental drifting that can cause the signal to change (e.g. lower intensities in same solution), a standard solution containing $2 \mu g/L$ of Cd and Se and 20 $\mu g/L$ of As, Pb,

Cu, Zn, Ni, Cr and Co was analyzed for every 20 samples run on the instrument during heavy metal analysis. A deviation in concentration of less than 10% was accepted.

For every time the plasma had been shut off for more than an hour, a performance test was conducted using a certified optimization solution containing reference concentrations of various elements. The performance test checked if the signal intensities from the optimization solution was above required signal intensity. The performance test was conducted to optimize the torch alignment, nebulizer gas flow, and ion optics to obtain a maximum signal intensity of the elements in the optimization solution.

For ICP-MS analysis of Mg for CEC determination the performance showed signal intensities below the required value for one or more elements in the optimizing solution, i.e. the performance test was not passed for Mg, but analysis was run. This results in an inaccurate analysis of the element.

For analysis of heavy metals, the performance test was passed.

3.6.4.2 DMA-80

The first two boats on the built-in autosampler of the DMA (Figure 3-13) did not contain any sample boats and the next three autosampler positions contained empty boats. The rest of the built in autosampler contained the soil samples and reference material. No boats were filled in the first two sample boats to clean the system for Hg traces. The system was considered clean if the last empty boat had a Hg content of <0.03 ng.
As the DMA-80 had a capacity of running 40 samples in total, only one sample series was run.

3.7 Data processing

3.7.1 Statistical analysis

Rstudio 1.1.463, Minitab 19, and Microsoft Excel 16.39 was used for statistical analysis of data obtained in the study. For the multivariate analysis, POPs data from the same soil samples were included (Nipen, 2020)

The POPs data can be used to differentiate between different types of pollution sources, as they have very distinct application areas. Dec syn and dec anti for examples are used in EEEs while the chlorinated paraffins are used in plastics and can thus represent general waste.

3.7.1.1 Principal component analysis

Principal component analysis (PCA) was performed to reduce the number of components in the dataset to a selection of principal components (PC) which explained maximum variation of the data. From a PCA plot one can observe patterns in metals and explanatory variables showing similarities or differences. A PCA plot in combination with sample scores (biplot) allowed for the illustration of trends for the different locations.

3.7.1.2 Dendrogram

A dendrogram was made using hierarchical clustering to observe grouping of heavy metals, physicochemical properties of the soils, POPs and distance to known sources with similar spatial patterns.

3.7.1.3 Wilcoxon Rank Sum test

To assess if the levels of heavy metals were significantly higher in the urban areas than the two rural transects, a Wilcox Rank Sum test was conducted. The Wilcoxon rank sum test is a non-parametric test on two independent groups, also known as Mann Whitney U Test.

4 Results and discussion

The spatial variation in concentrations of heavy metals are compared empirically to explanatory variables regarding the soils ability to hold heavy metals (pH, OM, CEC, clay content) and distance to known sources such as the city center (Kariakoo) and the waste dump in section 4.1. POPs data provided from the same soil samples (Nipen et.al., unpublished data) were included in the multivariate statistical analysis.

In chapter 4.2 the levels of heavy metals are presented and compared to the heavy metal concentrations found in natural background, urban and e-waste locations in other studies.

The physicochemical properties of the soil are described in chapter 4.3 in regard to the soils ability to bind metals to the levels of heavy metals

Based on the induced empirical relationships and our biogeochemical process understanding the main factors governing the levels of heavy metals in the tropical environment are deduced.

4.1 Multivariate analysis

To map the relationship between metals and their explanatory variables, dendrogram and PCA plots (Figure 4-1 and Figure 4-2) were made using the metal concentrations for all locations, including the explanatory parameters and POPs.

4.1.1 Dendrogram

The dendrogram in Figure 4-1 separates the metals and variables into different categories based on their inter-correlation. From the dendrogram it is assessed that the analyzed metals are arranged into 4 different clusters;

1. Pb, Cd
2. Zn, Cu
3. Ni, Cr, Co, As
4. Se
5. Hg

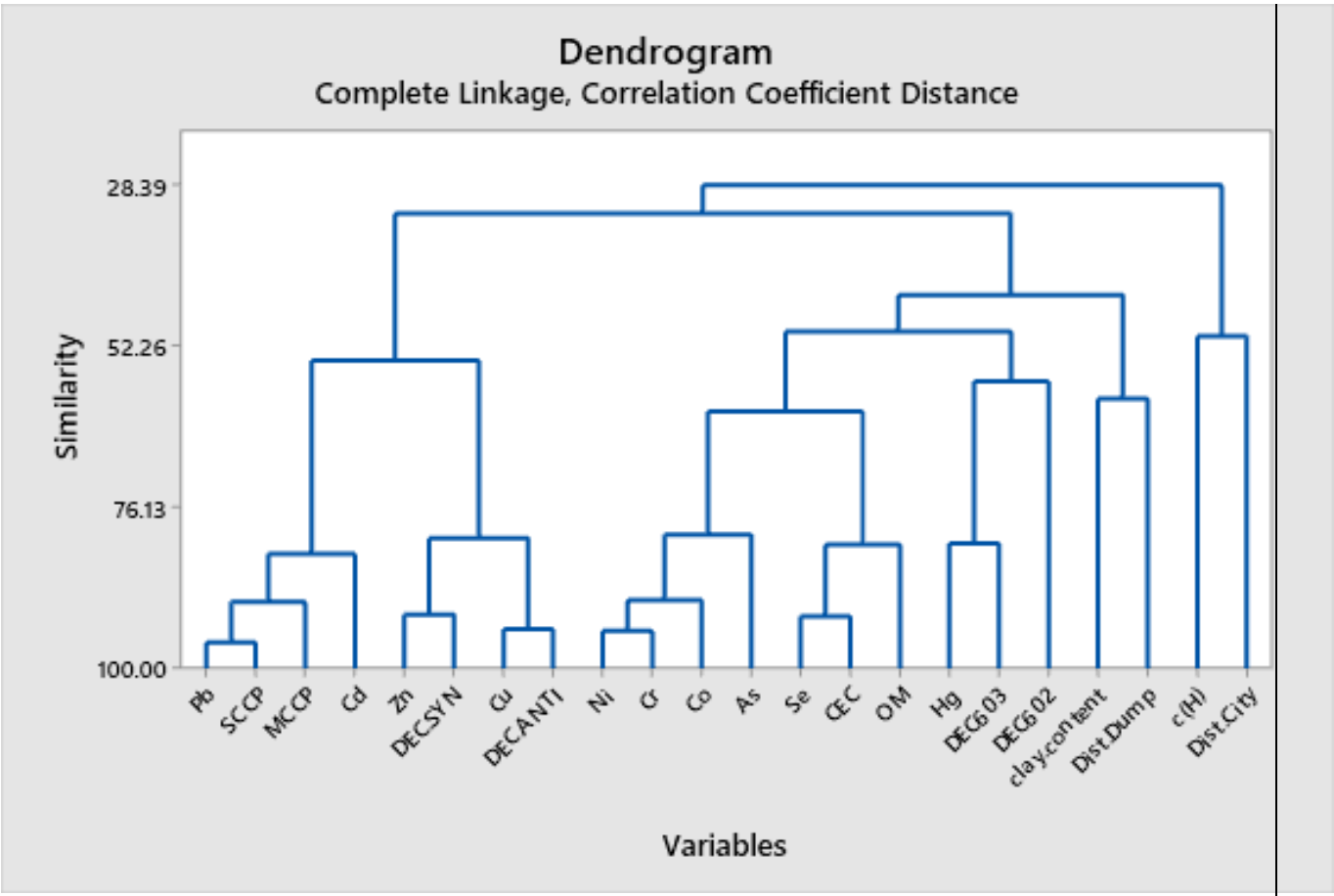

Figure 4-1: Dendrogram of all variables.

No distinct difference between these clusters in regard to ionic or covalent index was observed.

In cluster 1 Pb and Cd are strongly correlated with SCCP and MCCP. SCCP and MCCP are both frequently used as additives in plastics, which indicate that this cluster is related to general waste. Cluster 2 additionally includes Dechlorane syn and anti, the two isomers present in the flame retardant, Dechlorane Plus, which along with Cu and Zn are often used in EEE. This cluster therefore represent recycling of e-waste as pollution source of these compounds.

The metals in the 3rd cluster are correlated with each other but may also be extended to be correlated with Se, OM and CEC, where CEC reflects the reactivity of the soil.

Hg is in the 4th clustered, not correlating with other metals included in the study, or physicochemical properties. The measured concentration of Hg is low (Figure 4-14). It is indicated that the state of the climate in the region might be the reason for no correlation with physicochemical properties, such as low content of OM which minimizes the retention of Hg in soil and high temperatures which facilitates the re-emission of non-retained Hg to air. The pH of all the soil samples was in addition above 6.5 for all samples (Figure 4-15), indicating that the pH is a non-governing factor for Hg.

The dendrogram show indications that general waste pollution may be indicated by high levels of Pb, Cd, SCCP and MCCP, while e-waste may be indicated by high levels of Cu, Zn and dechlorane plus. The levels of As, Co, Cr, Ni and Se may be governed by physicochemical properties. This is further investigated in the PCA.

4.1.2 Principal Component Analysis

The PCA analysis gave a PC1 explaining 27.1 % of the variation in the data set and a PC2 explaining additional 23.9 % of the variation (Figure 4-2). PC1 is mainly governed by the distance to city, while PC2 is reflecting the physicochemical characteristics of the soil.

PC1: Distance to city

PC2: Physicochemical properties of the soil

The first two clusters (1 & 2 from Figure 4-1) have medium loadings opposite to PC2 and high loading along the positive PC1, while the third and fourth clusters of metals have strong loading along the positive PC1 and PC2 as illustrated in the PCA in Figure 4-2 . All metals are located opposite to the distance to city in the PCA, indicating decreasing concentration with increasing distance to city for all metals.

Metals in cluster 3 and 4 all have positive loading on PC2 along with a weak loading of distance to waste dump. The positive loading indicates increasing concentration with increasing distance from the waste dump, but to the very weak positive loading of distance to waste dump one may argue that the distance to the waste dump is not an explanatory factor for the spatial variation of the metals in this cluster. Thsese metals are also correlated with OM, CEC and clay content which can indicate that the physicochemical properties are governing factors for the spatial distribution of metals with high loading along the PC2.

Hg in cluster 5 has no loading along PC2 implying that it is not influenced by the physicochemical properties of the soil. Instead it has a significant loading along the PC1, implying that the distance to the city is the main factor explain its spatial distribution, rather than the physicochemical properties of the soil.

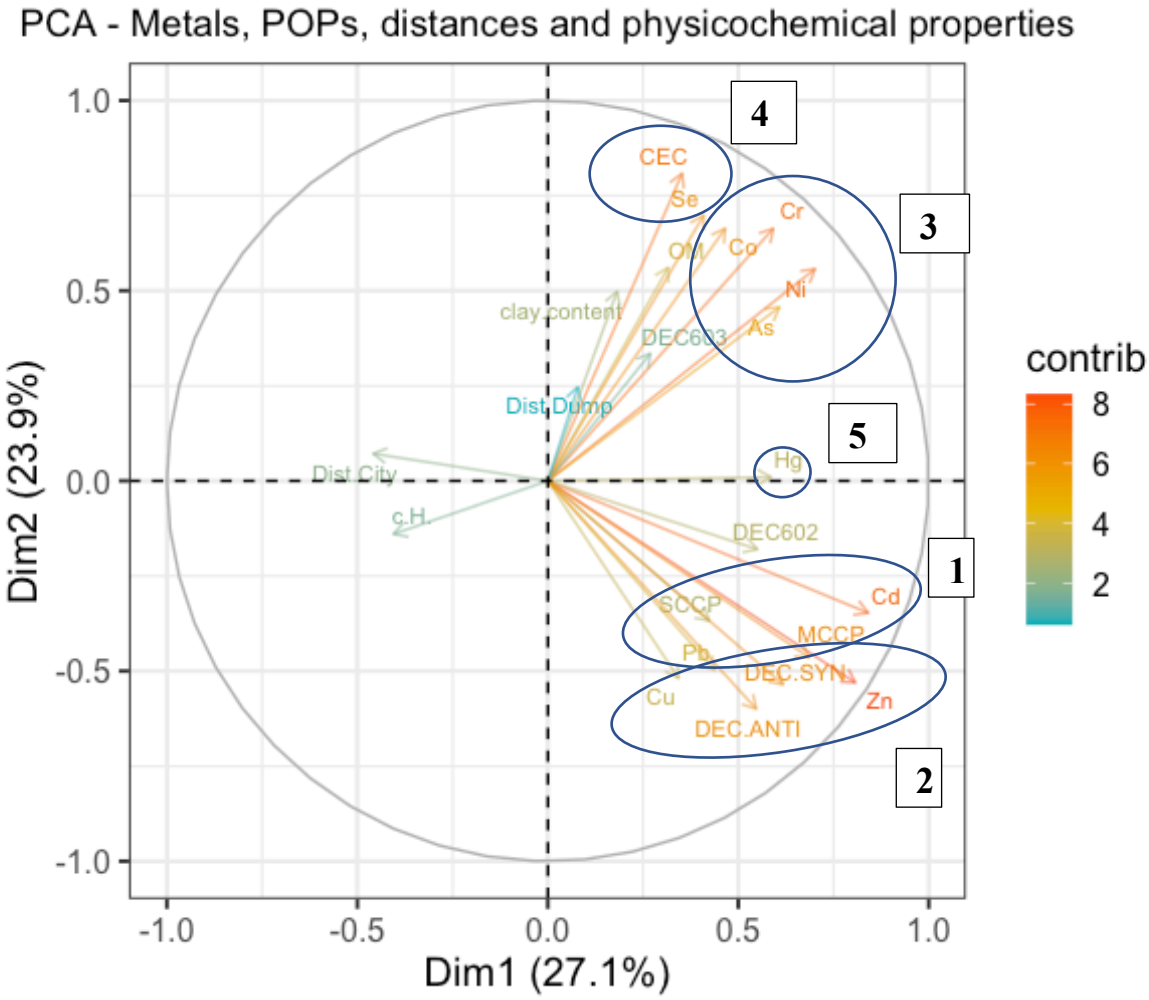

Figure 4-2: PCA of all variables

Sample scores on PC1 and PC2, illustrated in Figure 4-3, show that locations L-4, L-7, L-10, L-11 and L-13 are located positively on PC2 and have high levels of metals that also has positive loading along PC2 i.e., Se, Ni, As, Co and Cr. L-4, L-7, L-10 and L-11 has the highest concentrations of As and Ni in the whole dataset. The sites L-7, L-4 and L-11 have 17.5% clay content, which can explain why the samples have high value of these metals. The remaining two sites (L-10 and L-13) have 6.7 and 8.9 % OM respectively, which is of some of the higher OM contents in the studied soil (Figure 4-16) and L-13 additionally has one of the higher CEC (Figure 4-17).

The hotspot locations S-2, S-4 and L-6 are placed on the negative side of PC2. These are samples from the urban and suburban e-waste recycler plants (L-6 and S-4 respectively) as well as from the waste dump (S-2) implying strong local anthropogenic loading, which erases out the physicochemical properties affect towards the levels of heavy metals.

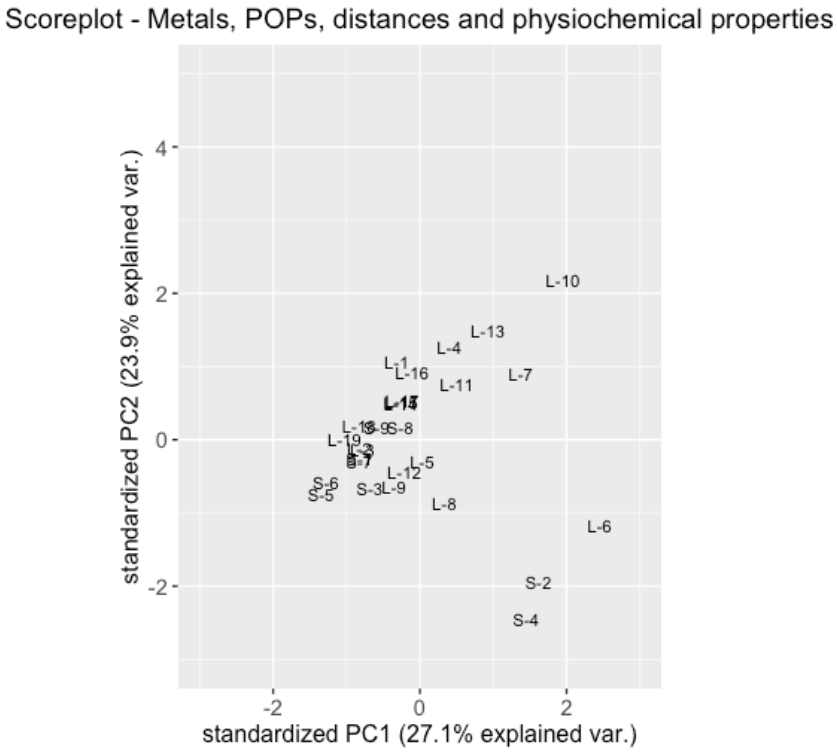

Figure 4-3: Sample scores on PC1 and PC2

Figure 4-4 shows the parameter loading along PC2 vs. PC3. PC3, explaining an additional 10.9% of the variation in the dataset, has a strong opposite loading of Pb, SCCP and MCCP on one side and Dec syn and Dec anti on the other.

PC3: Distinction between e-waste and general waste

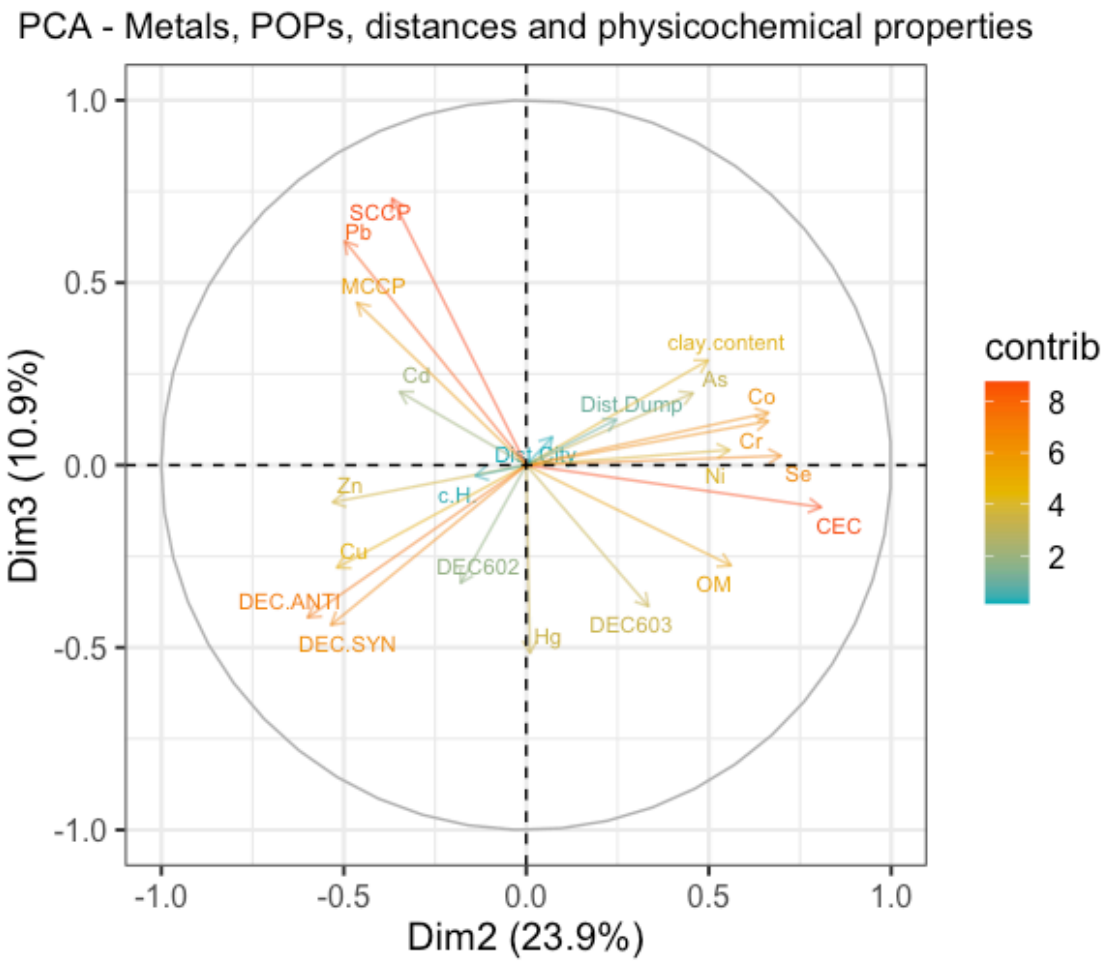

Figure 4-4: PC2 vs. PC3

The score plot in Figure 4-5 show strong loading of S-2 on PC3 which supports the idea of general waste pollution of Pb, SCCP and MCCP as the sample is from the site near the waste dump, though Cd has a weaker loading than expected from the dendrogram (Figure 4-1).

S-4 and L-6 both have a strong negative loading on along with the Cu, Dec syn and anti, which indicate e-waste pollution at these sites, though Zn had a weaker loading than expected from the dendrogram. These are the samples that were collected from inside of an e-waste recycler plant (S-4) and from an urban e-waste site (L-6).

L-13 and S-8 had the highest concentrations of Hg in the dataset (excluding hotspot locations) and some of the highest levels of OM in the dataset, which explains why the samples have a sample score close to Hg and positive on PC2. Hg levels are further discussed in section 4.2.5.

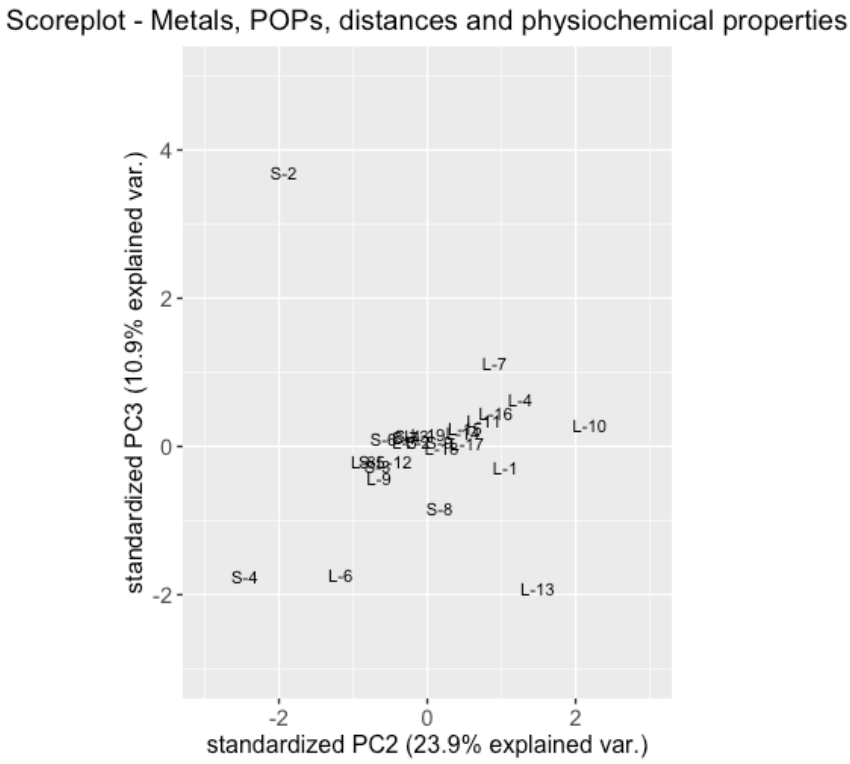

Figure 4-5: Scoreplot for samples on PC2 vs PC

Summing up, PC1 which represent the distance to city is the main governing factor concerning the levels of heavy metals in the region. Additionally, PC2 represent the physicochemical properties of the soil which governs the spatial trends of As, Co, Cr, Ni and Se. High levels of Hg were found in samples with high OM content, although this was not the case for all samples with high OM content.
In addition, PC3 allowed for the separation between general waste pollution and e-waste pollution. General waste is indicated by high levels of Pb, SCCP, MCCP and to some extent Cd. E-waste was indicated by high levels of Cu, Dec anti and syn.

4.1.3 **Rural and Urban trends**

A separate PCA plot of the rural-urban-rural transect was made to map potential spatial trends for assessing the effect of distance to the city.

The parameter loading and sample scores along PC1 and PC2, together explaining 58% of the variation in these data, are illustrated in Figure 4-6. The distance to the city has a positive loading on PC1, while all metals have opposite loading to the city. PC2 represents the physicochemical properties same as for the overall PCA (Figure 4-2). All the rural locations

(L-1, L-2, L-3, L-17, L-18, L-19) have positive scores on PC1, meaning low levels of heavy metals due to large distances from the city. L-4, L-7, L-10, L-11 and L-13 are correlating with the physicochemical properties, same as the overall PCA (Figure 4-2).

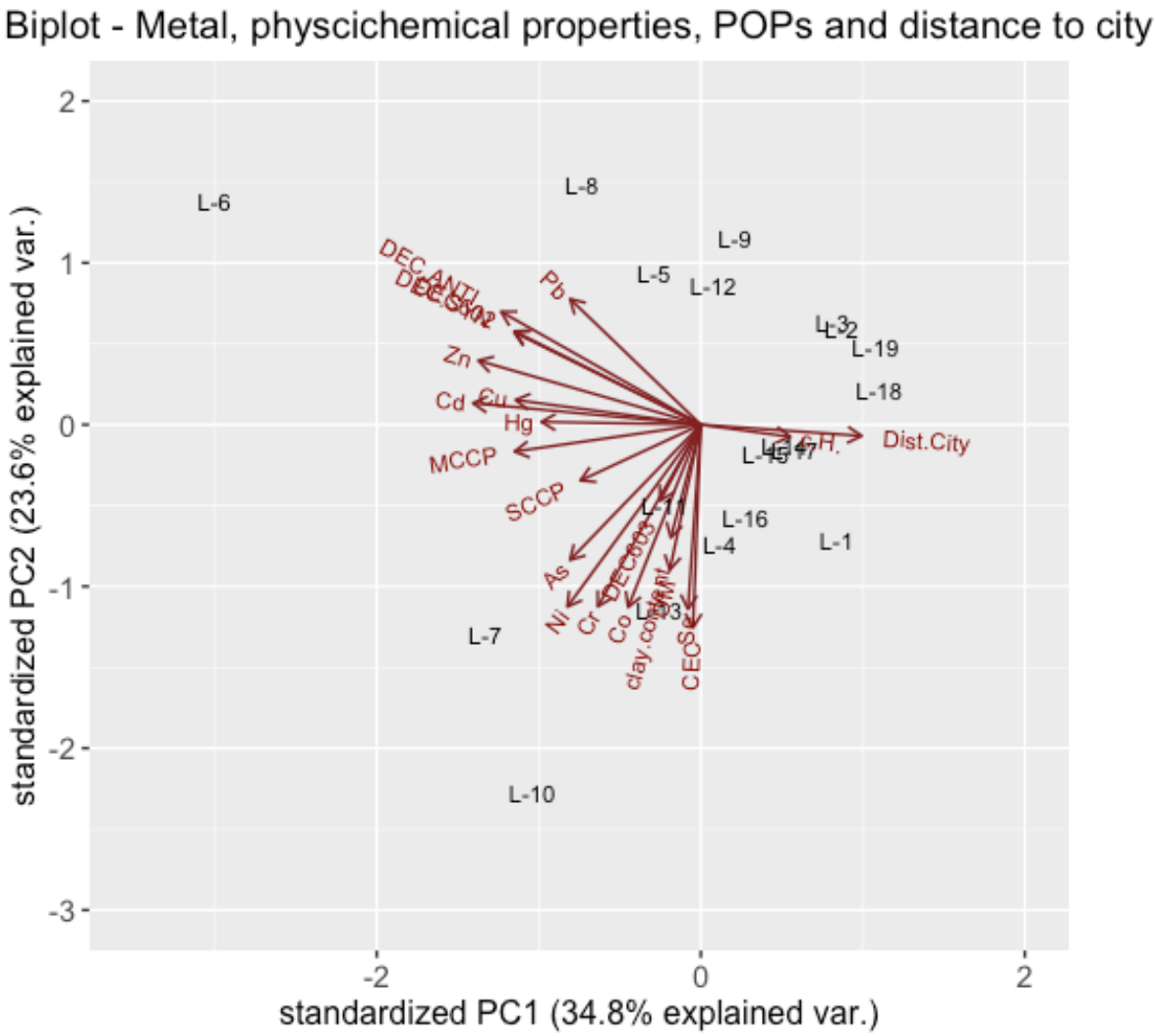

Figure 4-6:Biplot of scores for locations in urban, suburban and rural locations along with eigenvectors.

The PCA plot of PC1 and PC2 of the rural-urban-rural data show the same generals features as the corresponding PCA plot for all the data discussed above supporting the claim that the distance to city is the main governing factor concerning the spatial trends om heavy metals.

4.1.4 **Hotspot to background pattern**

A separate PCA plot of samples from the e-waste transect was made. A biplot of sample scores along with PC1 and PC2 are found in Figure 4-7. The biplot shows that the distance to the waste dump does not affect the levels of Zn, Cu, Pb, Ni, Cd and As.

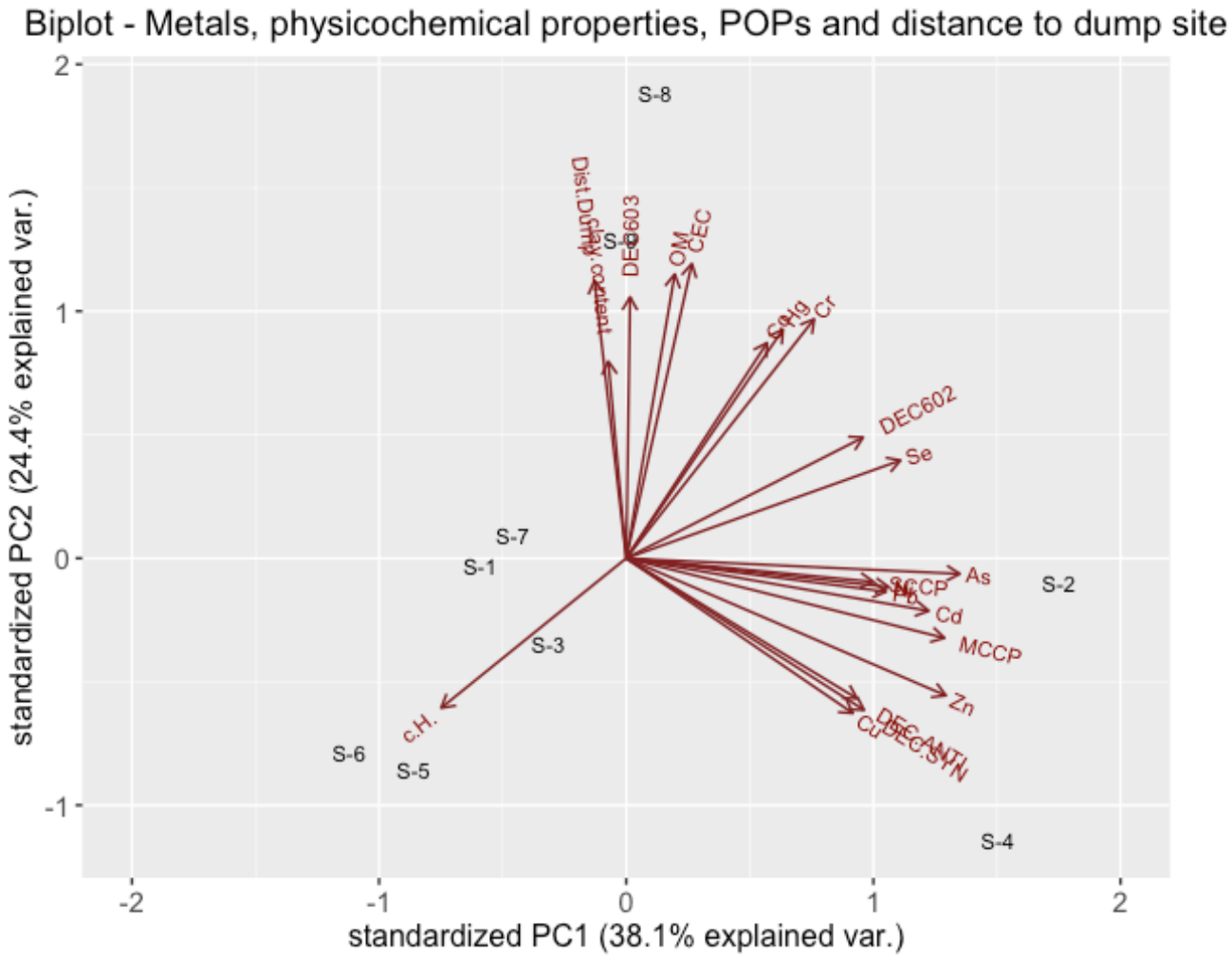

Figure 4-7: Biplot of samples and PC from E-waste transect

From Figure 4-7 It is observed that the levels of Co, Cr and Hg are determined by distance to waste dump, but the levels appear to increase with distance as it is positively correlated with distance to waste site in the biplot. It is thus concluded that the distance to the landfill is not an appropriate variable to explain the levels of Co, Cr, Se and Hg. This is also apparent from the overall all PCA (figure 4.1), indicating that the levels of these metals are not related to known sources in the e-waste transect. Co, Cr and Se are governed by physicochemical properties both in the rural-urban-rural transect as well as in the e-waste transect. S-8 had the highest levels of Hg in the transect, while S-9 had the highest levels of Co and Cr in the

transect. These locations are also the sites with the highest OM content and CEC supporting the fact that these elements are governed by the physicochemical properties of the soil.

Visualizing PC2 vs PC3 results in a separation of S-2 and S-4 (Figure 4-8). S-4 is strongly correlated with Cu and dec anti and syn, while S-2 is strongly correlating with SCCP and Pb supporting the fact that e-waste pollution is indicated by high levels of Cu and dechlorane Plus, while general waste pollution is indicated by high levels of Pb, Cd and CPs.

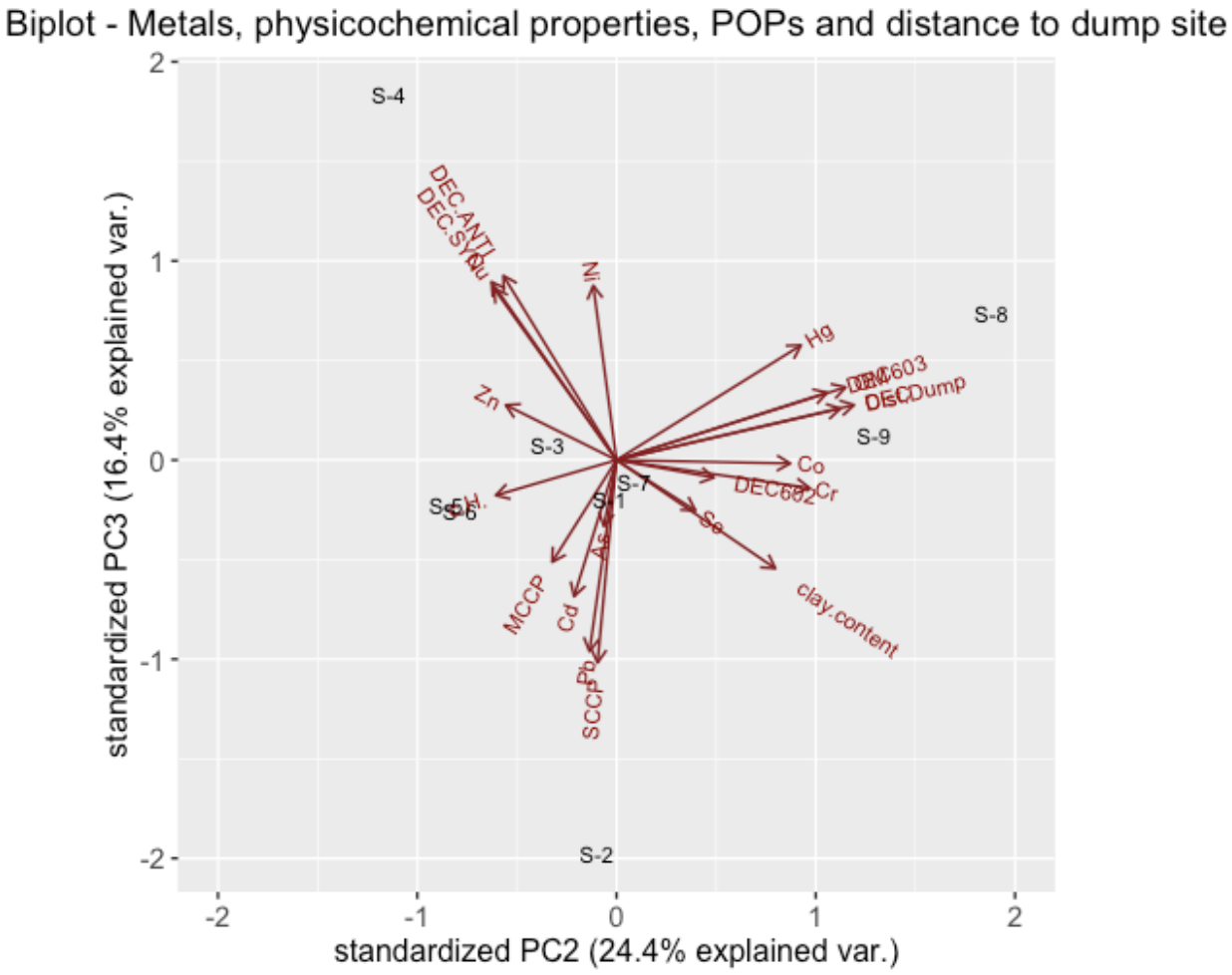

Figure 4-8: Biplot PC2 vs PC3 - e-waste transect

Summing up, Hg, Co and Cr are governed by the physicochemical properties of the soil in this transect. The inclusion of POPs supports the claim that high levels of Cu and dechlorane Plus are related to e-waste pollution, while high levels of Pb, Cd and CPs are related to general waste pollution.

4.2 Heavy metal concentrations

The total levels of measured heavy metals are shown in Figure 4-9.

Especially high levels of Cu, Zn and Pb were found at the main city garbage dump (S-2) and the suburban e-waste recycler (S-4). These heavy metals do not appear to be transported from the point of pollution as their levels are low at short distance from the sources. The emission at the hotspot locations may thus be released to water running rather than atmosphere which means that the contaminants are transported at a lower rate. A general observation made was also that the total levels appear to be higher in the urban areas than the rural transects which was also the conclusion for all the metals in the multivariate statistics.

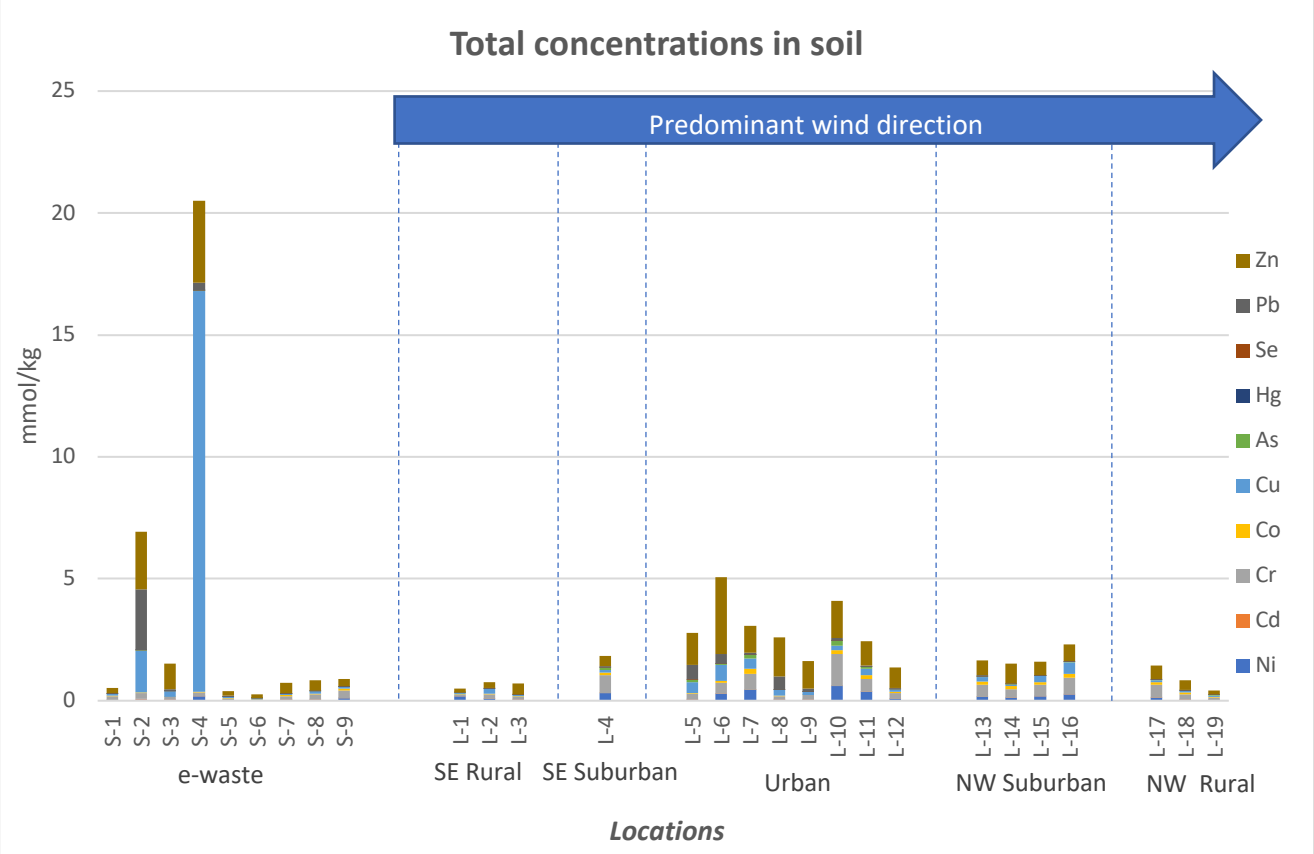

Figure 4-9: Total concentrations of heavy metals in mmol/kg in soil from different locations in and around Dar es Salaam, Tanzania.

The obtained levels of heavy metals were compared to the levels in other studies (Table 4-1) and the Tanzanian standards for agricultural soil (The National Environmental Standards Comittee of Tanzania Bureau of Standards, 2007). Cd, Co, Cr, Ni and Se did not exceed the acceptable limits and are discussed in section 4.2.6.

Table 4-1: Concentration (mg/kg) of heavy metals found in this study and different environments from literature.

	This study (Dar es Salaam city)	This study (Rural, SE and NW) (mg/kg)	This study (E-waste transect)	Natural background	Urban soil (Southwest China)	Urban soil (Italy)	Soils from E-waste site (Ghana)
Pb (mg/kg)	8-114	1-7	1-516	17	20-224	57-2516	207
Cu (mg/kg)	7-42	3-12	2-1045	2-50	19-163	10-34	222
Zn (mg/kg)	54-207	<MDL-37	<MDL-220	10-100	36-362	52-433	35
As (mg/kg)	0.6-15	0.4-2	<MDL-2	0.1-55	6-15	-	-
Hg (mg/kg)	0.01-0.1	0.007-0.06	0.007-0.03	0.05	-	0.04-56	-
Cd (mg/kg)	<MDL-0.3	<MDL-0.06	<MDL-0.4	0.1-1	-	0.27-4	0.53
Ni (mg/kg)	3-35	2-10	0.6-11	80	-	7-40	8
Cr (mg/kg)	6-68	4-28	2-18	100	-	12-100	3
Co (mg/kg)	0.9-12	0.7-6	0.2-4	25	-	2-15	3
Se (mg/kg)	<MDL-0.1	<MDL-0.9	<MDL-0.3	0.01-2	-	-	-
Reference	This study			Alloway (2013a)	Guo et al. (2012)	Manta et al. (2002)	Akortia et al. (2017)

4.2.1 **Lead**

A large range of Pb concentrations (1-516mg/kg) was found in the studied soil samples. Figure 4-10 show thus the log transformed concentrations of Pb in soil. Some soils had Pb concentrations that were even lower than 17mg/kg, which is the global average in uncontaminated soils (Table 4-1). Low concentrations were also found in all the rural samples, in addition to some soil samples from the urban area (L-5, L-8 and L-11) and the e-waste transect (all but S-2 and S-4 had concentrations below 17mg/kg). The highest level of Pb (516 mg/kg) was found in soil near the garbage dump (S-2). This was the only location where the accepted content of Pb for agricultural soils was exceeded. Elevated levels of Pb were as expected also found in some urban locations (L-5, L-6 and L-8) since elevated levels of Pb is commonly found in strongly anthropogenically influenced environments. Urban concentrations of Pb varies a great deal globally, though the Pb levels found in urban areas of Dar es Salaam are low compared to studies from China and Italy (Manta et al., 2002, Guo et al., 2012). L-6 is located in the city of Dar es Salaam and therefore experiencing pollution due to urban activities as well as e-waste related activities.

However, the Pb levels at both e-waste recyclers (S-4 and L-6) were lower than values found at the Agbogbloshie e-waste area in Ghana were informal e-waste recycling is occurring (Table 4-1).

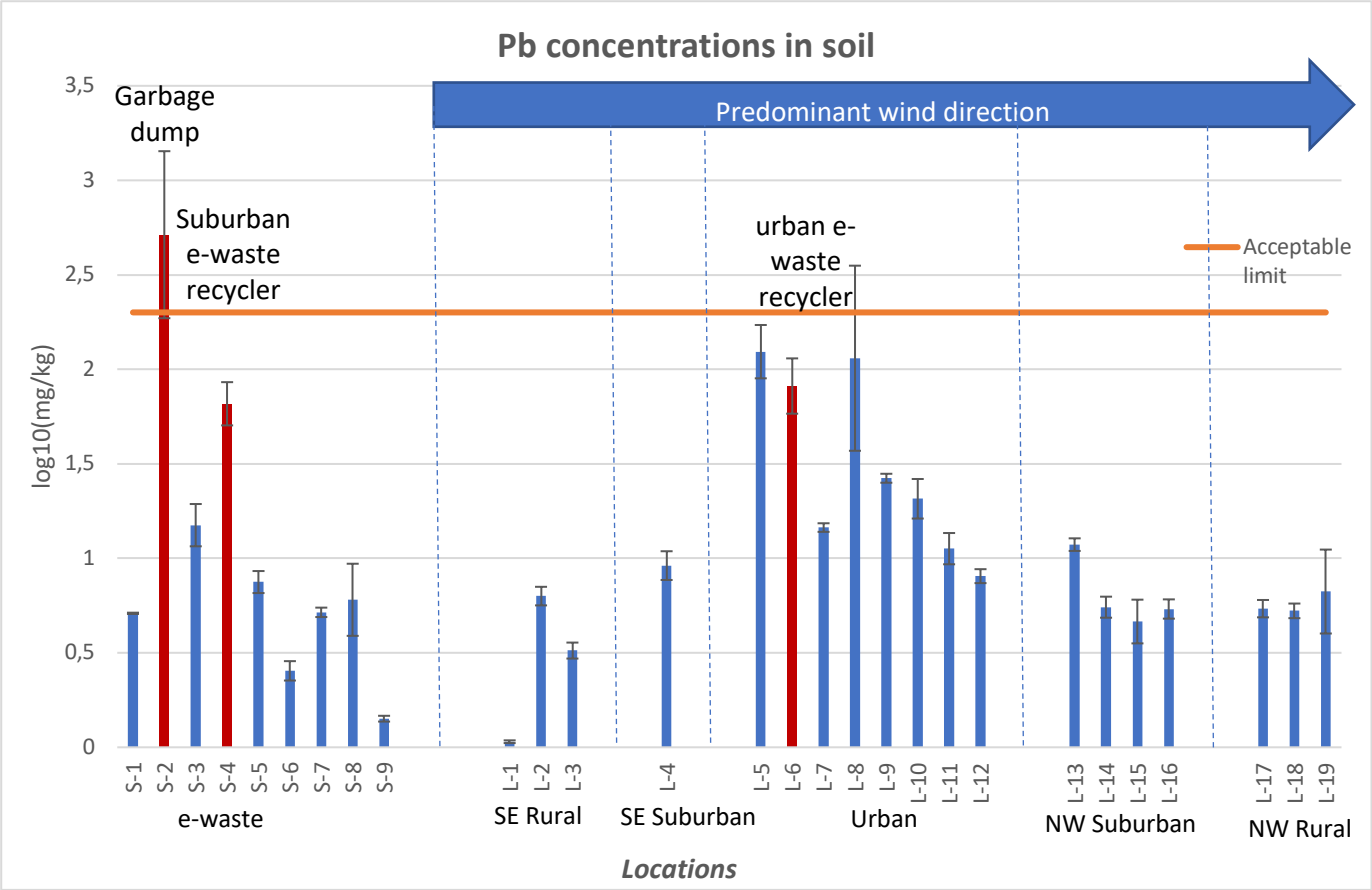

Figure 4-10: Pb concentrations in soils in and around Dar es Salaam, Tanzania. Data are log transformed.

The lowest Pb concentration (1 mg/kg) was found at a rural site 44km SE of Dar es Salaam (L-1). This was the starting point of the urban-rural transect going from the SE to the NW of Dar es Salaam. This transects follows the predominant wind direction, placing this site upwind of all local pollution sources and only downwind to the Indian Ocean. According to the Wilcoxon rank sum test, the urban locations contain significantly higher concentrations of Pb than both the SE rural and NW rural transects.

Summing up, Pb contamination was especially high at the waste site, though close to background levels within short distance from the source. Elevated Pb levels are also found in the urban environment and at e-waste sites.

4.2.2 **Copper**

Levels of Cu found in soils around Dar es Salaam are shown in Figure 4-11. The data is log transformed to observe potential patterns in the concentration distribution. The sample collected inside the suburban e-waste recycler plant (S-4) had Cu concentration (1045 mg/kg)

exceeding the acceptable limit. Elevated Cu concentrations was also found in the sample collected close to the nearby city dump (S-2). The high levels of Cu found at the e-waste sites (both S-4 and L-6) are higher than what has been found a large e-waste site located in Agbogbloshie, Ghana (Table 4-1)

There is an increase in Cu concentration from the rural SE locations (L-1) towards the city (L-2 to L-4). The opposite trend was observed with increasing distance from the urban area at the rural sites in the NW locations, with L-19 being the endpoint and having the lowest concentration in the NW transect. The concentrations are highest at the urban and suburban locations (L-4 to L-16). The range in Cu concentration in urban soils (7-42 mg/kg) is within the range of what has been found in urban soils in Italy (Table 4-1), but below levels found in China (Table 4-1). The range of Cu concentrations in urban soils are also within the range of what can be found naturally in soil on a global scale. This is also the case for the rural samples (3-12 mg/kg).

The SE and NW rural transects had Cu concentrations significantly lower than the urban locations (p-value = 0.006 for both transects).

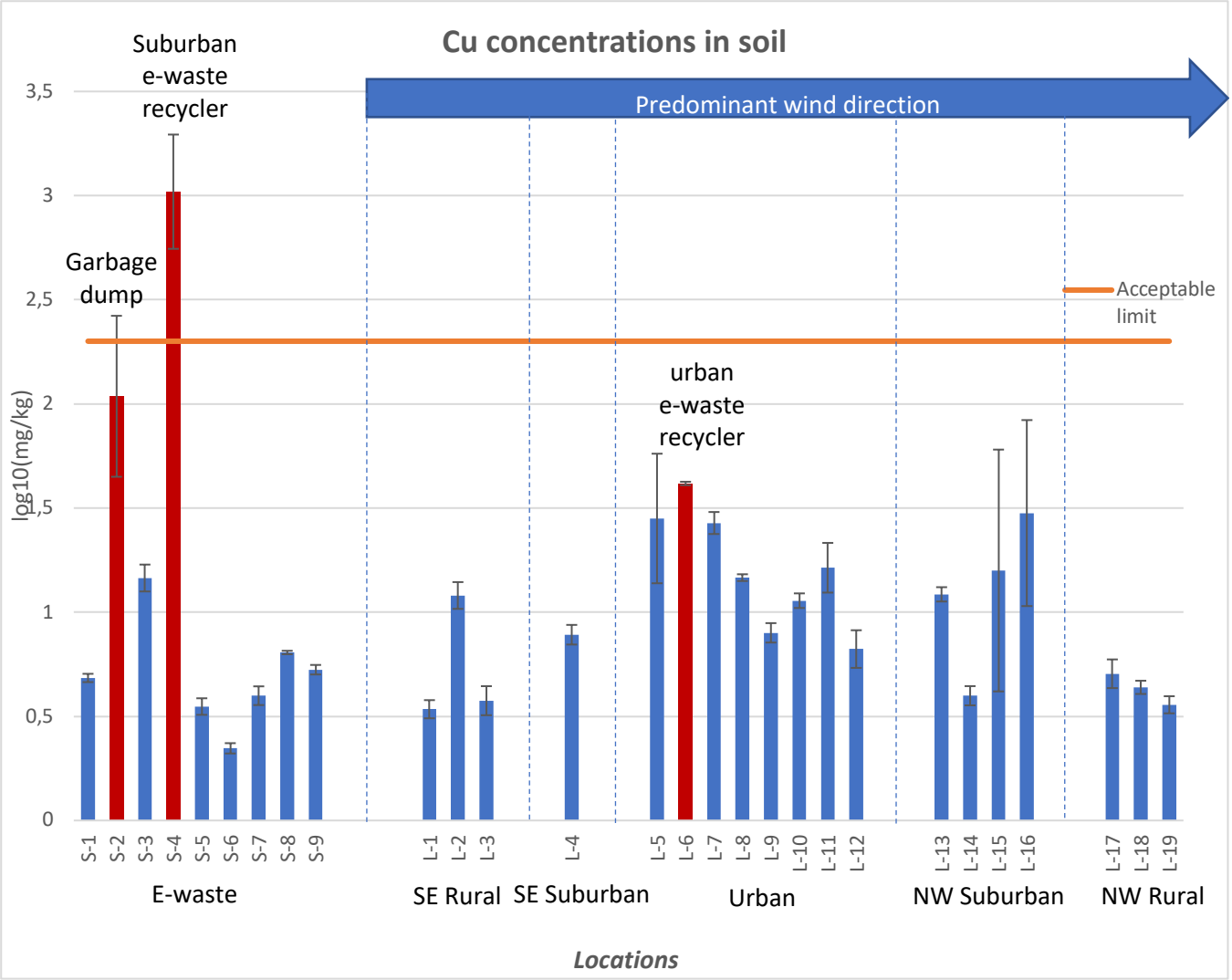

Figure 4-11: Cu concentrations (mg/kg) found in soils in and around Dar es Salaam, Tanzania. Data are log transformed.

Summing up, we find elevated levels of Cu close to e-waste recycling sites and the city garbage dump, though within a short distance from these sites the levels are low. Both rural transects had significantly lower concentrations of Cu than the urban locations which may indicate urban pollution of Cu.

4.2.3 **Zinc**

The concentration of Zn in the soil samples are shown in Figure 4-12. Soil from 5 locations exceeded the natural global background concentration of Zn in soil (>100mg/kg) (Table 4-1). These samples were collected in the e-waste transect (S-2 and S-4, i.e. the waste dump and e-

waste recycler plant which are both hotspots for heavy metals) and in urban areas (L6, L-8 and L-10).

Zn concentration in soil from the e-waste site in Agbogbloshie has been measured to be 35 mg/kg (Table 4-1) which is substantially lower than the concentrations found at the hotspots in this study.

As explained earlier, L-6 receives heavy metals pollution from both anthropogenic urban sources as well as the urban e-waste recycling plant.

Most soil samples from the rural locations (L-1, L-2, L-3, L-4, L-18 and L-19) had Zn levels under MDL for Zn. The Zn content in the soils increased sharply upon entering the urban region in the main wind direction from the SE (i.e. L-4 to L-5), and decreased gradually again with increasing distance from the city to the NW (from L-13 to L-19). This gradient along with the predominant wind direction indicates that Zn could be subject to atmospheric transport.

On the other hand, the Zn levels were below MDL in samples collected downwind in the close vicinity of the suburban e-waste recycler (S-4) and the city garbage dump (S-2), indicating no transportation from these hotspots to nearby locations. The higher Zn levels in the NW may therefore instead be due to more anthropogenic activities in the NWt of Dar es Salaam compared to the SE. In addition, the concentration gradient may be due to Zn being emitted to air in urban areas, and thus are prone to longer transport while in the waste dump and e-waste recycler is released to water which moves through these sites, which moves at a lower rate than wind masses.

Both the SE and NW rural transect had Zn levels significantly lower than the urban transect.

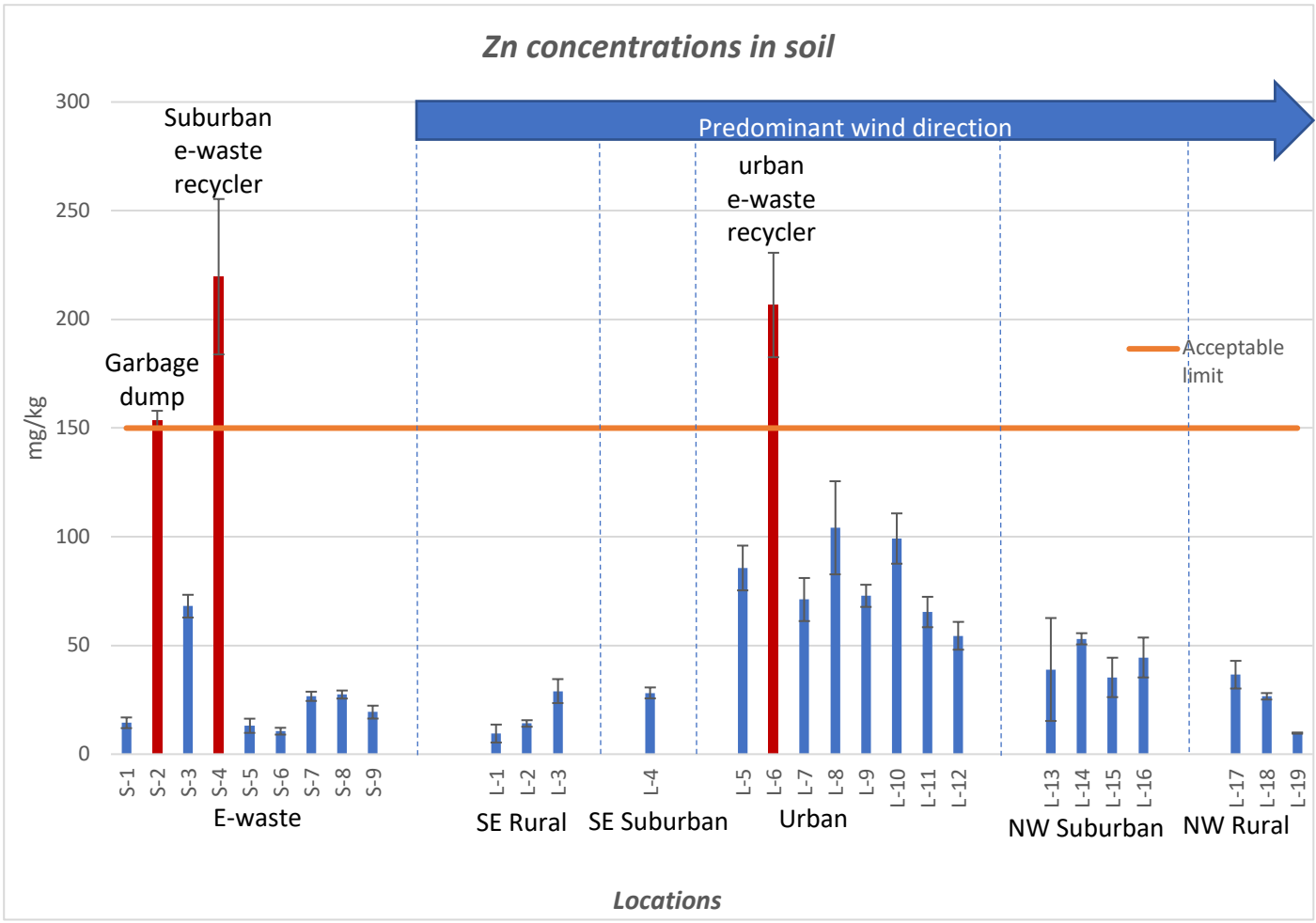

Figure 4-12: Zn concentrations (mg/kg) found in soils in and around Dar es Salaam, Tanzania. S-1, S-5,S-6, S-7, S-8, S-9, L-1, L-2, L-3, L-4. L-18 and L-19 had concentrations<MDL.

In short, the spatial distribution of Zn was similar to that of Cu. The highest levels were found close to the e-waste recycling plants, while the soil close to the city waste dump and urban soils had elevated levels of Zn.

4.2.4 **Arsenic**

As concentrations in soil samples are presented in Figure 4-13. As was found above the acceptable limit in several samples, most of which were collected in urban areas such as L-4, L-5, L-6, L-7, L-19, L-11 and L-12. L-4 is defined as a suburban location, but the location is in close proximity to an industrial area (Temeke), which can affect levels of As. The concentrations of As found in soil in this study in the urban areas (0.6-15 mg/kg) were similar to what has been found in urban areas of southwest China (Table 4-1).

There is globally a wide range of natural occurring concentrations of As in soil (0.1-55 mg/kg), and all the samples are within this range, although some were higher than the acceptable limit. Even the soil sample from the starting point of SE rural transect (L-1) had

higher concentration than the accepted limits, even though it is located far from the city and any significant anthropogenic activity. A possible explanation of this can be the soil´s physicochemical properties such as high content of OM (7.8%, Figure 4-16) and high CEC (20cmol+/kg, Figure 4-17), have a stronger role in the accumulation of As. The main species of As in soil are the oxyanions dihydrogen- and hydrogen arsenate ($H_2AsO_4^-$ and $HAsO_4^{2-}$). These interact very differently than the aqueous cations of Pb^{2+}, Cu^{2+} and Zn^{2+} in soil. The levels of As are not significantly higher in the urban area than the SE rural (p=0.14), but significantly higher than the NW rural transect (p=0.012).

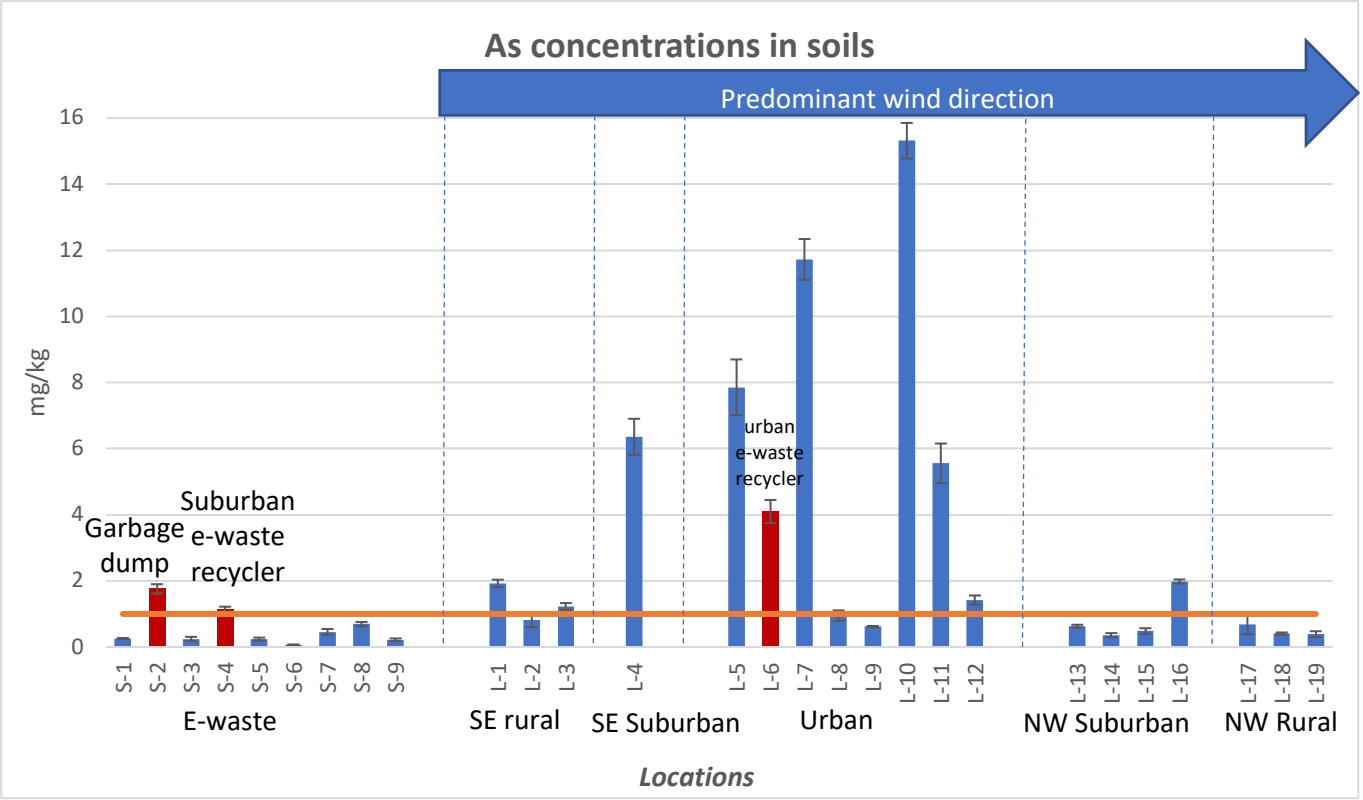

Figure 4-13: Arsenic concentrations (mg/kg) found in and around Dar es Salaam, Tanzania. S-1, S-3, S-5, S-6, S-9 and L-14 had concentrations<MDL

Although the levels of As are clearly influenced by anthropogenic activities, the spatial distribution was very different compared to Pb, Cu and Zn. This suggest other major anthropogenic sources as well as elevated background of As. In addition, the soils physicochemical characteristics may play a role in governing the spatial distribution of As in these soils as indicated and discussed from Figure 4-1 *and* Figure 4-2.

4.2.5 **Mercury**

The levels of Hg in the studied soils are shown in Figure 4-14.

Hg levels in all the samples were not above the acceptable limit, although some samples had levels above natural background concentration, and in the range of what could be found in Italian urban soil (0.04-56 mg/kg) (Table 4-1). The highest concentrations were found at the urban e-waste recycling site, L-6 (0.1 mg/kg) as well as the suburban sites, S-8 (0.06 mg/kg) and L-13 (0.09 mg/kg).

The high levels in L-13 and S-8 may be due to the soils ability to bind heavy metals as these samples have a high content of OM relative to other locations (6.7 and 8.9% respectively, Figure 4-16). Hg is a typical type B metal that is strongly bound to OM. If not strongly complexed, the reduced Hg^0 will rapidly evaporate and be transported away given the hot climate of the region. The spatial differences in the content of OM may thus explain the high concentrations found in these particular samples.

The NW and SE rural transects did not have significantly lower levels than the urban areas ($p=0.097$, 0.067 respectively).

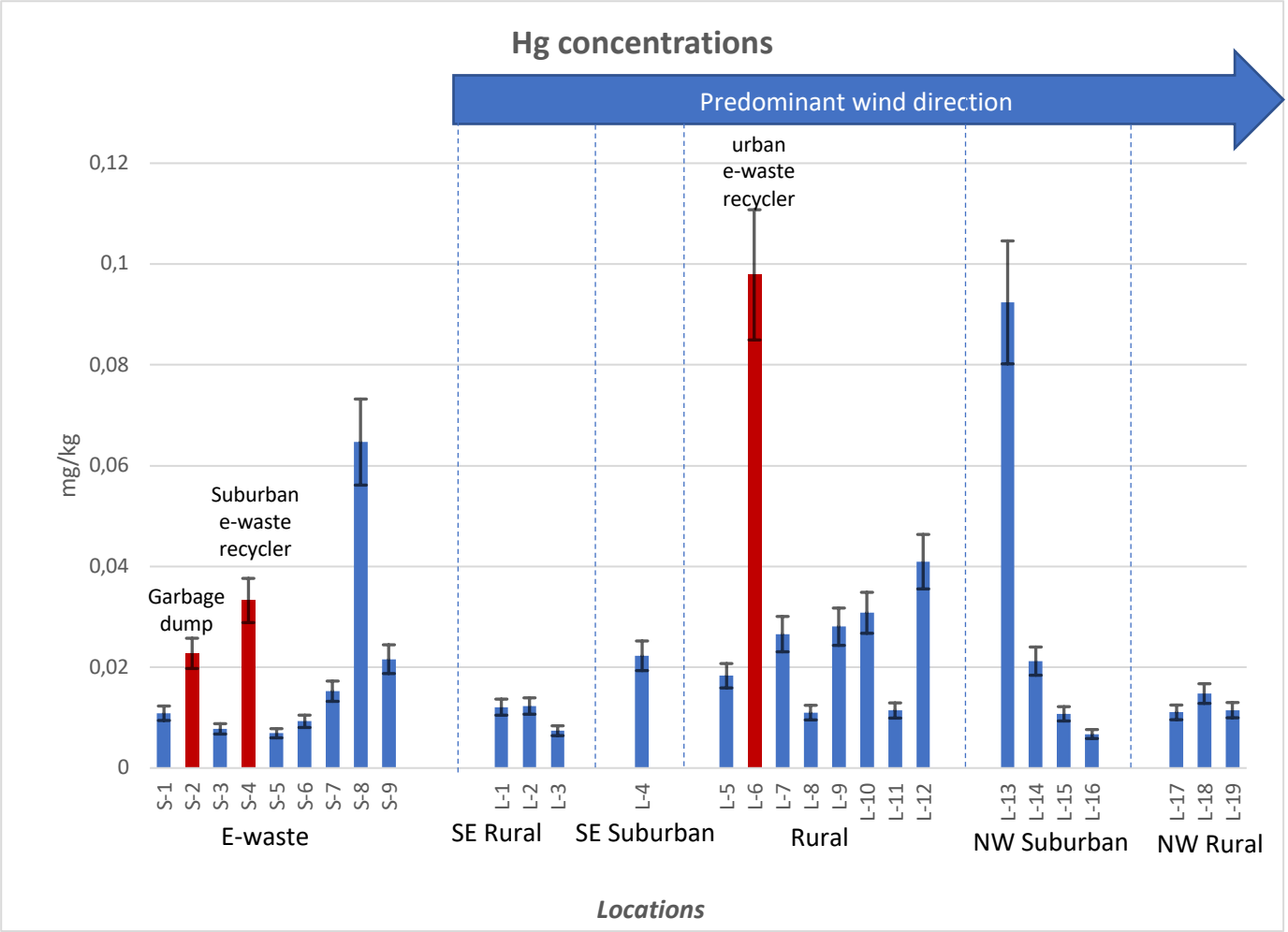

Figure 4-14: Hg concentrations (mg/kg) found in soil in and around Dar es Salaam,. No acceptable limit line drawn due to the concentrations being lower than the acceptable limit (2 mg/kg).

In conclusion, the Hg levels in the soils around Dar es Salaam were mainly governed by the direct contamination from e-waste handling or the soils OM content, dictating the soils ability to hold Hg.

4.2.6 Heavy metal concentrations below acceptable limits

The levels of several heavy metals were below the acceptable national limits. The barplots of these are found in Appendix G.

The highest value of Cd in the dataset was 0.3 mg/kg at L-6 (Figure G 1)

This is in the range of natural background for the element (Table 4-1).

The natural global average level of Cr in soil is an average of 100mg/kg globally. The highest concentration of Cr found in this study was 68mg/kg (Figure G 3). None of the samples

exceeded the natural background of Co at 25mg/kg (Figure G 4). The same applies for Ni (Figure G 2) which have a natural background of 80mg/kg (Table 4-1).

Se concentrations were also found to be within the range of natural background of 0.01-2mg/kg. The concentrations of Se found in this study was <MDL-0.9mg/kg (Figure G 5).

4.3 Physicochemical properties of soil samples

The results for pH, OM, CEC and estimated clay content of the soil samples are presented in Figure 4-15, 4-16, 4-17 and 4-18 respectively. As expected for the region, the pH of all the soil samples (Figure 4-15) was circumneutral (from 6.1 to 8.8). This is partly due to carbonate minerals in the soil as well as the low amount of OM shown in Figure 4-16. Low content of OM was expected, given the tropical savannah nature of the region. The highest relative amount of OM was 8.9% (L-13).

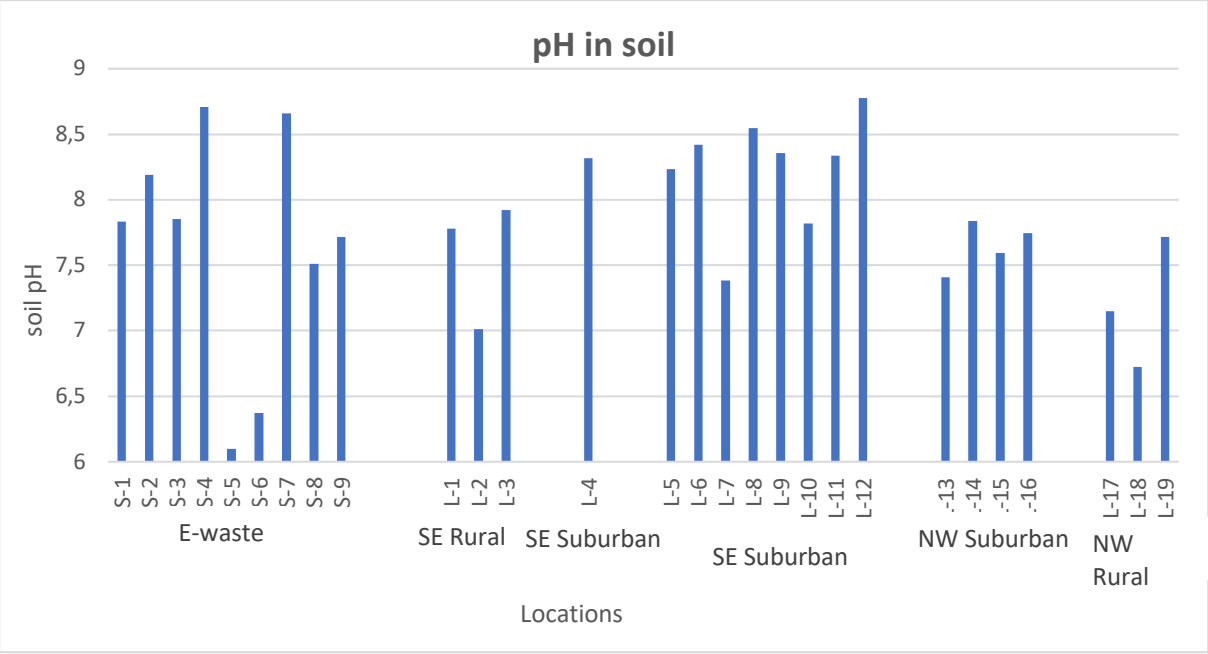

Figure 4-15: pH value of soil samples

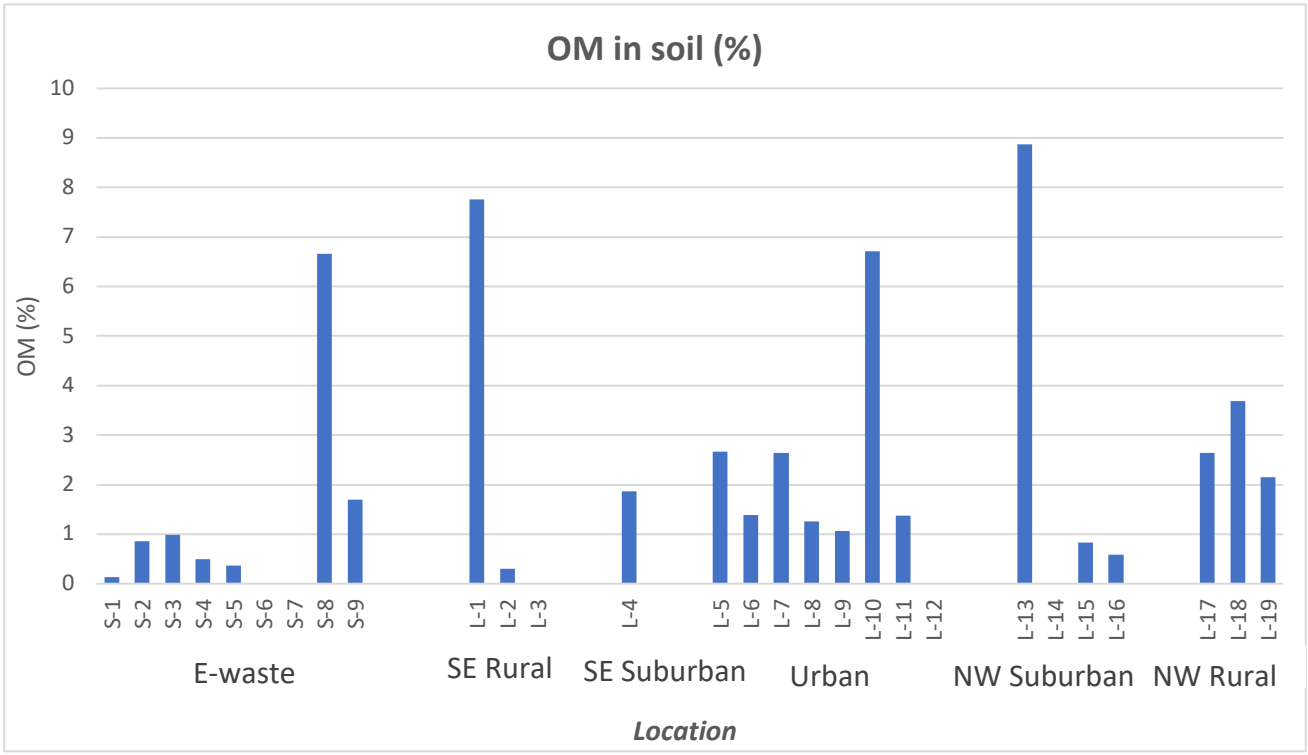

Figure 4-16: OM content in soil after LOI and correction for clay content.

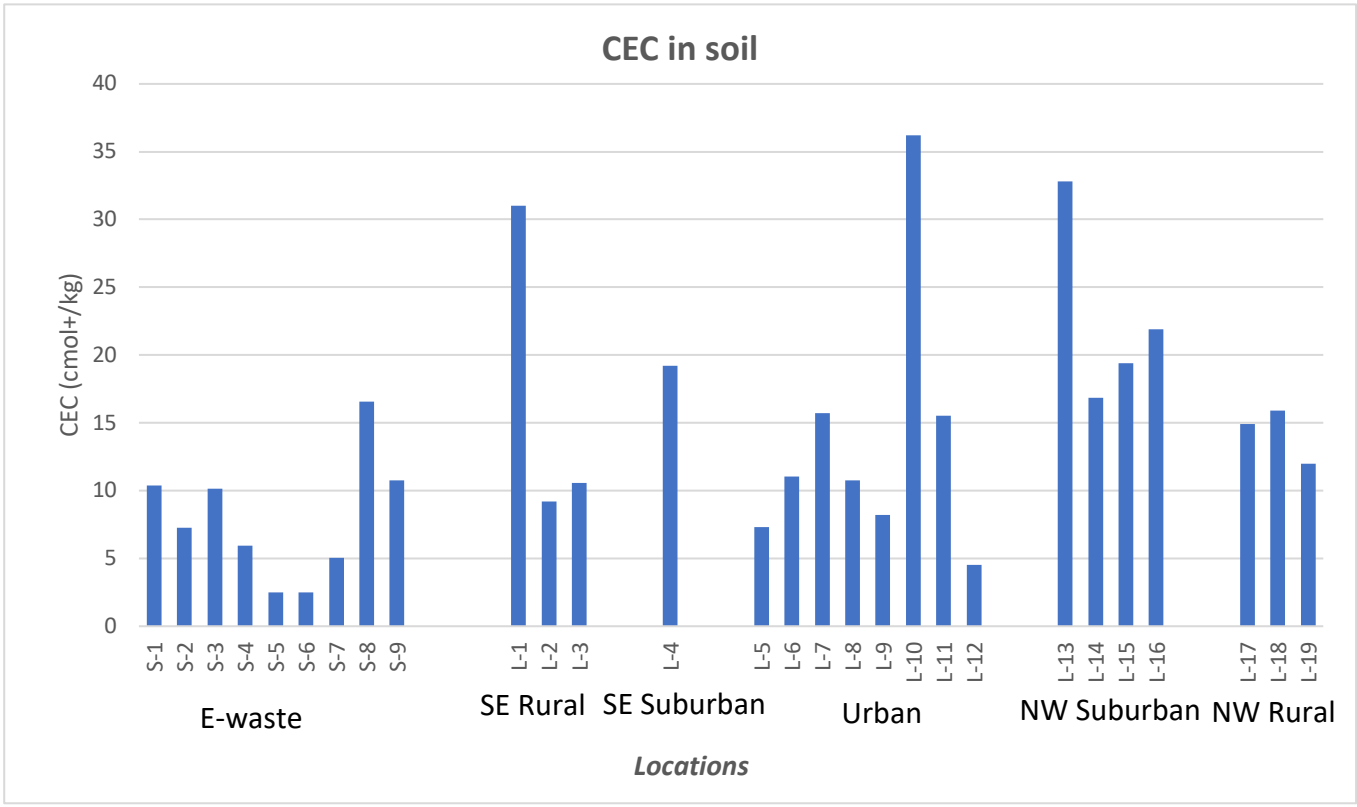

Figure 4-17: CEC of soil after treatment with $BaCl_2$

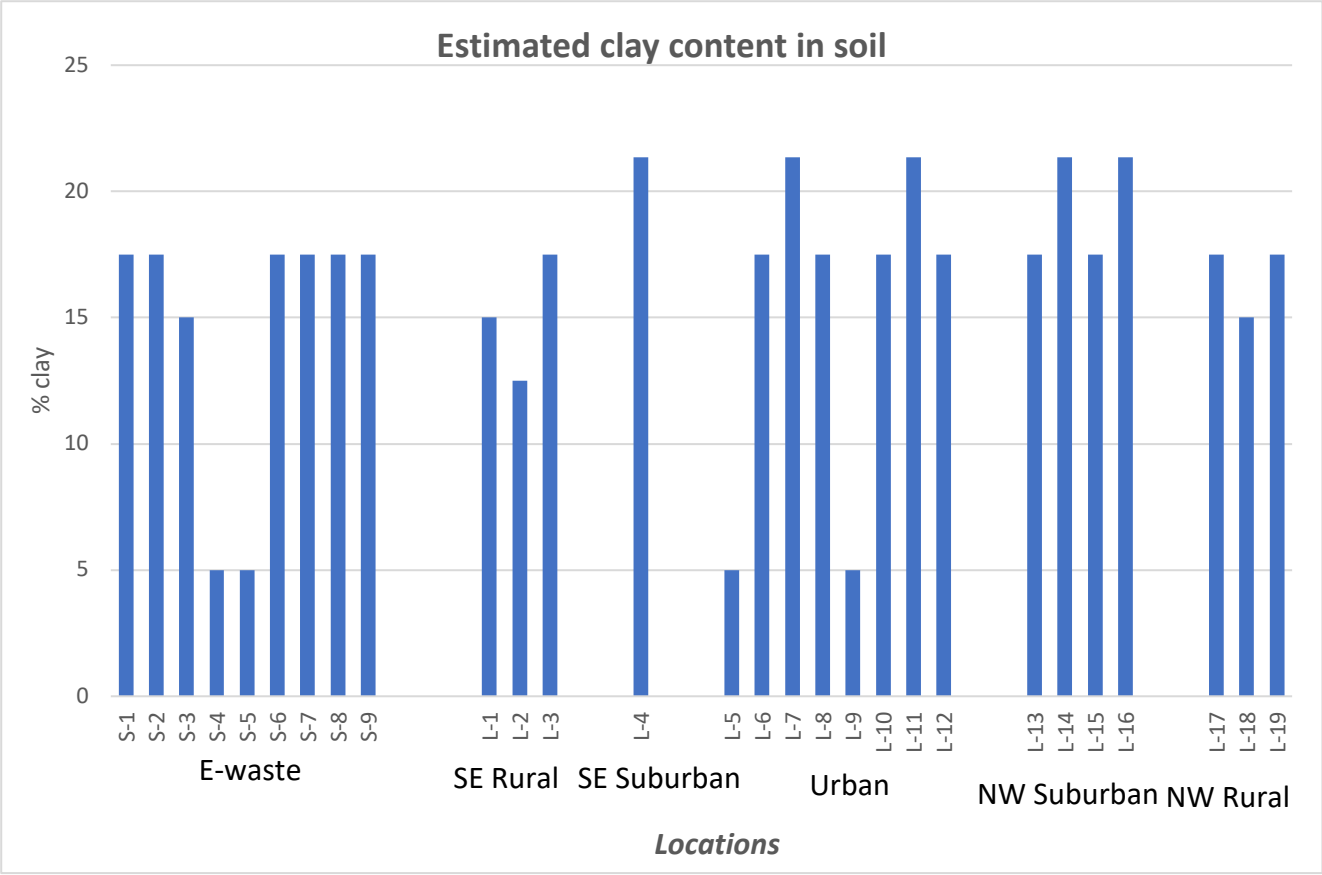

Figure 4-18: Estimated clay content after determining the soil texture by feel.

4.3.1 Correlation between heavy metals and physicochemical properties

A Correlation matrix and corresponding significance levels are found in Table 4-2.
Cd, Ni and slightly Zn were expected to be negatively correlated to H^+ concentration, due to the increase of sorption for these metals on soil particles in the range of pH found in the soils in this study (Figure 2-1 for pH dependency graph). The lack of correlations with pH may be due to the very small differences in pH in the circumneutral soils. Another likely reason for a lack of correlation to physicochemical properties may be the strong local anthropogenic input of heavy metals to these urban and suburban soils, which may overshadow the importance of the physiochemical properties of the soil. The lack of correlation with %OM is mainly due to the low overall amount of OM in the soil. The CEC can be interpreted as a measure of the reactivity of the soil as previously stated (section 2.1.2).

The correlation of Co and Cr with CEC and clay content supports the argument that these metals are governed by the physicochemical properties of the soil. Hg and Se are to some extent significantly correlated with OM. This supports the assumption that the reason for

generally low Hg concentrations are due to the low content of OM. The highest concentration of Hg was found in the sample with the highest OM content (excluding the hotspot locations).

Table 4-2: Correlation between metals and physicochemical properties.

	OM		H+ concentration		CEC		Clay content	
	R^2	p-value	R^2	p-value	R^2	p-value	R^2	p-value
Pb	-0.10	0.63	-0.13	0.51	-0.21	0.28	-0.050	0.82
Zn	-0.08	0.70	-0.29	0.14	-0.12	0.54	-0.21	0.28
Ni	0.36	0.062	-0.26	0.18	**0.62**	$3.9*10^{-4}$	**0.38**	0.046
Cd	0.09	0.64	-0.28	0.15	0.03	0.89	0.020	0.93
Cr	0.34	0.081	-0.26	0.19	**0.66**	$1.4*10^{-4}$	**0.43**	0.023
Co	0.24	0.22	-0.23	0.23	**0.58**	0.0012	**0.55**	0.0027
Cu	-0.12	0.54	-0.10	0.62	-0.19	0.34	-0.35	0.069
As	0.33	0.083	-0.19	0.34	**0.42**	0.027	0.17	0.38
Hg	**0.49**	$8.8*10^{-3}$	-0.20	0.30	0.25	0.20	0.11	0.59
Se	**0.63**	$2.0*10^{-3}$	-0.28	0.14	**0.84**	$1.6*10^{-8}$	0.28	0.15

5 Conclusion

The levels of Pb, Cu, Zn, As and Hg were above background levels at one or more locations. The highest levels of several heavy metals (Pb, Cu and Zn especially) were found at the hotspot locations such as the suburban e-waste recycler, the waste dump and the urban e-waste recycler, but a large variety of heavy metal concentrations were obtained. The levels of heavy metals close to the hotspot locations were generally low indication minimum transport from these locations.

The physicochemical properties of the soil were as expected in a tropical region with low content of OM and high pH values. The low content of OM and high temperature in the region facilitates the evaporation of elemental Hg from the soil surface as the metal is not retained by OM. This was supported by the fact that Hg levels were low compared to other studies and exceeded the natural background concentration in only two samples (excluding hotspot locations). These samples also had a high content of OM.

The multivariate analysis clearly showed that distance to the city of Dar es Salaam is the main governing factor regarding the spatial trends of all metals included in the study. This was additionally supported by the levels of Pb, Cu, Zn and Cd being significantly higher in the urban areas than in rural, as these are metals associated with urban pollution in several studies as previously stated.

In addition to distance to city, the physicochemical properties of the soil were shown to govern the spatial trends of As, Co, Cr, Ni and Se.

The multivariate analysis also resulted in a separation of e-waste pollution from general waste pollution with general waste being indicated by high levels of Pb, Cd and CPs and pollution from e-waste being characterized by high levels of Cu, Zn and dechlorane plus.

The results indicate pollution at hotspot locations, higher levels of heavy metals such as Pb, Cu, Cd and Zn in the city of Dar es Salaam (though Cd is not above background levels) and physicochemical governance of some heavy metals such as As, Co, Cr, Ni and Se. Co, Cr, Ni and Se was found in background levels in all samples.
Hg was found in low concentrations mainly due to the physicochemical properties of the soil and high temperature in the region which hinder the retention of the metal in soil.

6 Further studies

To gain knowledge about how and what the heavy metals are bound to in soil, a sequential fractionation procedure based on the procedure by Tessier may be considered (Tessier et al., 1979). This procedure differentiates the metals into 5 fractions; exchangeable, bound to carbonates, bound to Iron and Manganese, bound to OM and residual.

A comparative study between tropical and boreal areas should be conducted to assess the differences in the biogeochemical processes that governs the spatial trends of heavy metals.

As the clay content was only roughly estimated, a more thorough analysis of clay content should be conducted. Due to time limitations this was not conducted, but was to be determined following the method of ISO11277 - determination of particle size distribution in mineral soil and material – method by sieving and sedimentation (International Organizastion for Standardization, 2009).

The CEC analysis has poor precision, and optimization of the method is advised. Conducting the Mg analysis for CEC determination on the ICP-MS is not advised as the concentration of Mg are high and may wear down the detector, even though the Mg concentrations are within the linear range of the instrument.

References

Ahrland, S., Chatt, J. & Davies, N. R. 1958. The relative affinities of ligand atoms for acceptor molecules and ions. *Q. Rev., Chem. Soc.,* 12265-76.

Akortia, E., Olukunle, O. I., Daso, A. P. & Okonkwo, J. O. 2017. Soil concentrations of polybrominated diphenyl ethers and trace metals from an electronic waste dump site in the Greater Accra Region, Ghana: Implications for human exposure. *Ecotoxicol. Environ. Saf.,* 137247-255.

Alloway, B. J. 2013a. Heavy Metals in Soils : Trace Metals and Metalloids in Soils and their Bioavailability. 3rd ed. Dordrecht: Springer Netherlands : Imprint: Springer.

Alloway, B. J. 2013b. Sources of Heavy Metals and Metalloids in Soils. *In:* Alloway, B. J. (ed.) *Heavy Metals in Soils: Trace Metals and Metalloids in Soils and their Bioavailability.* Dordrecht: Springer Netherlands.

AMAP 2011. AMAP Assesment 2011: Mercury in the Arctic. *Arctic Montoring and Assessment Program,* xiv-193.

Anthrotox. 2017. *AnthroTox* [Online]. Available: https://www.uio.no/english/research/strategic-research-areas/life-science/research/convergence-environments/anthrotox/ [Accessed 18.06.20 2020].

Aoshima, K. 2016. Itai-itai disease: Renal tubular osteomalacia induced by environmental exposure to cadmium—historical review and perspectives. *Soil Science and Plant Nutrition,* 62**,4** 319-326.

Appelo, C. A. J. & Postma, D. 2005. *Geochemistry, groundwater and pollution,2nd edition.* Leiden, Balkema.

Ariya, P. A., Dastoor, A. P., Amyot, M., Schroeder, W. H., Barrie, L., Anlauf, K., Raofie, F., Ryzhkov, A., Davignon, D., Lalonde, J. & Steffen, A. 2004. The Arctic: A sink for mercury. *Tellus, Ser. B,* 56B**,5** 397-403.

Bye, R. 2009. *Dekomponeringsmetoder i Analytisk Kjemi,edition.* Oslo, Media Oslo AS.

Christophersen, O. A., Lyons, G., Haug, A. & Steinnes, E. 2013. Selenium. *In:* Alloway, B. J. (ed.) *Heavy Metals in Soils: Trace Metals and Metalloids in Soils and their Bioavailability.* Dordrecht: Springer Netherlands.

Compeau, G. C. & Bartha, R. 1985. Sulfate-reducing bacteria: principal methylators of mercury in anoxic estuarine sediment. *Applied and Environmental microbiology,* 50**,2** 498-502.

Denier van der Gon, H., van het Bolscher, M., Visschedijk, A. & Zandveld, P. 2007. Emissions of persistent organic pollutants and eight candidate POPs from UNECE–Europe in 2000, 2010 and 2020 and the emission reduction resulting from the implementation of the UNECE POP protocol. *Atmospheric environment (1994),* 41**,40** 9245-9261.

Duffus, J. H. 2002. "Heavy metals"-a meaningless term? (IUPAC technical report). *Pure Appl. Chem.,* 74**,5** 793-807.

Echegoyen, Y., Boyle, E. A., Lee, J.-M., Gamo, T., Obata, H. & Norisuye, K. 2014. Recent distribution of lead in the Indian Ocean reflects the impact of regional emissions. *Proceedings of the National Academy of Sciences,* 111**,43** 15328-15331.

EPA. 2019. *Mercury in Consumer Products* [Online]. Available: https://www.epa.gov/mercury/mercury-consumer-products [Accessed 17.08 2020].

Fayiga, A. O., Ipinmoroti, M. O. & Chirenje, T. 2018. Environmental pollution in Africa. *Environment, Development and Sustainability,* 20**,1** 41-73.
Fergusson, J. E. 1990. *The heavy elements : chemistry, environmental impact and health effects,edition.* Oxford [England], Pergamon Press.
Fiedler, H. 2010. Short-Chain Chlorinated Paraffins: Production, Use and International Regulations. *In:* Boer, J. (ed.) *Chlorinated Paraffins.* Berlin, Heidelberg: Springer Berlin Heidelberg.
Fischer, L., Bruemmer, G. W. & Barrow, N. J. 2007. Observations and modelling of the reactions of 10 metals with goethite: adsorption and diffusion processes. *Eur. J. Soil Sci.,* 58**,6** 1304-1315.
Frazzoli, C., Orisakwe, O. E., Dragone, R. & Mantovani, A. 2010. Diagnostic health risk assessment of electronic waste on the general population in developing countries' scenarios. *Environmental impact assessment review,* 30**,6** 388-399.
Gilmour, C. C., Elias, D. A., Kucken, A. M., Brown, S. D., Palumbo, A. V., Schadt, C. W. & Wall, J. D. 2011. Sulfate-Reducing Bacterium Desulfovibrio desulfuricans ND132 as a Model for Understanding Bacterial Mercury Methylation. *Appl. Environ. Microbiol.,* 77**,12** 3938-3951.
Guo, G., Wu, F., Xie, F. & Zhang, R. 2012. Spatial Distribution and pollution assesment of heavy metals in urban soils from southwest China. *Journal of Environmental Sciences,* 24**,4** 410-418.
Harada, M. 1995. Minamata disease: methylmercury poisoning in Japan caused by environmental pollution. *Crit. Rev. Toxicol.,* 25**,1** 1-24.
He, K., Sun, Z., Hu, Y., Zeng, X., Yu, Z. & Cheng, H. 2017. Comparison of soil heavy metal pollution caused by e-waste recycling activities and traditional industrial operations. *Environ. Sci. Pollut. Res.,* 24**,10** 9387-9398.
Herat, S. 2008. Green electronics through legislation and lead free soldering. *Clean: Soil, Air, Water,* 36**,2** 145-151.
International Organizastion for Standardization 1993. ISO11465:1993 - Soil Quality - Determination of Dry Matter and Water Content on a Mass Basis - Gravimetric Method. Geneve, Switzerland.
International Organizastion for Standardization 1994a. ISO10390:1994 - Soil Quality-Determination of pH. Geneva, Switzerland.
International Organizastion for Standardization 1994b. ISO11260:1994 - Soil Quality - Determination of Effective Cation Exchange Capacity and Base Saturation Level using Barium Chloride Solution. Geneva, Switzerland.
International Organizastion for Standardization 2006. ISO11464:2006 - Soil Quality - Preatreatment of Samples for Physico-Chemical Analysis. Geneva, Switzerland.
International Organizastion for Standardization 2009. ISO11277:2009 - Determination of Particle Size Distribution in Mineral Soil Material - Method by Sieving and Sedimentation. Geneva, Switzerland.
Jaerup, L., Berglund, M., Elinder, C. G., Nordberg, G. & Vahter, M. 1998. Health effects of cadmium exposure. A review of the literature and a risk estimate. *Scand. J. Work, Environ. Health,* 24,**Suppl. 1** 1-51.
Kalpage, F. S. C. P. 1976. *Tropical Soils: Classification, Fertility and Managment,Revised edition.* London, The Macmillian Press LTD.
Karim, Z., Qureshi, B. A., Mumtaz, M. & Qureshi, S. 2014. Heavy metal content in urban soils as an indicator of anthropogenic and natural influences on landscape of Karachi-A multivariate spatio-temporal analysis. *Ecol. Indic.,* 4220-31.

Krogstad, T. 1992. Metoder for Jordanalyser. Institutt for jordfag, Ås-NLH: Jordbunnslære.
Landis, W. G., Sofield, R. M. & Yu, M. H. 2018. *Introduction to Environmental Toxicology: Molecular Substructures to Ecological Landscapes,5th edition.* Boca Raton, Florida, CRC Press.
Leaner, J. J., Dabrowski, J. M., Mason, R. P., Resane, T., Richardson, M., Ginster, M., Gericke, G., Petersen, C. R., Masekoameng, E., Ashton, P. J. & Murray, K. 2009. Mercury emissions from point sources in South Africa. *In:* Mason, R. & Pirrone, N. (eds.) *Mercury Fate and Transport in the Global Atmosphere: Emissions, Measurements and Models.* Boston, MA: Springer US.
Lindberg, S. E. & Stratton, W. J. 1998. Atmospheric Mercury Speciation: Concentrations and Behaviour of Reactive Gaseous Mercury in Ambient Air. *Environmental Science & Technology,* 32**,1** 49-57.
Lindqvist, O., Johansson, K., Aastrup, M., Andersson, A., Bringmark, L., Hovsenius, G., Håkanson, L., Iverfeldt, Å., Meili, M. & Timm, B. 1991. Mercury in the Swedish Environment - Recent Research on Causes, Consequences and Corrective Methods. *Water, air and soil pollution,* 55**,1-2** xi-261.
Mahenge, R. S., Ulanga, P., Malabeja, M., Pilly, J. & Massoy, W. 2018. Performance Audit Report on Electronic Waste Managment. Dar es Salaam: National Audit Office.
Manta, D. S., Angelone, M., Bellanca, A., Neri, R. & Sprovieri, M. 2002. Heavy metals in urban soils: a case study from the city of Palermo (Sicily), Italy. *Sci. Total Environ.,* 300**,1-3** 229-243.
Metoblue. 2020. *Climate Dar es Salaam* [Online]. Available: https://www.meteoblue.com/en/weather/historyclimate/climatemodelled/dar-es-salaam_tanzania_160263 [Accessed 21.04.2020 2020].
Milestone 2018a. DMA-80 Direct Mercury Analyzer. Sorisole, Italy.
Milestone. 2018b. *DMA-80 evo, Direct Mercury Analyzer* [Online]. Sorisole, Italy. Available: https://www.holgerhartmann.no/getfile.php/1323319-1542290940/Produkter/Laboratorie/Kvikksølvanalysator/DMA%2080%20evo/DMA-80-brochure.pdf [Accessed 01.10.2019].
Nieboer, E. & Richardson, D. H. S. 1980. The replacement of the nondescript term 'heavy metals' by a biologically and chemically significant classification of metal ions. *Environ. Pollut., Series. B: Chem. Phys.,* 1**,1** 3-26.
Nipen, M. 2020. Unpublished work.
Nriagu, J. O. 1983. Occupational exposure to lead in ancient times. *Sci. Total Environ.,* 31**,2** 105-16.
Perdue, E. M. 2009. Natural Organic Matter. *In:* Likens, G. E. (ed.) *Encyclopedia of Inland Waters.* Oxford: Academic Press.
Poulain, A. J. & Barkay, T. 2013. Cracking the Mercury Methylation Code. *Science (American Association for the Advancement of Science),* 339**,6125** 1280-1281.
Ritchey, E. L., McGrath, J. M. & Gehring, D. 2015. Determining Soil Texture by Feel. *Agriculture and Natural Resources Publications,* 139.
Robinson, B. H. 2009. E-waste: An assessment of global production and environmental impacts. *Sci. Total Environ.,* 408**,2** 183-191.
Schlesinger, W. H. & Bernhardt, E. S. 2013. Chapter 4 - The Lithosphere. *Biogeochemistry: An analysis of global change.* 3rd ed. Boston: Academic Press.
Schuster, E. 1991. The behavior of mercury in the soil with special emphasis on complexation and adsorption processes - a review of the literature. *Water, Air, Soil Pollut.,* 56**,1** 667-80.

Slemr, F., Seiler, W. & Schuster, G. 1981. Latitudinal Distribution of Mercury Over the Atlantic Ocean. *Journal of Geophysical Research,* 82**,C2** 1159-1166.
Smolders, E. & Mertens, J. 2013. Cadmium. *In:* Alloway, B. J. (ed.) *Heavy Metals in Soils: Trace Metals and Metalloids in Soils and their Bioavailability.* Dordrecht: Springer Netherlands.
Steinnes, E. 2013a. Lead. *In:* Alloway, B. J. (ed.) *Heavy Metals in Soils: Trace Metals and Metalloids in Soils and their Bioavailability.* Dordrecht: Springer Netherlands.
Steinnes, E. 2013b. Mercury. *In:* Alloway, B. J. (ed.) *Heavy Metals in Soils: Trace Metals and Metalloids in Soils and their Bioavailability.* Dordrecht: Springer Netherlands.
Sverko, E., Tomy, G. T., Reiner, E. J., Li, Y.-F., McCarry, B. E., Arnot, J. A., Law, R. J. & Hites, R. A. 2011. Dechlorane Plus and Related Compounds in the Environment: A Review. *Environ. Sci. Technol.,* 45**,12** 5088-5098.
Tessier, A., Campbell, P. G. C. & Bisson, M. 1979. Sequential extraction procedure for the speciation of particulate trace metals. *Anal. Chem.,* 51**,7** 844-51.
The European Parliament and the Council of the European Union 2011. Directive 2011/65/EU of the European Parliamaent and of the Council of 8th June 2011on the restriction of the use of certain hazardous substances in electrical and electronic equipment. *Official Journal of the European Union*.
The National Environmental Standards Comittee of Tanzania Bureau of Standards 2007. The Environmental Managment (Soil Quality Standards Regulations).
The World Data Bank 2009. *Tanzania Country Brief,edition.*, The World Bank.
Thomas, R. 2013. *Practical guide to ICP-MS: a tutorial for beginners,edition.*, CRC Press.
Tolcin, A. C. 2020. 2017 Minerals Yearbook: Cadmium [advance release]. U.S Geological Survey.
Tong, S., von Schirnding, Y. E. & Prapamontol, T. 2000. Environmental lead exposure: a public health problem of global dimensions. *Bulletin of the World Health Organ,* 78**,9** 1068-1077.
U.S Environmental Protection Agency 1994. Method 200.8:Determination of Trace Elements In Waters and Wastes by Inductively Coupled Plasma - Mass Spectrometry. Cincinnati, OH.
U.S Environmental Protection Agency 2016. Definition and Procedure for the Determination of the Method Detection Limit, Revision 2. Washington, DC.
UN Environment 2019. Global Mercury Assesment 2018. Geneva, Switzerland: Chemcials and health branch.
UNECE. 1998. *The 1998 Aarhus Protocol on Heavy Metals* [Online]. Aarhus, Denmark. Available: https://www.unece.org/fileadmin/DAM/env/lrtap/full%20text/1998.Heavy.Metals.e.pdf [Accessed 01.09.20].
UNEP 2002. Global Mercury Assessment 2002. Geneva, Switzerland: UNEP Chemicals.
UNEP 2010a. Final Review of scientific information on cadmium. Geneva Switzerland: UNEP Chemicals.
UNEP 2010b. Key scientific findings for Lead: An excerpt from Final Review of scientific information on Lead. Geneva, Switzerland: Chemicals Branch.
UNEP 2011. Stockholm Convention on Persistant Organic Pollutants(POPs). Revised in 2017 ed.: Secretariat of the Stockholm Convention (SSC).
UNEP 2013. Minamata Convention on Mercury. Kumamoto, Japan: UN Treaty Collection.
USDA:Natural Resources Conservation Service Soils. 2020. *Soil Texture Calculator* [Online]. Available:

https://www.nrcs.usda.gov/wps/portal/nrcs/detail/soils/survey/?cid=nrcs142p2_054167 [Accessed 25.07 2020].
Vandecasteele, C. 1993. *Modern methods for trace element determination,edition.* Chichester, Wiley.
VanLoon, G. W. & Duffy, S. J. 2011. *Environmental chemistry : a global perspective,3rd edition.* Oxford, Oxford University Press.
Vice President's Office: Division of Environment 2017. Minamata Initial Assesment in Tanzania. *First Draft.* United Republic of Tanzania.
Vogt, R. D. 2020. *RE: Environmental Chemistry II, KJM5700. Lecture on Environmental Chemistry of Colloids and Surfaces*,University of Oslo.
Wania, F. & Mackay, D. 1996. Tracking the distribution of persistent organic pollutants. *Environ. Sci. Technol.,* 30**,9** 390-396.
World Health Organization. Regional Office for Africa 2015. *Lead exposure in African children: contemporary sources and concerns,edition.* Brazzaville, World Health Organization. Regional Office for Africa.
Young, S. D. 2013. Chemistry of Heavy Metals and Metalloids in Soils. *In:* Alloway, B. J. (ed.) *Heavy Metals in Soils: Trace Metals and Metalloids in Soils and their Bioavailability.* Dordrecht: Springer Netherlands.
Zhang, H., Feng, X., Larssen, T., Qiu, G. & Vogt Rolf, D. 2010. In Inland China, Rice, Rather than Fish, Is the Major Pathway for Methylmercury Exposure. *Environmental Health Perspectives,* 118**,9** 1183-1188.

List of Appendencies

Appendix A Locations

Appendix A contains information about the locations such as their GPS coordinates (A.1) and photographs for description of the sites (A.2).

A.1 GPS coordinates

Table A 1: Sample locations and their GPS coordinates.

Locations	Latitude ($°N$)	Longitude($°E$)	Transect
S-1	-6.9317	39.14074	e-waste
S-2	-6.92834	39.12823	e-waste
S-3	-6.92525	39.12572	e-waste
S-4	-6.92644	39.12468	e-waste
S-5	-6.92864	39.12368	e-waste
S-6	-6.92526	39.12017	e-waste
S-7	-6.91611	39.11291	e-waste
S-8	-6.90065	39.09197	e-waste
S-9	-6.91072	39.03234	e-waste
L-1	-7.12269	39.53052	SE Rural
L-2	-6.93528	39.44984	SE Rural
L-3	-6.86737	39.36371	SE Rural
L-4	-6.8384	39.33624	SE Suburban
L-5	-6.87291	39.283092	Urban
L-6	-6.84019	39.25724	Urban
L-7	-6.81215	39.28951	Urban
L-8	-6.82966	39.26955	Urban
L-9	-6.83541	39.20857	Urban
L-10	-6.78262	39.28333	Urban
L-11	-6.77439	39.24934	Urban
L-12	-6.78428	39.23887	Urban
L-13	-6.78019	39.20539	NW Suburban
L14	-6.7986	39.13759	NW Suburban
L-15	-6.78753	39.05656	NW Suburban
L-16	-6.76502	38.99271	NW Suburban
L-17	-6.76059	38.94704	NW Rural
L-18	-6.72598	38.854	NW Rural
L-19	-6.67816	38.76045	NW Rural

A.2 Visual description of locations

Figure A 1: S-1

Figure A 2: S-3

Figure A 3: S-5

Figure A 4: S-6

Figure A 5: S-7

Figure A 6: S-8

Figure A 7: S-9

Figure A 8: L-2

Figure A 9: L-3

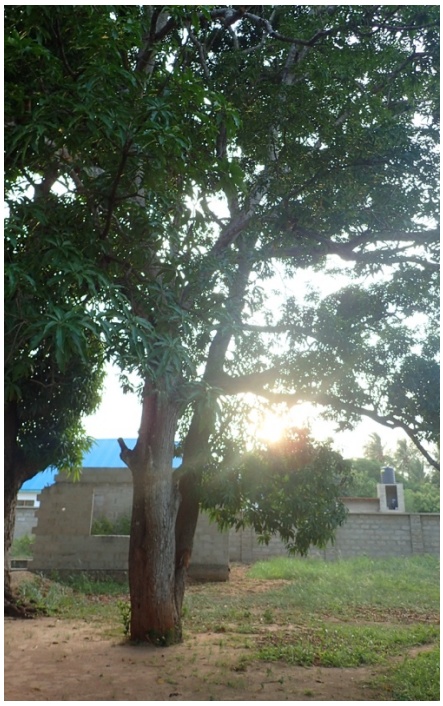

Figure A 10: L-4

Figure A 11: L-5 (Photo: Rolf Vogt)

Figure A 12: L-7

Figure A 13: L-9

Figure A 14: L-10

Figure A 15: L-11

Figure A 16: L-12

Figure A 17: L-14

Figure A 18: L-15

Figure A 19: L-16

Figure A 20: L-17

Figure A 21: L-18

Appendix B Physicochemical properties

Appendix B contains results for the physicochemical properties of the soil. The results for pH is located in B.1, OM in B.2 , CEC in B.3 and clay content in B.4. The flow chart followed to estimating the clay content is found in B.5.

Additionally, the hygroscopic humidity (%H_2O) can be found in B.6.

B.1 pH

pH values are found in Table B 1, the average (avg) H^+ concentration was used to calculate the pH value of the samples.

Table B 1:average H^+concentrations in the soil sample and resulting pH.

Sample	mol/L H^+	pH
S-1	1.48E-08	7.83
S-2	9.09E-09	8.04
S-3	1.40E-08	7.85
S-4	1.95E-09	8.71
S-5	7.95E-07	6.10
S-6	4.29E-07	6.37
S-7	2.19E-09	8.66
S-8	3.09E-08	7.51
S-9	1.89E-07	6.72
L-1	1.70E-08	7.77
L-2	9.77E-08	7.01
L-3	1.22E-08	7.91
L-4	4.85E-09	8.31
L-5	5.82E-09	8.23
L-6	3.81E-09	8.42
L-7	4.12E-08	7.38
L-8	2.85E-09	8.54
L-9	4.45E-09	8.35
L-10	1.52E-08	7.82
L-11	4.76E-09	8.32
L-12	1.68E-09	8.77
L-13	3.91E-08	7.41

Sample	mol/L H^+	pH
L-14	1.45E-08	7.84
L-15	2.62E-08	7.58
L-16	1.91E-08	7.72
L-17	7.08E-08	7.15
L-18	1.92E-07	6.72
L-19	1.94E-08	7.71

B.2 OM

OM content is found in Table B 2 and B 3. The %LOI are corrected for clay content.

Table B 2: %LOI for the three sample replicates as well as the average value and stdanrd deviation.

Sample	OM (%LOI)			After correcting average %LOI for clay content
	Replicate 1	Replicate 2	Replicate 3	
S-1	2.07	2.15	2.19	0.137
S-2	2.91	2.77	2.89	0.860
S-3	2.15	1.95	1.85	0.985
S-4	1.24	1.33	1.93	0.500
S-5	1.29	1.55	1.25	0.361
S-6	1.02	1.00	1.02	0
S-7	0.758	0.883	0.881	0
S-8	8.77	8.60	8.62	6.66
S-9	3.70	3.60	3.78	1.70
L-1	9.99	10.2	9.09	7.76
L-2	2.19	2.36	2.34	0.306
L-3	1.65	1.80	1.81	0
L-4	3.83	4.05	3.73	1.87
L-5	3.77	3.81	3.43	2.67
L-6	4.73	2.80	2.61	1.38
L-7	4.83	4.39	4.69	2.64
L-8	3.27	2.95	3.55	1.26
L-9	2.08	2.17	1.96	1.07
L-10	8.82	8.75	8.58	6.71

Sample	%LOI			
	Replicate 1	Replicate 2	Replicate 3	After correcting average %LOI for clay content
L-11	3.45	3.26	3.43	1.38
L-12	1.66	1.62	1.53	0
L-13	10.8	11.0	10.9	8.87
L-14	1.75	1.92	1.88	0
L-15	2.96	2.76	2.76	0.824
L-16	2.68	2.60	2.46	0.578
L-17	3.52	3.81	3.59	2.64
L-18	4.59	4.87	4.60	3.69
L-19	3.03	2.98	3.44	2.15

B.3 CEC

Average CEC and RSD of the three sample replicates are fund in Table B 4 and B 5.

Table B 3: CEC for the three sample replicates as well as the RSD.

Sample	AVG (Cmol+/kg)	RSD(%)
S-1	10.4	28.8
S-2	7.3	73.0
S-3	10.1	29.0
S-4	5.94	62.4
S-5	2.50	65.4
S-6	2.51	49.5
S-7	5.03	66.6
S-8	16.6	11.4
S-9	10.8	24.0
L-1	31.0	5.89
L-2	9.18	37.8
L-3	10.6	13.7
L-4	19.2	10.9
L-5	7.32	21.1

Sample	AVG (cmol+/kg)	RSD(%)
L-6	11.0	19.6
L-7	15.7	4.9
L-8	10.7	30.1
L-9	8.22	43.5
L-10	36.2	0.972
L-11	15.5	0.551
L-12	4.53	30.8
L-13	32.8	0.923
L-14	16.9	13.6
L-15	19.4	15.2
L-16	21.9	8.22
L-17	14.9	13.0
L-18	15.9	18.3
L-19	12.0	10.2

B.4 Clay estimates

The estimates for clay content following the flow chart in figure B 1 are found in Table B 6 and B 7, along with the correction factor used to correcting the OM content for clay content.

Table B 4: Estimates of clay content (%) in soil and the resulting correction factors.

Sample	Clay content (%)	Correction factor for OM
S-1	17.5	2
S-2	17.5	2
S-3	15	1
S-4	5	1
S-5	5	1
S-6	17.5	2
S-7	17.5	2
S-8	17.5	2
S-9	17.5	2
L-1	15	2
L-2	12.5	2
L-3	17.5	2

Sample	Clay content (%)	Correction factor for OM
L-4	21.35	2
L-5	5	1
L-6	17.5	2
L-7	21.35	2
L-8	17.5	2
L-9	5	1
L-10	17.5	2
L-11	21.35	2
L-12	17.5	2
L-13	17.5	2
L-14	21.35	2
L-15	17.5	2
L-16	21.35	2
L-17	17.5	2
L-18	15	2
L-19	17.5	2

B.5 Flow chart used for estimation of clay content

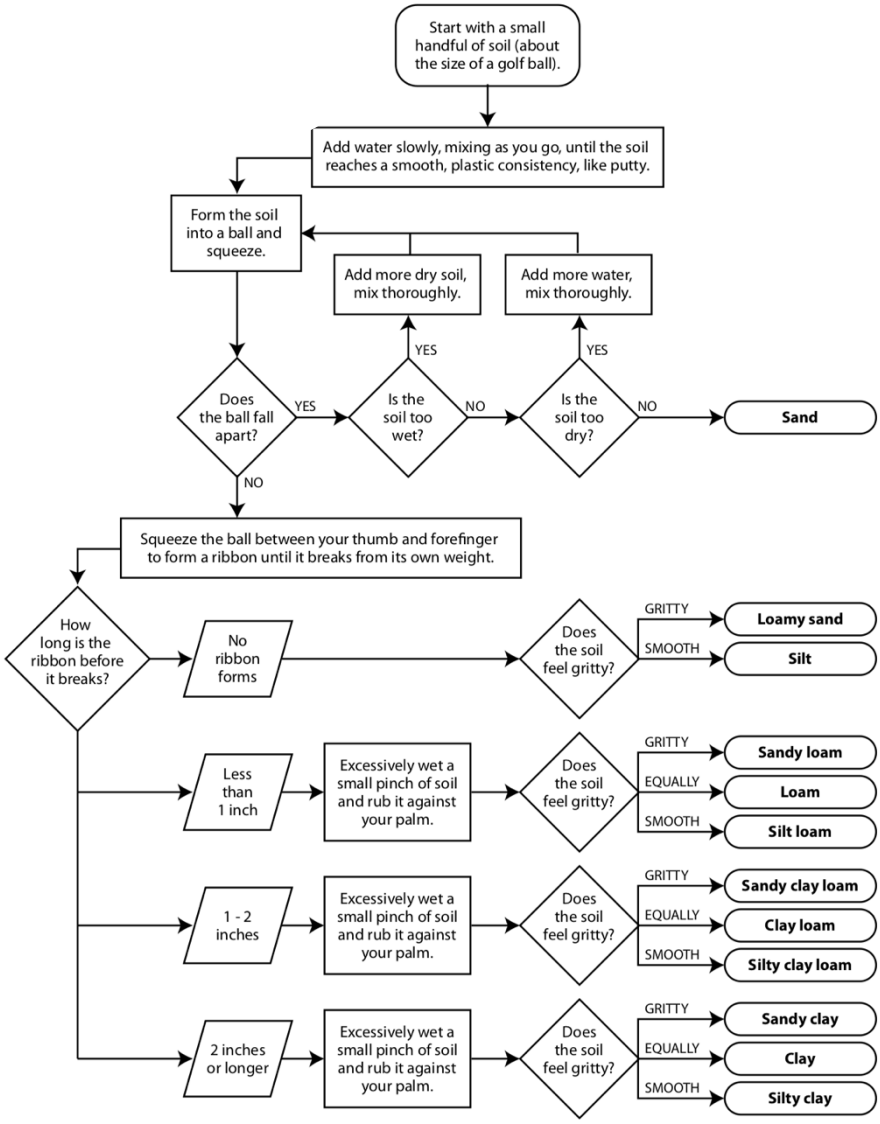

Figure B 1: Flow chart used to determine the soil texture of sample, reproduced from Ritchey et al. (2015).

B.6 Hygroscopic humidity

Hygroscopic humidity values are found in Table B 5. Heavy metal concentrations and OM content are corrected for content of water.

Table B 5: Hygroscopic humidity of soil samples (%H_20).

Sample	%H_2O			
	Replicate 1	Replicate 2	Replicate 3	AVG
S-1	0.64	0.64	0.67	0.65
S-2	0.75	0.74	0.81	0.76
S-3	0.75	0.74	0.79	0.76

Sample	%H_2O			
	Replicate 1	**Replicate 2**	**Replicate 3**	**AVG**
S-4	0.49	0.50	0.43	0.47
S-5	0.40	0.53	0.48	0.47
S-6	0.31	0.38	1.1	0.60
S-7	1.1	0.49	0.45	0.66
S-8	2.0	2.1	2.1	2.1
S-9	2.5	2.2	2.5	2.4
L-1	2.7	2.9	2.8	2.8
L-2	1.4	1.3	1.3	1.3
L-3	0.72	0.72	0.89	0.78
L-4	2.8	2.9	2.9	2.9
L-5	1.3	1.3	1.5	1.4
L-6	0.78	1.0	0.84	0.88
L-7	2.2	2.2	2.3	2.2
L-8	1.0	1.0	1.0	1.0
L-9	0.81	0.74	0.74	0.76
L-10	5.6	5.7	5.7	5.7
L-11	2.2	2.3	2.2	2.2
L-12	0.85	0.86	0.82	0.84
L-13	4.1	4.0	4.1	4.1
L-14	2.5	2.7	2.7	2.6
L-15	3.1	3.0	3.0	3.0
L-16	3.3	3.3	3.2	3.3
L-17	2.5	2.4	2.3	2.4
L-18	1.6	1.6	1.6	1.6
L-19	1.1	1.2	1.2	1.2
BCR142	*2.9*	*3.3*	*4.0*	*3.4*

Appendix C Calculations and statistics

C.1 and C.2 describes the calculations of average concentrations, STD and relative standard deviation (RSD). C.3 Gives the calculation for Grubbs test of outliers.

A description of the Wilcoxon rank sum test is found in C.4.

Loadings for different variables in the overall PCA are found in table C 2 in C.5

C.1 Average concentration

$$\bar{x}_N = \frac{x_1 + x_2 + x_3 + \cdots + x_N}{N} \qquad \text{Equation C 1}$$

Where,

$$x_1 = concentration\ in\ replicate\ 1$$

$$N = number\ of\ replicates$$

$$\bar{x}_N = average\ concentration\ (avg)$$

C.2 Standard deviation and relative standard deviation

$$STD = \sqrt{\sum \frac{(x_1 - \bar{x}_N)^2 + (x_2 - \bar{x}_N)^2 + (x_3 - \bar{x}_N)^2 + (x_N - \bar{x}_N)^2}{N - 1}} \qquad \text{Equation C 2}$$

Where,

$$STD = standard\ deviation$$

$$RSD = \frac{STD}{\bar{x}_N} * 100 \qquad \text{Equation C 3}$$

Where,

$$RSD = relative\ standard\ deviation\ (\%)$$

C.3 Grubbs test for outliers

$$G - value = \frac{(\bar{x}_N - x_s)}{S}$$ Equation C 3

Table C 1: Critical values of G for a two-sided test (P=0.05)

Sample Size	Critical values of G
3	1.155
4	1.481
5	1.715
6	1.887
7	2.020
8	2.126
9	2.15
10	2.290

A G-value above G-critical was considered an outlier.

C.4 Wilcoxon Rank Sum Test

The Wilcoxon rank sum test gives each observation in the two independent group ranks between 1 to N_A+N_B.

Where,

N_A=Number of observations in group A (e.g. urban locations)

N_B= Number of observations in group B (e.g. SE rural locations)

Want to test the hypothesis that the distribution of the data in A is the same as B;

H_0 : A=B

H_a : A>B

The sum of the ranks for A if H_0 is true is denoted W_A, while sum of ranks for A is denoted w_A if H_1 is true. If H_0 is true, then W_A is comparable to the sum of ranks for B. If H_1 is true, then w_A is higher and the observations in A has more of the higher ranks. P-value is given as the probability that $W_A \geq w_A$. Any p-value below 0.05 was considered significant.

$$\text{p-value} = \text{pr}(W_A \geq w_A)$$

C.5 Loadings in PCA

Table C 2: Loadings for the first three principal components.

	PC1	PC2	PC3
Pb	0,180	-0,217	0,397
Zn	0,331	-0,232	-0,066
Ni	0,288	0,243	0,0268
Cd	0,345	-0,152	0,130
Cr	0,243	0,290	0,0778
Co	0,191	0,290	0,0928
Cu	0,141	-0,227	-0,182
As	0,249	0,199	0,127
Hg	0,240	0,00440	-0,333
Se	0,168	0,305	0,0166
OM	0,130	0,245	-0,178
c,H,	-0,166	-0,0610	-0,019
CEC	0,145	0,353	-0,0747
clay,content	0,075	0,217	0,186
Dist,City	-0,188	0,031	0,0499
Dist,Dump	0,0323	0,108	0,0807
SCCP	0,174	-0,161	0,472
MCCP	0,281	-0,203	0,288
DEC602	0,225	-0,079	-0,209
DEC603	0,110	0,146	-0,250
DEC,SYN	0,253	-0,234	-0,283
DEC,ANTI	0,224	-0,262	-0,270

Appendix D DMA-80

Appendix D contains information about the DMA procedure (D.1, D.2 and D.3), as well as the measured concentrations (D.4), certificate of analysis for the reference material (D.5), the values for STD and MDL (D.6 and D.7). Recovery of reference material is foun in D.8.

D.1 Application note

Application Note: HG/SC-10 Field: Standard/Certified **BCR-141 (Calcareous Loam Soil)**

Summary

Precise and rapid determination of total mercury in BCR 141 can be performed using Direct Mercury Analyzer. Such an instrument requires no sample wet chemistry or pre-treatment.

Once a weighed sample portion is introduced into the instrument, analysis is completed in six minutes. Direct analysis of mercury, using the integrated sequence of Thermal Decomposition, Catalyst Conversion, Amalgamation, and Atomic Absorption Spectrophotometer, is described in EPA 7473 and is validated for laboratory as well as field analysis.

Instrumentation

Direct Mercury Analyzer apparatus and supplies

Milestone DMA-80, 660-1660 terminal with DMA-80 software or DMA-80 PC software, metal boats.

Analytical balance, spatula, pipette, or appropriate mechanical pipette and volumetric flask (Class A), 50 or 100 ml.

Sample weight :

40-100 mg

Procedure

1. Place a boat on the balance plate, tare it and weigh the sample.
2. Introduce the boat into sample tray.
3. Run the DMA-80 program to completion.

DMA-80 program

N° step	Time	Temperature
1	00:00:10	200°C
2	00:02:00	650°C
3	00:01:00	650°C
Max start temp: 200°C Purge: 60 sec		

Results

N°	µg/kg
1	52.84
2	53.91
3	54.02
4	52.30
5	54.14

Certified value of Hg : 52.5 – 61.1 µg/kg

Avg: 53.44 µg/kg SD: 0.74 µg/kg RSD: 1.38 %

Conclusion

The DMA-80 Mercury Analyzer successfully processed BCR 141 sample. Total analysis time per sample was less than 6 minutes, including the time employed to weigh each sample into the boat.

D.2 Instrumental set up

Table D 1: Instrumental set up of DMA-80

Parameter	Value
Max start T (°C)	500
Purge time (sec)	30
Amalgamator time (sec)	12
Signal recording time (sec)	24

Table D 2: DMA-80 program used to wuantify Hg.

Step	Temperature (°C)	Time (hour:min:sec)
Ramp to drying step	200	00:00:30
Drying	200	00:00:10
Ramp to decomposition step	650	00:02:00
Decomposition	650	00:01:00

D.3 Calibration

Due to the instrument's stability and the long lifetime of the catalyst and gold amalgamator, calibration of the system on a daily basis was not required. The calibration conducted by liquid reference solutions was done in 2017 by the supplier of the instrument (Holger Hartmann). Both Cell 1 (low concentrations) and Cell 2 (high concentrations) calibration curves utilize a squared approximation method.

	Low concentration	High concentration
Equation	$0.061x - 0.001x^2$	$1.000 * 10^{-3}x - 2.765 * 10^{-7}x^2$
R^2	1.000	0.9999

D.4 Measured Hg levels

Table D 3: Concentration of Hg in samples.

Sample	mg/kg
S-1	0.0109
S-2	0.0228
S-3	0.00777
S-4	0.0332
S-5	0.0069
S-6	0.00927
S-7	0.0152
S-8	0.0647
S-9	0.0216
L-1	0.0121
L-2	0.0123
L-3	0.0074
L-4	0.0223
L-5	0.0183
L-6	0.0979
L-7	0.0266
L-8	0.0110
L-9	0.028
L-10	0.0308
L-11	0.0114
L-12	0.0409
L-13	0.0924
L-14	0.0212
L-15	0.0108
L-16	0.00675
L-17	0.011
L-18	0.0148
L-19	0.0115

D.5 Reference material

EUROPEAN COMMISSION

JOINT RESEARCH CENTRE

Institute for Reference Materials and Measurements

CERTIFIED REFERENCE MATERIAL
BCR® – 142R

CERTIFICATE OF ANALYSIS

LIGHT SANDY SOIL			
Element	Mass fraction based on dry mass		Number of accepted sets of results p
	Certified value [1] [mg/kg]	Uncertainty [2] [mg/kg]	
Total content			
Cd	0.34	0.04	4
Co	12.1	0.7	6
Cu	69.7	1.3	8
Pb	40.2	1.9	4
Mn	970	16	9
Hg	0.067	0.011	6
Ni	64.5	2.5	7
Element	Mass fraction based on dry mass		Number of accepted sets of results p
	Certified value [3] [mg/kg]	Uncertainty [2] [mg/kg]	
Aqua regia soluble content			
Cd	0.249	0.010	4
Pb	25.7	1.6	7
Ni	61.1	1.5	9
Zn	93.3	2.7	9

1) Unweighted mean value of the means of p accepted sets of data, each set being obtained in a different laboratory and/or with a different method of determination. The certified values are traceable to the SI.

2) Half-width of the 95 % confidence interval of the mean defined in 1) or 3).

3) Unweighted mean value of the means of p accepted sets of data, each set being obtained in a different laboratory and/or with a different method of determination. The certified values are traceable to the aqua regia extraction method as described in the report (DIN 38414-S7).

This certificate is valid for one year after purchase.

Sales date:

The minimum amount of sample to be used is 250 mg.

NOTE

This material has been certified by BCR (Community Bureau of Reference, the former reference materials programme of the European Commission). The certificate has been revised under the responsibility of IRMM.

Brussels, April 1993
Latest revision: April 2007

Signed:

Prof. Dr. Hendrik Emons
Unit for Reference Materials
EC-JRC-IRMM
Retieseweg 111
2440 Geel, Belgium

Figure D 1: Certificate of analysis for the reference material. The measured Hg levels were compared with the total content, while levels of metals obtained with ICP-MS were compared with the aqua regia soluble content.

D.6 Calculating STD of the Hg quantification method

Table D 4: Sample L-1 used to determine STD.

Sample	mg/kg
L-1-1	0.0116
L-1-2	0.0126
L-1-3	0.0101
L-1-4	0.0144
L-1-5	0.0116
AVG	**0.0121**
STD	**0.002**
RSD (%)	**13.196**

D.7 Determining MDL

Table D 5: Amount of Hg in blank samples as well as standard deviation and MDL.

Boat #	ng Hg
1	0.0158
2	0.0137
3	0.0114
4	0.00971
5	0.0104
6	0.0113
7	0.00919
8	0.00976
9	0.00960
10	0.00964
Average	**0.01106**
STD	**0.002**
MDL (mg/kg)	**0.004**

D.8 Recovery of reference material

Table D 6: Recovery of Hg in reference sample.

	Measured concentration (mg/kg)	**Reference concentration (mg/kg)**	**Recovery (%)**
BCR142	0.064	0.067	95.7

Appendix E Decomposition of soil

Appendix E contains the application note followed to decompose the soil samples (E.1), the microwave program for decomposing and cleaning(E.2 and E.3 respectively). The microwave program stated in the application note was edited because the method had not previously been tested on the Milestone Ethos 1 microwave.

E.1 Application note

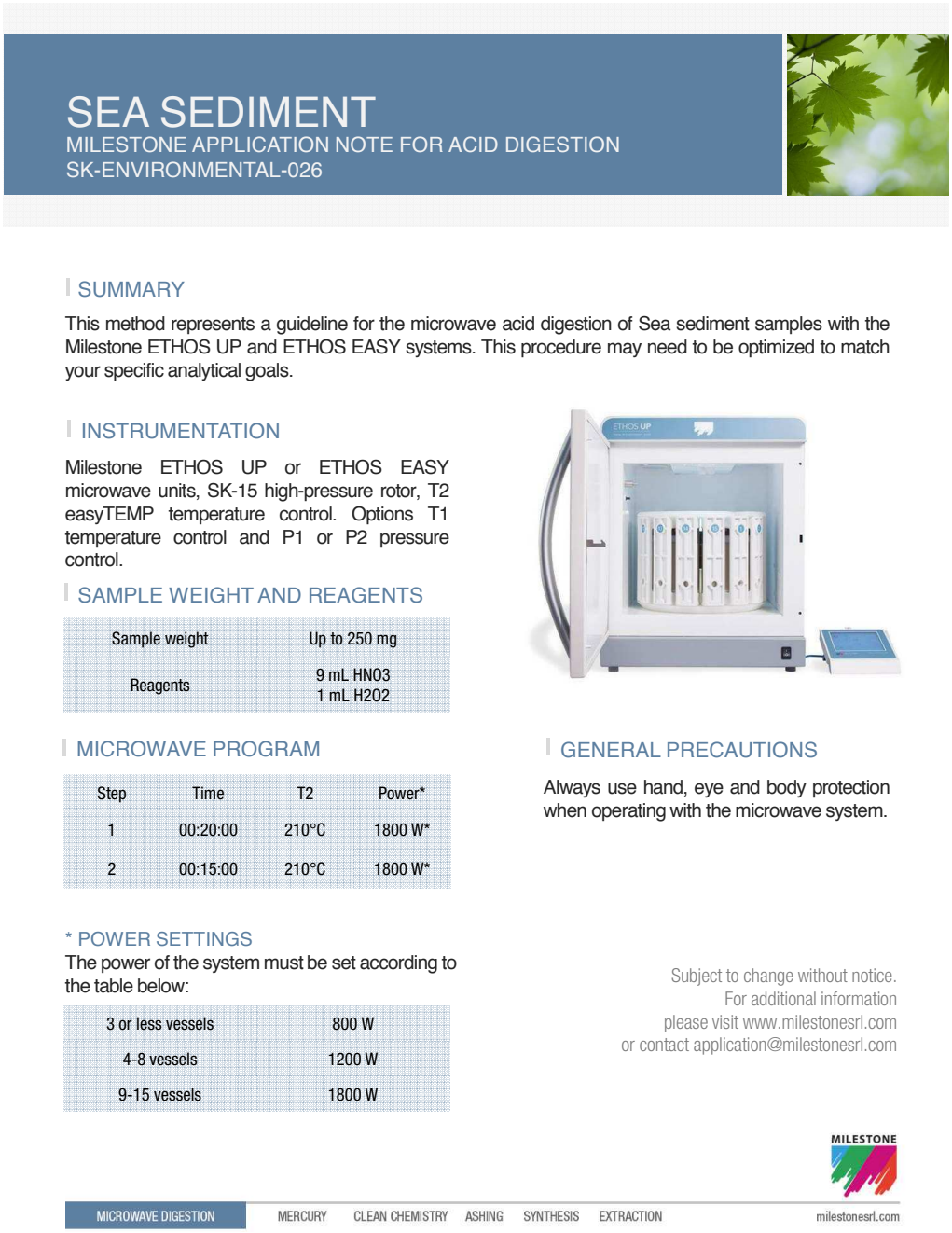

SEA SEDIMENT

MILESTONE APPLICATION NOTE FOR ACID DIGESTION
SK-ENVIRONMENTAL-026

SUMMARY

This method represents a guideline for the microwave acid digestion of Sea sediment samples with the Milestone ETHOS UP and ETHOS EASY systems. This procedure may need to be optimized to match your specific analytical goals.

INSTRUMENTATION

Milestone ETHOS UP or ETHOS EASY microwave units, SK-15 high-pressure rotor, T2 easyTEMP temperature control. Options T1 temperature control and P1 or P2 pressure control.

SAMPLE WEIGHT AND REAGENTS

Sample weight	Up to 250 mg
Reagents	9 mL HNO3 1 mL H2O2

MICROWAVE PROGRAM

Step	Time	T2	Power*
1	00:20:00	210°C	1800 W*
2	00:15:00	210°C	1800 W*

* POWER SETTINGS

The power of the system must be set according to the table below:

3 or less vessels	800 W
4-8 vessels	1200 W
9-15 vessels	1800 W

GENERAL PRECAUTIONS

Always use hand, eye and body protection when operating with the microwave system.

Subject to change without notice.
For additional information
please visit www.milestonesrl.com
or contact application@milestonesrl.com

MICROWAVE DIGESTION MERCURY CLEAN CHEMISTRY ASHING SYNTHESIS EXTRACTION milestonesrl.com

Figure E 1: Application note for Sea sediment.

E.2 Microwave digestion reagents and program

Table E 1: Reagents used for microwave digestion.

Reagents	Concentration (%)	Volume (mL)	Grade
HNO_3	65	9	Suprapur
H_2O_2	35	1	Purum Pa.

Table E 2: Microwave program.

Time (hour:min:sec)	Temperature (°C)	Maximum power (Watt)	Step
00:07:30	100	1000	Ramp
00:04:00	100	1000	Delay
00:07:30	180	1000	Ramp
00:20:00	180	1000	Decomposition
00:20:00	40	0	Cooling

E.3 Cleaning of microwave vessels

Table E 3: Cleaning program for microwave vessels.

Reagents	Concentration (%)	Volume (mL)	Grade
HNO_3	65	5	Reag. Ph Eur
H_2O_2	33	1	Technical grade
water	-	2	Type 1

Table E 4: Reagents used for cleaning of microwave vessels.

Time	Temperature (°C)	Power (watt)	Step
00:05:00	180	1000	Ramp
00:10:00	180	1000	
00:10:00	-	0	Cooling

Appendix F ICP-MS

Appendix F contains information about the ICP-MS analysis procedure (F.1, F.2, F.3) and the resulting concentrations measured of the soil samples (F.4). The concentrations measured of the reference material are found in F.5, while MDL calculation are shown in F.6.

Evidence for Cd contamination are found in F.7

F.1 Set up

Table F 1: Instrumental setup of ICP-MS Nexion300d.

Component/Parameter	Type/value/Mode
Nebulizer	Meinhard glass concentric
Spray chamber	Glass cyclonic
Triple cone interface material	Nickel/Aluminum
Plasma gas flow	17.0L/min
Auxiliary gas flow	1.2L/min
Nebulizer gas flow	Ca. 0.96L/min
Peristaltic pump	24rpm
RF power	1000W
Integration time	1000ms
Replicates per sample	3
Mode of operation	Standard

F.2 Isotopes measured

Table F 2: Isotopes selected for ICP-MS analysis.

Analyte	Mass (amu)
Cr	52
Co	59
Ni	60
Cu	63
Zn	66
As	75
Se	82

Analyte	Mass (amu)
Cd	111
In	115
Sb	121
Pb	208

F.3 Calibration curves

Table F 3: Calibration approximation equations and R^2

Elements	1st run (30.01.20)		2nd run (30.01.20)		3rd run (31.01.20)		4th run (31.01.20)	
	Linear through zero	R^2	Linear through zero	R^2	Linear through zero	R^2	Linear through zero	R^2
Pb	14193x	1	40651x	0.9991	41501x	0.9992	38856x	0.9987
Zn	2534.1x	1	5523.8	1	5845.2x	0.9999	5417.9x	1
Ni	5832.9x	0.9999	14183x	1	14915x	0.9996	14261x	0.9998
Cd	3968.3x	0.9999	7275x	1	7514	0.9999	7608.5x	1
Cr	20764x	0.9996	53766x	0.9999	56325x	0.9997	52752x	0.9983
Co	24442x	0.9997	65337x	1	68709x	0.9999	64754x	1
Cu	11903x	0.9989	29537x	0.9998	30959x	0.9995	29649	0.9998
As	2715.2x	1	5492.1x	1	5739.1x	0.9999	5512.3x	1
Se	289.42x	0.9999	627.01x	1	657.77x	1	620.57x	0.9999

F.4 Concentrations

Table F 4: Concentrations (mg/kg) of heavy metals for all the three sample replicates of each soil sample.

Sample	mg/kg								
	Pb	Zn	Ni	Cd	Cr	Co	Cu	As	Se
S-1-1	5.09	18.1	1.95	0.0163	7.09	1.21	4.96	0.277	0.190
S-1-2	5.13	20.1	1.99	0.164	7.84	1.28	4.85	0.246	0.165
S-1-3	5.13	15.2	1.99	0.0474	7.33	1.26	4.68	0.248	0.205
S-2-1	445	149	3.74	0.335	11.7	2.21	98.4	1.86	0.360
S-2-2	493	158	3.31	0.357	12.6	2.00	133	1.60	0.318

Sample	mg/kg								
S-2-3	608	156	3.74	0.388	13.6	2.10	95.4	1.82	0.305
S-3-1	14.6	71.6	2.43	0.0923	5.42	0.954	14.8	0.210	0.196
S-3-2	13.8	62.1	2.22	0.0982	5.31	0.926	13.7	0.207	0.227
S-3-3	16.5	70.6	2.41	0.101	5.91	1.03	15.3	0.317	0.232
S-4-1	66.4	187	13	0.128	9.65	1.51	958	1.13	0.254
S-4-2	61.3	258	7.79	0.148	6.47	1.72	1.03*10^3	1.05	0.299
S-4-3	69.5	214	12.7	0.182	8.33	1.61	1.15*10^3	1.22	0.232
S-5-1	6.95	9.40	0.848	0.0237	3.41	0.639	3.24	0.242	0.205
S-5-2	7.59	15.7	1.06	0.0217	4.23	0.722	3.59	0.200	0.238
S-5-3	7.93	14.1	0.896	0.0248	3.33	0.733	3.74	0.285	0.193
S-6-1	2.34	10.0	0.499	0.0140	2.22	0.193	2.05	0.0630	0.122
S-6-2	2.36	9.35	0.561	0.0142	1.83	0.176	2.25	0.0595	0.107
S-6-3	2.91	12.3	0.631	0.108	2.85	0.227	2.36	0.0791	0.0940
S-7-1	5.39	25.7	2.83	0.0202	8.24	1.89	3.63	0.558	0.204
S-7-2	5.09	29.0	2.27	0.0256	7.25	1.90	4.14	0.400	0.199
S-7-3	5.06	25.1	2.50	0.0211	7.85	1.99	4.15	0.415	0.163
S-8-1	5.18	28.4	3.75	0.0451	12.4	1.66	6.47	0.746	0.217
S-8-2	5.18	28.6	3.56	0.0396	10.0	1.66	6.41	0.715	0.212
S-8-3	7.74	25.3	2.40	0.0373	8.52	1.61	6.34	0.623	0.217
S-9-1	3.75	16.6	3.88	0.0467	13.2	3.21	4.61	0.211	0.316
S-9-2	4.52	22.5	7.07	0.0670	22.6	5.02	5.99	0.234	0.314
S-9-3	3.91	19.0	4.99	0.0491	17.0	3.85	5.28	0.214	0.296
L-1-1	1.37	7.59	10.8	0.0520	3.82	0.750	3.71	2.03	1.00
L-1-2	0.908	6.63	9.89	0.0510	3.47	0.705	3.39	1.94	0.922
L-1-3	0.932	14.2	9.47	0.0809	3.93	0.721	3.16	1.80	0.804
L-2-1	6.72	15.7	4.80	0.0596	9.87	2.94	12.3	0.851	0.329
L2-2	6.27	14.0	5.14	0.0228	12.5	3.11	11.2	1.04	0.346
L-2-3	5.95	12.7	3.54	0.0268	4.80	2.39	12.6	0.594	0.301
L-3-1	3.00	25.6	1.84	0.0241	4.40	1.56	3.41	1.11	0.279
L-3-2	3.22	26.1	2.59	0.0278	5.76	1.69	3.59	1.30	0.316
L-3-3	3.53	35.4	2.52	0.0818[1]	5.95	1.82	4.28	1.27	0.317
L-4-1	9.98	31.1	18.2	0.349[1]	36.9	4.88	7.36	5.84	0.625
L-4-2	8.84	26.5	19.4	0.106	40.2	5.10	7.86	6.93	0.508
L-4-3	8.63	26.9	18.7	0.105	38.3	4.90	8.17	6.31	0.573
L-5-1	131	97.1	3.69	0.117[1]	12.6	1.85	34.9	8.8	0.587
L-5-2	115	82.5	3.62	0.0966	13.3	1.74	26.3	7.60	0.347

Sample	mg/kg								
L-5-3	126	77.3	0.598	0.0959	13.1	1.70	23.3	7.18	0.421
L-6-1	78.9	186	18.3	0.327	27.2	3.89	148[1]	4.50	0.414
L-6-2	77.2	200	14.8	0.304	20.7	3.22	41.4	3.94	0.413
L-6-3	88.7	233	16.6	0.360	23.6	3.68	41.7	3.86	0.402
L-7-1	14.4	65.0	25.6	0.122	33.5	11.6	26.7	11.5	0.511
L-7-2	14.4	65.8	24.7	0.117	34.0	11.6	25.9	11.2	0.447
L-7-3	14.9	82.3	29.1	0.131	34.3	14.1	27.9	12.4	0.501
L-8-1	96.4	129	3.37	0.166	6.55	1.44	14.7	1.129	0.202
L-8-2	146	92.4	3.13	0.179	6.33	1.37	14.8	0.833	0.216
L-8-3	101	91.2	3.33	0.179	6.38	1.43	14.4	0.888	0.207
L-9-1	26.6	68.4	2.58	0.0974	8.62	0.883	7.84	0.594	0.260
L-9-2	26.1	78.4	2.94	0.0894	9.51	0.914	7.63	0.620	0.247
L-9-3	26.9	71.7	3.06	0.0807	9.32	0.968	8.42	0.634	0.280
L-10-1	19.4	102	34.1	0.169	65.4	9.36	11.0	15.04	0.747
L-10-2	20.0	109	37.1	0.184	69.3	10.5	11.8	15.93	0.833
L-10-3	22.5	86.4	35.1	0.163	68.5	10.05	11.3	15.0	0.809
L-11-1	12.3	73.1	24.1	0.136	30.0	10.1	18.2	6.24	0.46
L-11-2	10.9	63.5	20.4	0.114	26.5	9.10	15.2	5.33	0.426
L-11-3	10.6	59.5	19.2	0.111	26.5	8.47	15.6	5.11	0.439
L-12-1	8.02	61.7	5.09	0.0667	13.1	3.28	7.08	1.50	0.229
L-12-2	7.74	49.7	3.30	0.0549	9.52	3.01	5.81	1.27	0.229
L-12-3	8.39	51.9	5.16	0.0737	12.6	3.34	7.07	1.51	0.188
L-13-1	11.9	51.9	9.6	0.112	25.9	7.33	11.8	0.619	0.606
L-13-2	12.1	11.6	9.3	0.165	25.7	7.62	12.1	0.679	0.621
L-13-3	11.4	53.3	10.1	0.109	26.1	7.24	12.6	0.601	0.540
L-14-1	5.17	55.1	7.11	0.0306	19.2	6.87	4.29	0.323	0.438
L-14-2	5.97	50.2	7.86	0.0598[1]	21.9	7.94	3.94	0.429	0.547
L-14-3	5.39	54.0	5.85	0.0294	14.9	7.01	3.68	0.328	0.487
L-15-1	4.99	33.6	10.4	0.0278	26.5	6.50	19.7	0.469	0.478
L-15-2	3.71	27.2	7.59	0.0180	20.5	5.10	7.03	0.407	0.412
L-15-3	5.19	45.1	12.4	0.0447	29.5	7.35	20.9	0.575	0.525
L-16-1	4.97	34.5	15.0	0.0337	36.7	8.16	25.2	0.502	0.400
L-16-2	5.51	52.5	13.7	0.0313	31.5	8.17	24.2	0.485	0.514
L-16-3	5.69	46.4	15.9	0.0753[1]	40.8	8.66	40.3	0.598	0.461
L-17-1	5.76	29.8	7.72	0.0336	32.4	6.15	4.62	1.01	0.616

sample	mg/kg								
L-17-2	5.08	37.4	5.61	0.0383	21.7	5.73	4.97	0.522	0.579
L-17-3	5.41	42.5	8.72	0.0345	29.5	6.16	5.60	0.505	0.523
L-18-1	4.99	25.2	2.90	0.0220	9.13	4.73	4.15	0.380	0.286
L-18-2	5.27	28.1	3.05	0.0203	10.3	4.76	4.34	0.445	0.324
L-18-3	5.56	26.6	3.75	0.0289	12.3	4.96	4.58	0.396	0.315
L-19-1	5.56	9.90	2.16	0.0423[1]	4.23	1.60	3.81	0.320	0.332
L-19-2	5.71	9.81	2.23	0.0218	5.62	1.65	3.67	0.363	0.391
L-19-3	8.74	9.39	2.08	0.0198	5.60	1.62	3.30	0.488	0.373

[1]Ruled an outlier by Grubbs test.

F.5 Concentrations measured of reference material

Table F 5: Concentrations measured of the reference material.

	Pb (mg/kg) Referance conc:	Cd (mg/kg)	Ni (mg/kg)	Zn (mg/kg)
BCR-142-1	27.0	0.717[1]	38.5	92.7
BCR-142-2	25.3	0.237	35.4	89.0
BCR-142-3	25.5	0.239	45.8	90.9

[1]Ruled an outlier by Grubbs test

F.6 Determining MDL

Table F 6: concentrations of analytes in blank samples and MDL.

Blank Sample	Concentration(ug/L)								
	Pb	Cd	Co	Cr	Cu	Ni	Zn	As	Se
1301	0.0946	0.00578	0.00669	1.06	0.161	0.125	1.00	0.0622	0.0946
0512	0.556	0.00956	0.0111	0.961	0.354	0.192	31.8	0.482	0.556
0901	0.0688	0.00561	0.00686	1.08	0.131	0.135	1.45	0.00811	0.0688
1112	0.0730	0.00644	0.00723	1.10	0.181	0.114	4.15	0.00980	0.0730
1501	0.0985	0.0112	0.00916	1.08	0.125	0.412	9.85	0.104	0.0985
0601	0.0849	0.00447	0.00607	1.06	0.178	0.125	0.930	0.0126	0.0849
2711	0.0716	0.00522	0.00693	1.06	0.622	0.124	20.4	0.0385	0.0716

Blank sample	Concentration(ug/L)								
0801	0.0609	0.00518	0.0102	1.02	0.159	0.137	1.99	0.0450	0.0609
1212	0.0561	0.00395	0.00650	1.07	0.168	0.114	1.18	0.00667	0.0561
2911	0.0760	0.0100	0.0106	1.00	0.320	0.112	1.57	0.128	0.0760
1601	0.0228	0.0566	0.00641	1.06	0.263	0.153	16.2	0.0214	0.0228
STD (ug/L)	0.2	0.02	0.002	0.04	0.1	0.1	10	0.1	0.1
MDL (mg/kg)	0.7	0.05	0.011	0.94	0.5	0.4	31	0.4	0.4

F.7 Evidence of Cd contamination

Table F 7: Signal intensities of Cd in blank samples.

	Intenstiy
Blank1	100
Blank2[1]	1500
Blank3	100
Blank4	160
Blank5	300
Blank6	260
Blank7[2]	-40
Blank8	120
Blank9	140
Blank10[2]	-60
avg	335
std	476.505

[1]Ruled an outlier by Grubbs test
[2]Below instrument LOD and omitted from calculation

Appendix G Concentrations below accepted limits

G.1 Cadmium

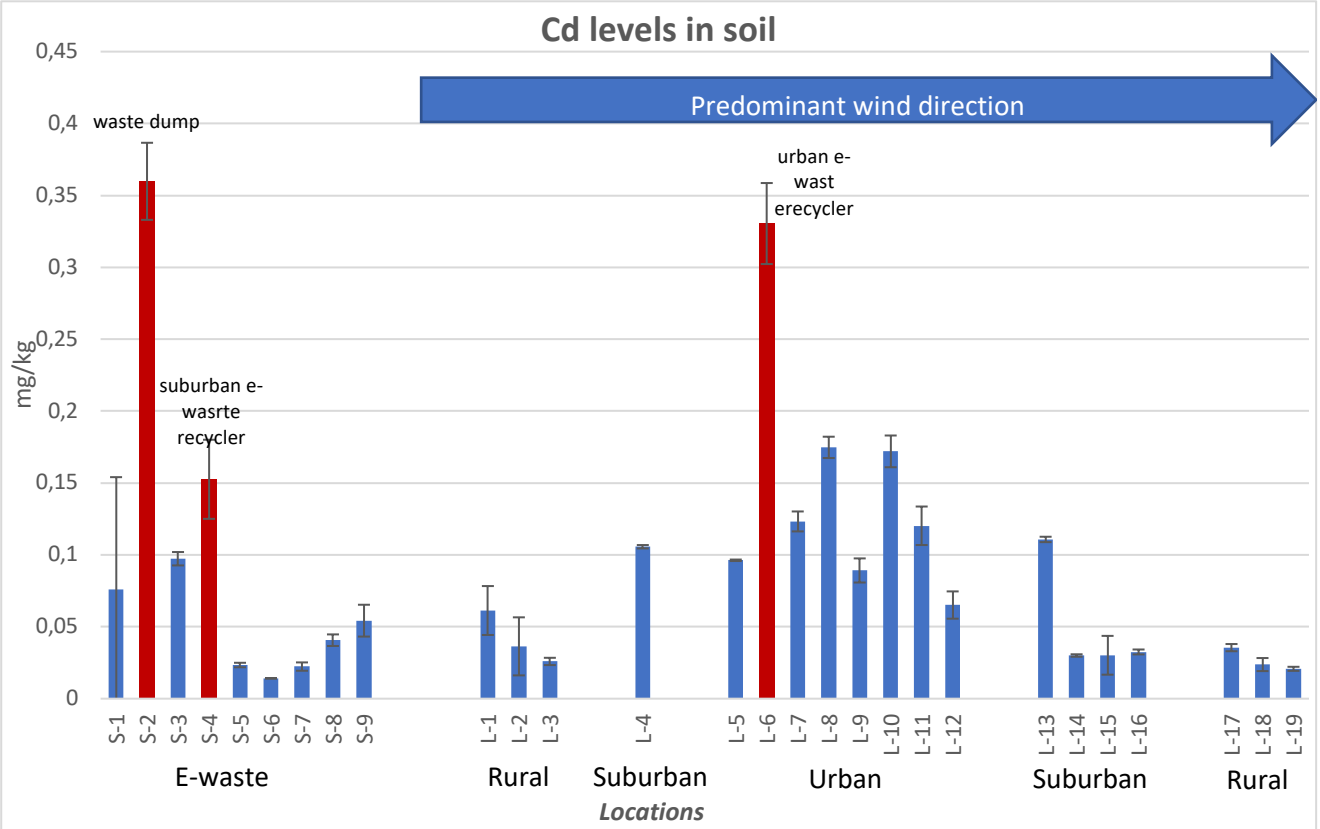

Figure G 1: Cd concentrations found in soils in and around Dar es Salaam, Tanzania.S-5, S-6, S-7, S-8, L-14, L-15, L-17, L-18 and L-19 had concentrations<MDL.

G.2 Nickel

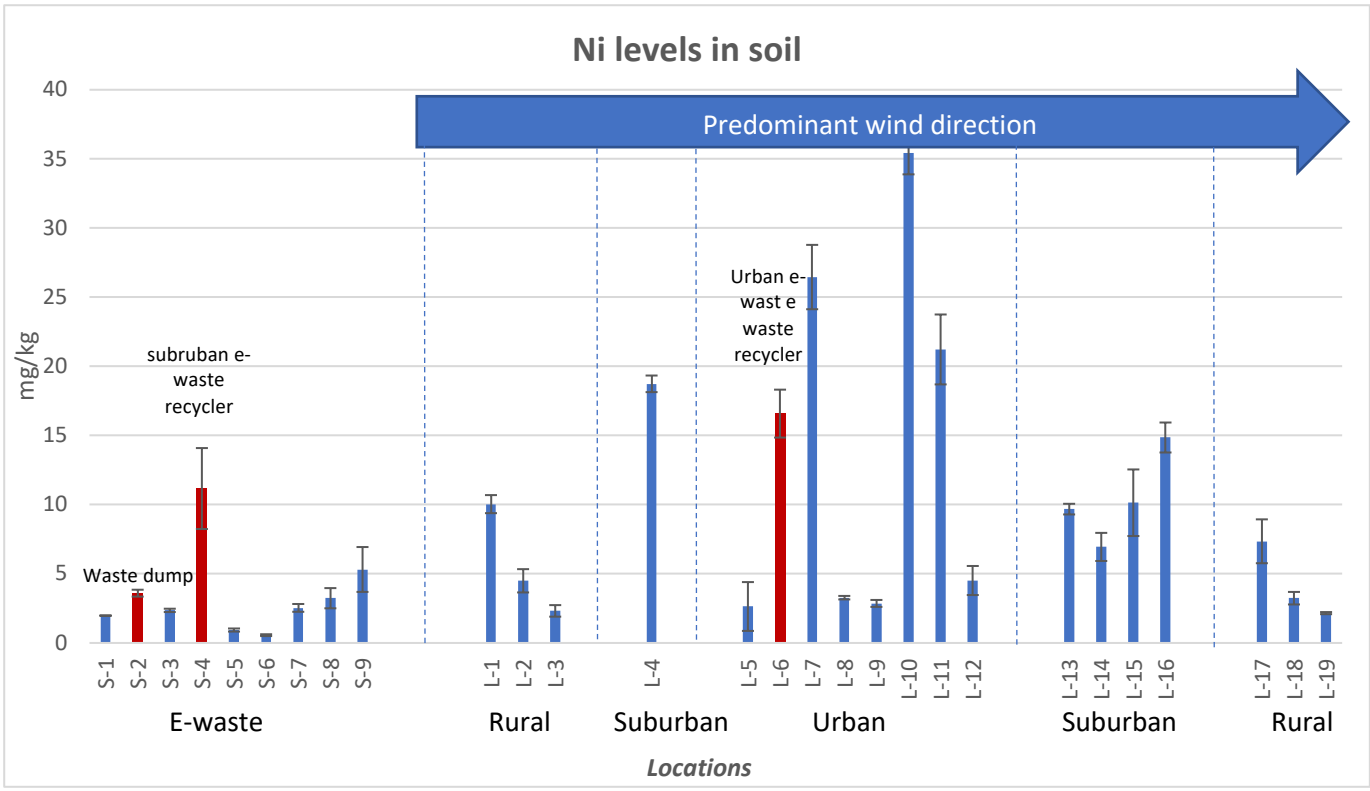

Figure G 2:Zn concentrations found in soils in and around Dar es Salaam.

G.3 Chromium

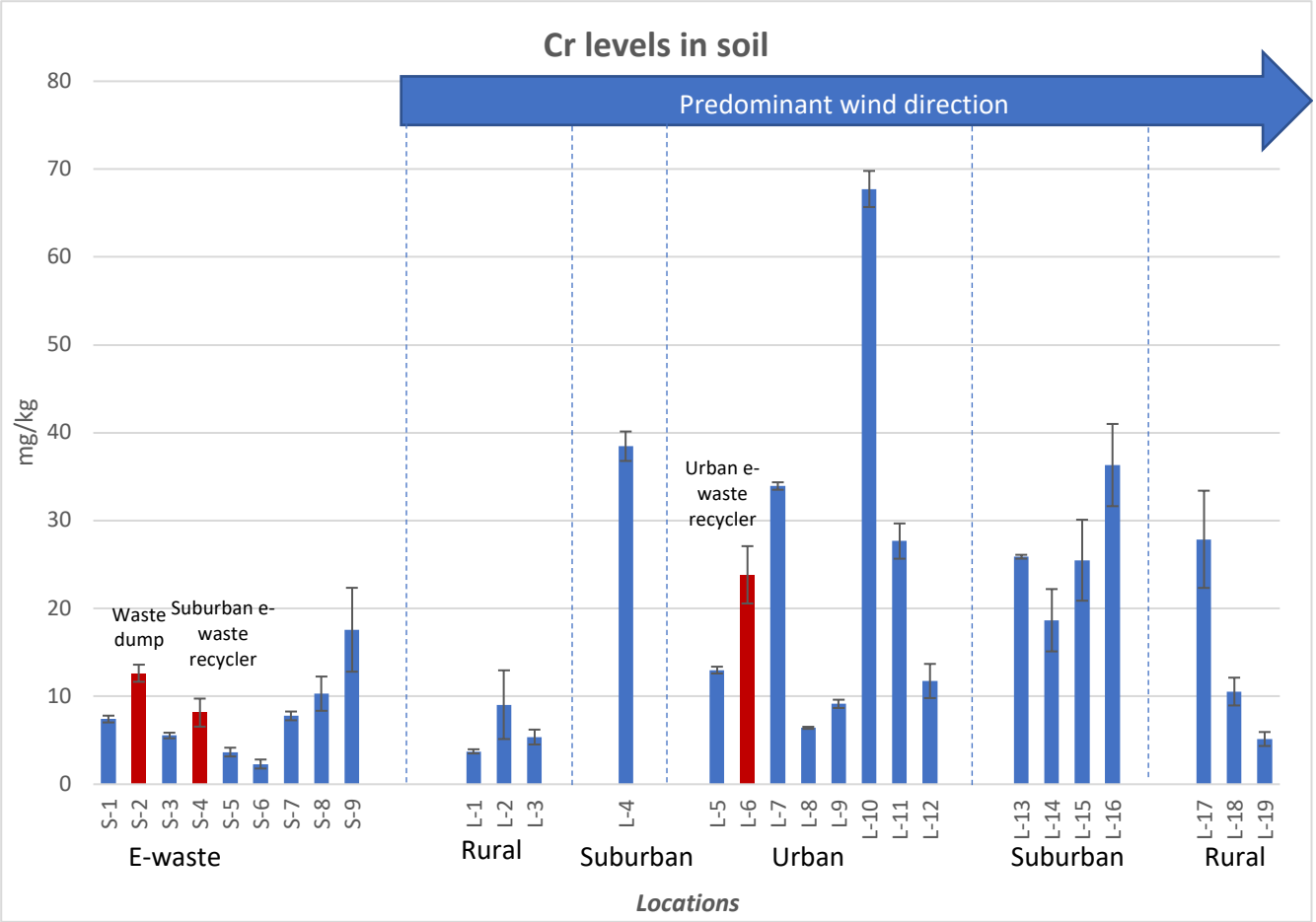

Figure G 3: Cr concentrations found in soils in and around Dar es Salaam.

G.4 Cobalt

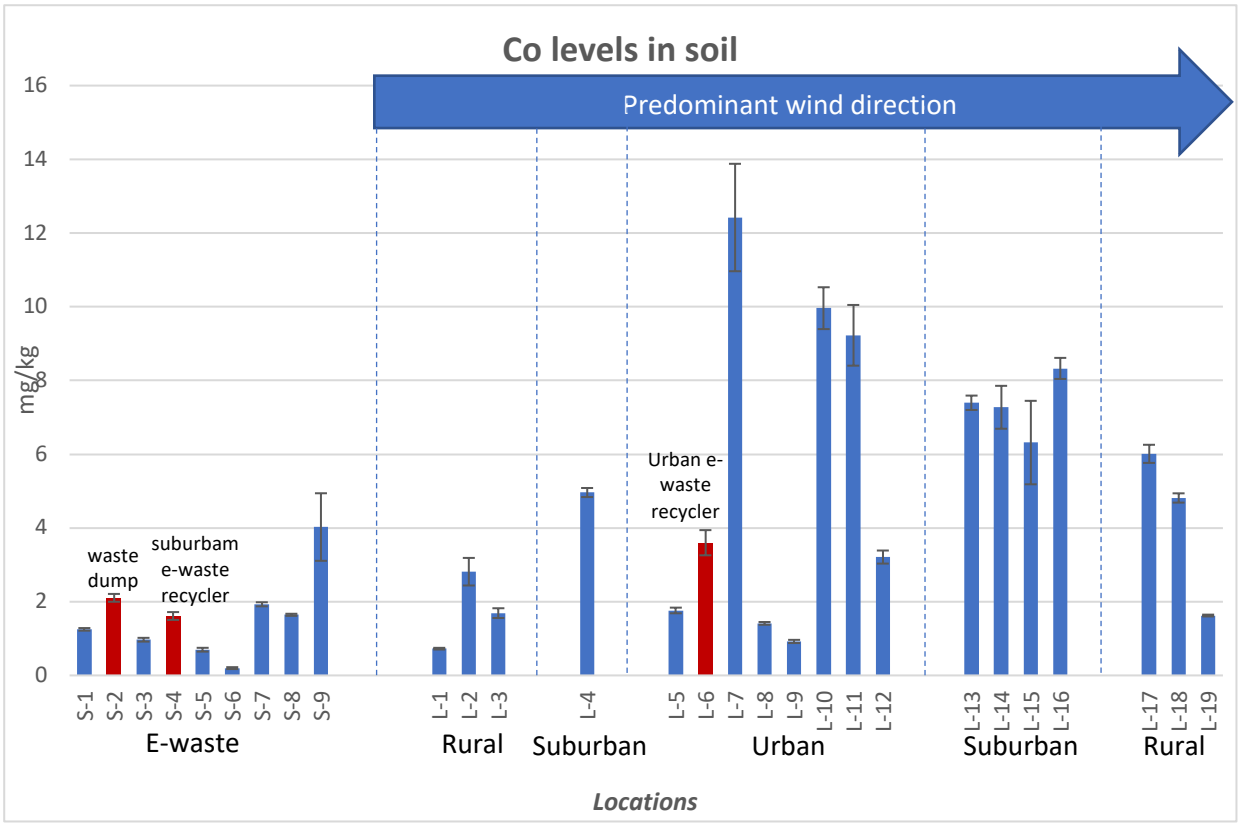

Figure G 4:Co concentrations found in soils in and around Dar es Salaam.

G.5 Selenium

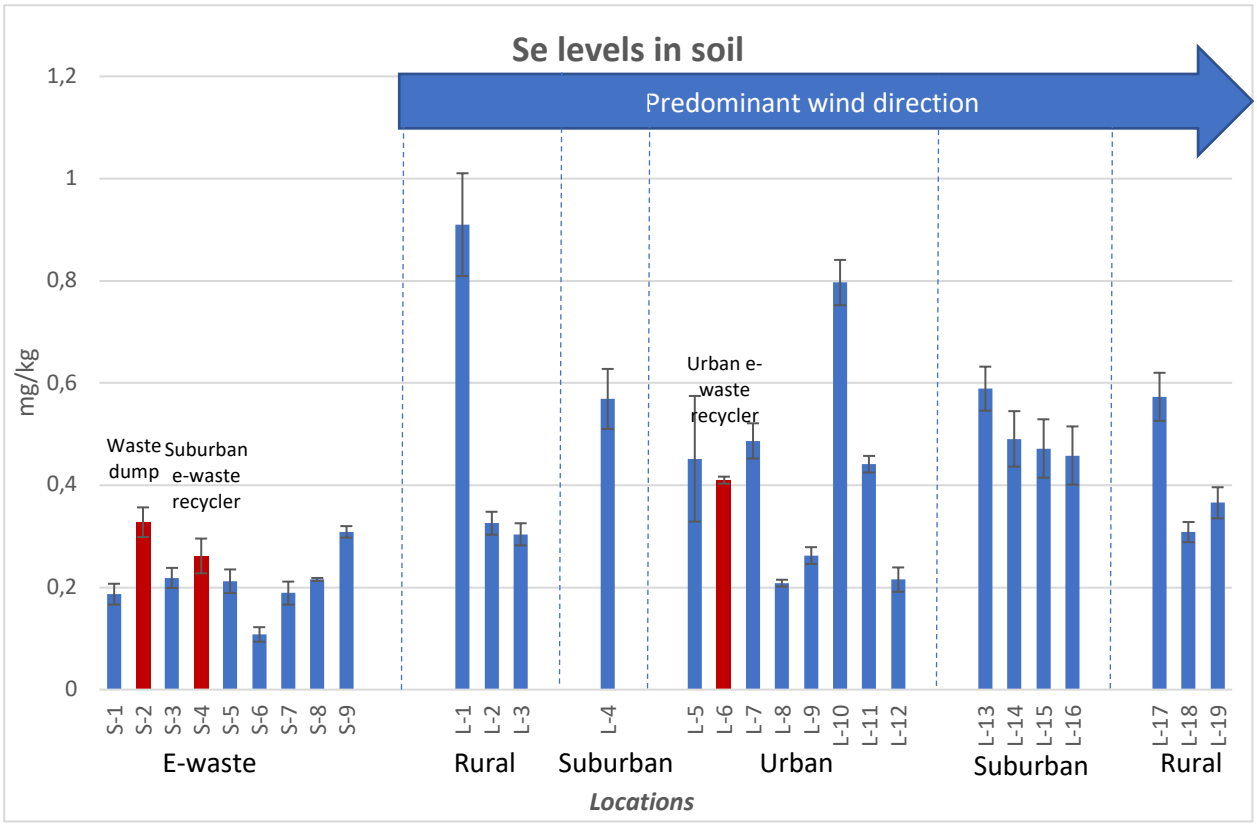

Figure G 5 :Se concentrations found in soils in and around Dar es Salaam. S-1, S-2, S-3, S-4, S-5, S-6, S-7, S-8, S-9, L-2, L-3, L-6, L-8, L-9, L-12, L-18 and L-19 had concentrations<MDL.